NEW METALLO-SILICATE MOLECULAR SIEVES AND SELECTIVE OXIDATION CATALYSIS

A THESIS
SUBMITTED TO THE
UNIVERSITY OF PUNE
FOR THE DEGREE OF
DOCTOR OF PHILOSOPHY
(IN CHEMISTRY)

by

ASIM BHAUMIK

CATALYSIS DIVISION
NATIONAL CHEMICAL LABORATORY
PUNE - 411 008, INDIA

AUGUST 1996

---TO MY BELOVED PARENTS

CERTIFICATE

It is to certify that the work incorporated in the thesis **"New Metallo-Silicate Molecular Sieves and Selective Oxidation Catalysis"** submitted by **Mr. Asim Bhaumik**, for the Degree of ***Doctor of Philosophy***, was carried out by the candidate under my supervision in National Chemical Laboratory, Pune, INDIA. Such material as has been obtained from other sources has been duly acknowledged in the thesis.

Dr. Rajiv Kumar
Research Guide

ACKNOWLEDGEMENTS

I wish to express my gratitude to Dr. Rajiv Kumar for his valuable guidance and encouragement throughout the course of investigation.

I am also deeply indebted to Dr. A.V. Ramaswamy, Dr. S. Sivasanker, Dr. B.S. Rao for their stimulating discussions and constant personal help they rendered throughout the present course of investigation.

I am greatful to Dr. A.N. Kotasthane, Dr. C. Gopinathan, Dr. A.P. Singh for their encouragement and stimulating discussions.

I wish to express my thanks to Dr. Mrs. A.A. Belhekar, Dr. M.K. Dongare and Dr. S. Ganapathy for their direct scientific contributions and their help during this study.

I would like to thank to Ms. R.K. Ahedi, Dr. Eric Lowenthal and other scientific and supporting staff of Catalysis Division, and my numerous friends for their wholehearted help and discussion.

It gives me great pleasure to thank my parents, sister Manisha for their love, unfailing support, tremendeous patience, trust and encouragement that they have shown to me.

Finally, my thanks are due to the Council of Scientific & Industrial Research, New Delhi, for my fellowship award and to Dr. P. Ratanasamy, Director, National Chemical Laboratory, for permitting me to carry out my research work at NCL.

Asim Bhaumik

ASIM BHAUMIK

Contents ....

CHAPTER I

INTRODUCTION AND BACKGROUND

1.1 DEFINITION AND CLASSIFICATION :

Zeolites are crystalline, porous aluminosilicate molecular sieves[1-8] composed of three dimensional network, formed by the sharing of oxygens of the $[SiO_4]^{4-}$ and $[AlO_4]^{5-}$ tetrahedra such that two Al tetrahedra are never adjacent to each other. The crystallographic unit cell of the zeolites may be represented as :

$$M_{x/n}[(SiO_2)_x (AlO_2)_y]\ z\,H_2O$$

Where M is a charge compensating cation with valency n, generally selected from the metal ions of group I A or II A or an organic cation. When M is a proton the Brönsted acidity is generated in the zeolites. The ratio of x/y can be one to infinity. Since Al^{3+} does not occupy adjacent tetrahedral sites, the Si/Al molar ratio corresponds the density of the acid in the zeolites. The number of water molecules, which can be reversibly adsorbed and desorbed in the zeolite pores, is represented by z. The pores of zeolites are of molecular dimensions ranging between 0.5 and 1.0 nm in diameter. Accordingly, zeolites are also known as molecular sieves[8] because of their ability to discriminate the molecules of different size and shape. The characteristics which make molecular sieves useful as catalysts are :

* Generation of highly acidic sites when exchanged with protons.
* Shape selective catalytic properties.
* High surface area and thermal stability.
* Ease of regeneration to the initial activity.

These crystalline, porous molecular sieves / zeolites exhibit eco-friendly shape selective catalytic, adsorption and ion-exchange (viz. as water softener, detergent builders etc.) properties along with the raggedness in high temperature and high pressure environments. They are also compared with catalytic antibodies[9] and

metalloenzymes[10]. The key role played by synthetic zeolites in petroleum refining and petrochemical industry[7] can hardly be over emphasized.

Table 1.1 Silica based molecular sieves (zeolites) are classified as follows :

(i) Pore openings :	Small pore (8-membered rings[11], MTN, NU-1, etc.)
	Medium pore (10-membered rings[12], MFI, MEL, etc.)
	Large pore (12-membered rings[13,14], MTW, BEA etc.)
	Extra large pore (14-membered rings[15], UTD-1)
(ii) Si/Al mole ratio :	Low silica (Si/Al = 1-5, LTA, FAU, LTL etc.)
	High silica (Si/Al = 5-500, MFI, BEA etc).
	All silica, Si/Al = ∞, e.g. Si-MFI (Silicalite-1), Si-MEL (Silicalite-2), Si-TON, Si-MTW, Si-ZSM-48, Si-NCL-1, Si-UTD-1, etc.

1.2 METALLOSILICATES :

Well characterized metallosilicates may be classified as follows :

(b) Metallosilicates
- $\underline{M}^{3+}$; B^{3+}, Al^{3+}, Cr^{3+}, Fe^{3+}, Ga^{3+} and As^{3+}.
- $\underline{M}^{4+}$; Si^{4+} (Silicalites), Ti^{4+}, V^{4+}, $Ge^{4+}$and Zr^{4+}.
- $\underline{M}^{5+}$; As^{5+}.

While the incorporation of M^{3+} and M^{4+} ions in a regular tetrahedrally coordinated silicate network are known to give anionic and neutral frameworks, respectively, the incorporation of M^{5+} (like V^{5+} or As^{5+}) is expected to lead a cationic framework. However, a cationic zeolite framework with anion-exchange properties is not known yet.

However, with the substitution of various trivalent hetero elements e.g. B^{3+}, Fe^{3+}, Ga^{3+} [16-18] in the silicate matrix in the framework positions, these molecular sieves are termed as borosilicates (B-Si), ferrisilicates (Fe-Si), gallosilicates (Ga-Si) and so on. These boro-, galo- and ferri-silicates show different acidic and catalytic properties than their corresponding aluminosilicate zeolites because of the inherent chemical nature associated with the heteroelements. The extent of incorporation is also dependent on these inherent factors like ionic size, stability in tetrahedral environment, etc.

In the incorporation of tetravalent cations, like Ge^{4+}, Ti^{4+}, etc., a neutral framework as that of the pure silica polymorph of zeolites is obtained[19-21]. The discovery of titanium silicate molecular sieve, TS-1[20,21] (titanium silicate analog of ZSM-5) has given a philip to heterogeneous oxidation catalysis in liquid phase. TS-1 has shown remarkable catalytic activity in numerous oxidation reactions including alkane oxidation[22], alkene epoxidation[23], aromatic hydroxylation[24] ammoximation of carbonyls[25] (in presence of liquid ammonia), selective oxidation of primary and secondary amines[26], sulphoxidation of organic sulfides[27], etc. using dilute aqueous hydrogen peroxide as oxidant. Similarly, titanium silicate-2, TS-2[28] (titanium silicate analogue of ZSM-11) was synthesized and quite expectedly shows almost similar catalytic properties as that exhibited by TS-1. Then the trend continues with more emphasis on the synthesis of new titanium silicates and their use in other organic transformations. As an outcome of these efforts till date Ti-ZSM-48[29], titanium aluminum beta[30,31] (Ti-Al-β, partial titanium substitution in BEA structure), Ti-MCM-41[32], Ti-MCM-48[33], etc. have been prepared, promising bright future for titanium silicates in synthesis of organic fine chemicals[34-36].

1.3 ORGANIC ADDITIVES IN ZEOLITE SYNTHESIS : BACKGROUND AND RECENT DEVELOPMENTS :

Ever since the discovery of the role of organic amines and quaternary ammonium ions as a structure directing agent by Barrer[2] in early 1960 and more importantly of high silica molecular sieves such as ZSM-5[12,37] and its aluminum free analog, Silicalite-1[37], a tremendous activity is going on till date to synthesize new structures using new organic templates. As an outcome of these efforts till today around 130 zeolites have been reported. With the synthesis of Silicalite-1[17], it was realized that aluminum is not an essential component in the formation of microporous structures. Apart from the basic requirements of gel composition, pH, temperature, time and aging, the organic templates directs the crystalline phase and its rate of crystallization. Generally, mono and bi quaternary ammonium compounds or amines are used as templates. Although, the exact mechanism of templating effect is still not fully understood, it is visualized that the zeolite structure grows around the templates, thus stabilizing certain porous structures or subunits. In the presence of these template organic species, the crystallization of various structures can be directed. Conversely, one structure can be directed by different templates[6,38]. These templates or structure directing agents find tremendous utility in synthesizing various zeolite structures specially high silica molecular sieves.

Recently, Szostak[6,38] has compiled various amines and quaternary ammonium salts along with corresponding zeolite structures. In Table 1.2 a list of diquaternary ammonium cations along with the corresponding zeolite structure formed is given. Various high silica medium and large pore structures are formed by varying either the number of methylene group [-$(CH_2)_x$-] or the side chain attached to both the nitrogens[45-52].

Table 1.2 : Various diquaternary ammonium salts in zeolite synthesis :

Entry	Diquaternary ammonium salts $(R)_3\overset{+}{N}-(CH_2)_x-\overset{+}{N}(R)_3$	R	x	Zeolite	Reference
1.	Trimethylene bis (trimethyl ammonium bromide)	$-CH_3$	3	ZSM-39 EU-1	39 40
2.	Tetramethylene bis (trimethyl ammonium bromide)	$-CH_3$	4	EU-1	39
3.	Pentamethylene bis (trimethyl ammonium bromide)	$-CH_3$	5	EU-1	41
4.	Hexamethylene bis (trimethyl ammonium bromide)	$-CH_3$	6	ZSM-48 EU-1	42 43
5.	Heptamethylene bis (trimethyl ammonium bromide)	$-CH_3$	7	ZSM-23 MCM-10	44 45
6.	Octamethylene bis (trimethyl ammonium bromide)	$-CH_3$	8	ZSM-23	44
7.	Nonamethylene bis (trimethyl ammonium bromide	$-CH_3$	9	EU-2	42
8.	Decamethylene bis (trimethyl ammonium bromide)	$-CH_3$	10	NU-87	39
9.	Tetramethylene bis (ethyl dimethyl ammonium bromide)	$-C_2H_5$, $-(CH_3)_2$	4	ZSM-12	46
10.	Hexamethylene bis (ethyl dimethyl ammonium bromide)	$-C_2H_5$, $(-CH_3)_2$	6	ZSM-12	46
11.	Hexamethylene bis (tripropyl ammonium bromide)	$-C_3H_7$,	6	ZSM-5	47
12.	Pentamethylene bis (tributyl ammonium bromide)	$-C_4H_9$	5	ZSM-5	47
13.	Hexamethylene bis (triethyl ammonium bromide)	$-C_2H_5$	6	ZSM-57	41
14.	Hexamethylene bis (triethyl ammonium bromide).	$-C_2H_5$	6	NCL-1	48, 49

1.4 SYNTHESIS OF ZEOLITES AND THEIR METALLOSILICATE ANALOGS :

1.4.1 Alumino-Silicates :

Conventional synthesis procedure designed for aluminosilicate involves the hydrothermal crystallization of basic alkali metal alumino-silicate gel (at elevated temperature) under autogeneous pressure[50]. In the presence of fluoride as mineralizing agent, a method has been developed where crystallization takes place in neutral to acidic medium[51]. Various factors influencing the zeolite crystallization are:

(i) Molar composition of the hydrogel :

The molar chemical composition of a synthesis hydrogel is expressed in terms of oxide formula of the following form :

$$a\ SiO_2 : Al_2O_3 : b\ M_xO :\ c\ R : d\ H_2O$$

in which M and R stand for alkali metal ion(s) and organic template, respectively. The a, b, c and d values (i.e. SiO_2 / Al_2O_3, SiO_2 / M_xO, SiO_2 / R, SiO_2 / H_2O molar ratio) can influence the nucleation and crystallization kinetics affecting the nature of the crystalline material, the lattice Al content, crystal size and morphology[52-54].

(ii) Alkalinity :

The pH of the alkaline synthesis solution, which is generally between 9 to 12, is of vital importance in zeolite crystallization as the OH^- concentration fulfills the crucial role of mineralizing (mobilizing) of Si and Al oxides / hydroxides, and thus forming soluble and useful precursor species having T atoms in tetrahedral coordination and contain condensable ligands[55]. In this way a supersaturation state is created which makes nucleation and crystal growth possible.

(iii) Temperature and time :

With the increase in temperature, both nucleation and crystal growth rate increase upto certain limit of the stability of the particular phase. The thermodynamically least stable phase will crystallize fast, and will be successively replaced by more stable phases with time[56]. A typical example is the crystallization sequence : amorphous ⟶ Faujasite ⟶ Na P.

(iv) Template (organic structure directing agent) :

These are basically organic amines and mono and di- quaternary ammonium salts which contribute to the formation of zeolite lattice during the crystallization process (i) by influencing the gelation and / or nucleation process, where the TO_4 units are supposed to be clathrated in a particular geometry around themselves, these basic template molecules provide the precursor species for further nucleation and crystal growth[57], and probably (ii) by lowering the chemical potential of the lattice formed upon inclusion of templates during zeolite synthesis. The relative hydrophobicity of the hydrocarbon part of the template may direct the water structure of clathrated silica polyanionic units in ring formation and structure direction[57,58].

(v) Charged molecules (alkali metal cations) :

Inorganic cations such as Na^+, K^+, Li^+, Ca^{2+}, Mg^{2+} also influence the rate of crystallization and the structure of zeolite formed from the hydrogel. These cations in aqueous solution can influence the ordering of water molecules through its structure making and structure breaking ability. These organized water molecules surrounding the cations can be (partially) replaced by silicate and aluminate tetrahedra and this way contributes the formation of cage-like structure[58].

(vi) Neutral molecules :

Next to its templating effect by interaction with cations, as discussed above, water has its solvating and hydrolyzing ability which are of key importance in zeolite

synthesis. It enhances the formation of zeolitic structure by filling the micro pore system (as guest molecule) and thereby stabilizing the porous lattices.

(vii) Seeding :

Seeding is a technique in which the supersaturated system is inoculated with small particles of material to be crystallized. These seed crystals are supposed to readily provide nuclii which grow in size as crystalline material is deposited on them. As through this operation the nucleation stage is in fact by-passed, and significant reduction in the induction period can be achieved.

Broadly, zeolite crystallization follows three basic steps. In the first supersaturation stage, the polymeric silicate species present in the hydrogel first depolymerize into monomeric Q^0, and branched Q^1, Q^2, Q^3 and Q^4 silicate species[59,60]. These silicate species (Q^0- Q^4) oligomerize or condense with soluble aluminate anions to form aluminosilicate species in the solution phase itself. After the supersaturation stage is reached, the aluminosilicate species condense to form Q^1 (1 Al), Q^2 (1 Al), Q^2 (2 Al), Q^3 (3 Al), (or oligomers of Q^4 species in case of pure silicate solution) cyclic hexamer and tetramer precursor species[61] at the nucleation stage which in turn condense to form the cages and channel structure, and thus zeolite crystals grows.

However, this supersaturation, nucleation and crystallization stages vary largely form one structure to another. Thus full crystallization process takes few hours to several weeks for various zeolites even at the optimized recipes of that particular structure. Further, this long crystallization process, as Inui[62] has delineated, casues (i) extensive labor coupled with delays and expenses, (ii) low reproducibility and (iii) formation of larger crystals with inhomogeneous particle size distribution mainly because of secondary crystallization.

1.4.2 Metallosilicates :

The synthesis of other metallosilicates can be achieved by direct synthesis through addition of metal ions in gel[63-65] (with proper precaution to avoid precipitation of the corresponding metal hydroxide /oxide during addition) as well as post synthesis methods[66,67]. Liquid phase post synthesis incorporation of Fe, Si and Ti into various zeolite framework structures has been reported using ammonium salts of the corresponding metal hexafluorides ((NH_4MF_6))[67,68]. In the vapor phase method the zeolite is first dealuminated by acid treatment or hydrothermal treatment to form silanol nests. These nests are then heated with the vapor of a volatile compound of metal to be replaced[69]. Complete replacement of aluminum is not possible by these methods. However, the addition of metal ions in the gel (absolutely free from aluminum) leads to the synthesis of aluminum free analogue of zeolites. Although the literature covers the synthesis of various metallosilicates (Al, B, Be, Ga, Ge, Cr, Fe, Zr, Sn, Ti, V, Mn, etc.), only a few metallosilicate (viz. Al, Ti, V, Fe and Ga) have been studied and characterized in detail.

Metal ions may occupy one or more or all of the following locations in the solid after subsequent hydrothermal crystallization :

* Lattice framework position either in regular corner-sharing or edge-sharing tetrahedral (Si-O-Al-O-Si) form.
* Surface defect sites (Si-O-M or Si-O-$\overset{O}{\overset{\|}{M}}$-).
* Cation exchange sites.
* Finely dispersed oxide clusters inside / outside the pores.
* Bulk oxides on the external surface.

Formation of a good metallosilicate gel is necessary to achieve successful incorporation of metal ions in the zeolite framework, during crystallization by direct hydrothermal synthesis. Since the final metallosilicate gel is generally basic (pH ≅ 10-

13) in nature, the solubility of metal oxide / hydroxide in that medium guides the mode of incorporation. Based on the solubility of the oxide / hydroxide of the metal ions in basic medium the metal ions can be divided into two classes :

(i) Metal ions forming soluble oxide in basic medium (viz. B, Al, V, Ga, As etc.), where the dissolution of metal oxide, if formed, helps in the formation of metallosilicate species, a prerequisite for the metal ion incorporation in the zeolite network.

(ii) Metal ion forming insoluble / sparingly soluble metal oxides (viz. Ti, Cr, Fe, Zr etc.) in basic medium, where such metal ions are expected to from precipitate of metal oxide / hydroxide, thereby hindering the formation of metallosilicate gel and the incorporation of metal ions in zeolite network. Hence, the choice of reagent and the sequence of addition is very important in these cases and the formation of metal oxide / hydroxide can be prevented by a careful and calculated addition of reactants. For example, in the case of titanium silicates this is achieved by first hydrolyzing the tetra ethyl orthosilicate with alkaline template (which is absolutely free from alkali and alkaline earth metal cations) followed by the addition of titanium alkoxide taken in isopropyl alcohol[21] or complexing agent acetyl acetone[65]. In the case of ferrisilicates, this is achieved either by careful addition of basic silicate solution to the acidified Fe^{3+} salt solution or by using oxalate as complexing agent for Fe[63,64].

1.5 PHYSICO-CHEMICAL CHARACTERIZATION :

For characterization of zeolite and related molecular sieves, several instrumental and chemical techniques are required[70]. Powder X-ray diffraction (PXRD) is the single most powerful tool used in the study of these materials. It is used in the qualitative identification of the crystalline phase (by finger printing), in the calculation of unit cell

parameters and to find out the degree of crystallinity of the sample. A phase is assumed to be pure when the x-ray pattern matches exactly with that of the reported one[6,38] and some or all peak positions are differing with those of the reported structures in case of a new structure. For phase identification by X-ray diffraction (PXRD), generally the 2θ range in between 4^0 and 40^0 is preferred, since within this range most intense peaks characteristics of zeolite structure occur. Lattice spacing d can be calculated from the measured reflection 2θ by the Brag's equation $n\lambda = 2d \sin\theta$, (where λ is the wave length of CuK_α). Lattice parameters as well as unit cell volume can be calculated depending upon the symmetry of the structure.

Infrared (IR) spectroscopy is an important tool, complementary to XRD, as it is a sensitive analytical technique for the investigation of structural details of the zeolite framework vibrations. The lattice vibrations of zeolites in the IR spectrum are observed in the range 300 - 1300 cm^{-1}. These vibrations can be classified into two groups, (I) internal vibrations of TO_4 units or structure insensitive vibrations : which appear for (i) asymmetric stretching in the range of 1250 - 950 cm^{-1}, (ii) symmetric stretching at 720 - 650 cm^{-1} and (iii) for T-O bond at 420 - 500 cm^{-1}; and (II) vibrations due to external linkages of the TO_4 units or structure sensitive vibrations[71,72] which appear for (i) asymmetric stretching in the range 1050 - 1150 cm^{-1}, (ii) symmetric stretching at 750 - 820 cm^{-1}, (iii) double ring at 500 - 650 cm^{-1} and pore openings at 300 - 420 cm^{-1}. Crystallization of zeolites during synthesis can be studied by monitoring the changes in important vibrational frequencies and their comparison with those of the fully crystalline sample[73].

Apart from structural characterization FTIR spectroscopy is also generally used to characterize the acidic properties of zeolites. Strength of Brönsted acid sites affects hydroxyl absorption band (3600 - 3700 cm^{-1}). Both Brönsted and Lewis acidity are characterized using probe molecules such as ammonia, pyridine, CO_2 etc[74]. The

substitution of lighter elements such as B (vis-à-vis Si) shifts the framework vibrations to higher wave number[75], whereas the incorporation of heavier elements such as Fe, Ga etc. shifts them towards lower wave number[76]. In the case of titanium and vanadium silicates an additional stretching vibration attributed to Si-O-M (M = Ti, V, etc.) linkages[77,78] at around 960 is reported.

Molecular absorption spectroscopy in ultraviolet-visible region of spectra is widely used to determine metals, cationic species, anionic species and complex ions in either solid or liquid state. This spectroscopic technique is used to determine specific coordination state of metal ions substituted in the silicate matrix. As the coordination number of the metal ion decreases the charge transfer band shifts to lower wave length.

NMR spectroscopy is also an important tool to rationalize the understanding of the structure of zeolites at the molecular level and to characterize the local environment of framework metal ions. Ever since Lippmaa et al[79]. showed that ^{29}Si MAS (Magic Angle Spinning) NMR spectra are sensitive to the nature and chemical environment of the atoms, considerable knowledge has been gained during last few years about the structures of zeolites from the study of their ^{29}Si and ^{27}Al MAS NMR spectra[80,81]. It has been shown that the position of ^{29}Si NMR resonance is not only dependent on the number of tetrahedral (T) atoms in the first cationic sphere of Si but also the actual geometry of the T-O-T linkages[82]. Through variable angle spinning NMR spectra of ^{27}Al, octahedral and tetrahedral[83-85] coordination can be distinguished. Liquid state ^{29}Si NMR has also been used to understand the intriguing problem of zeolite crystallization process[86] identifying various building units from silicate and alumino-silicate species in the hydrogel.

EPR spectroscopy is the resonance absorption of the electromagnetic (microwave) radiation by magnetically split states of unpaired electrons. The unpaired

electron undergoes a transition to the excited state by the absorption of microwave energy when it is matched by the splitting caused by the field. The splitting of the magnetic levels can give information regarding the symmetry around the metal (M^{n+}) ion. This technique has been applied to know the isomorphous substitution of metal ions particularly Fe^{3+} and V^{4+}, in zeolite framework ($g \approx 4.3$ corresponds to rhombically distorted Fe which is incorporated in the molecular sieve lattice[87]), even in a dilute system. EPR of vanadium containing zeolites is used extensively as a proof for atomically dispersed vanadium[88] which gives rise to a hyperfine spectrum split into eight (8) component peaks ($I = 7/2$, $S = 2nI + 1$ states).

By virtue of zeolitic properties such as (i) three dimensional lattice with uniform pores and internal channels of molecular dimensions, (ii) a high surface area accessible to molecules of comparable size to diffuse through the pores and (iii) remarkable thermal stability, they are suitable as selective sorbents and catalysts. The molecular sieving properties of zeolites are uniquely determined by their pore dimensions and characterized by their equilibrium sorption capacities for various sorbed molecules. The void volume of porous zeolite solids are often determined by low temperature (77 K) nitrogen sorption. Analysis of such sorption isotherms have been found to be useful in determining the micropore volume and pore size distribution of composite materials containing molecular sieves[89]. Olson et al[90]. observed that the ion-exchange capacity, catalytic activity and hydrophobicity are linearly dependent on the aluminum / heteroelement content in the framework. Thus aluminum / heteroelement content affects the diffusion and adsorption processes, which in turn controls the overall rate of the catalytic chemical transformations.

Thermoanalytical technique has been used[91,92] over the years to get the information on the thermal behavior of the synthesized zeolite. The thermal stability of zeolites and related molecular sieves is an important parameter for their application as

selective sorbent and potential catalyst. The nature of high temperature exotherm is often used in characterizing the thermal stability[92,93] of zeolites. Similarly the shape and splitting of low temperature endotherm[94] helps to identify the location and desorption of the water molecules[95].

Ion exchange properties of the zeolites and related molecular sieves is one of the most important parameter which determine their potential as catalyst and as ion-exchanger in water softening and detergents[96]. It is an indirect way of the determination of framework trivalent (Al^{3+}, B^{3+}, Fe^{3+}, Ga^{3+} etc.) element. Since only framework M^{3+} generate cation exchange property, the molar ratio of Na / M^{3+} or K / M^{3+} determined by chemical analysis, indicates the extent of M^{3+} ions in the framework in a semiquantitative way.

1.6 CATALYSIS :

Catalysis over zeolites and related molecular sieves has shown enormous expansion over the years[97,98]. Not only a multiplicity of new reactions has been explored over various zeolite structures, but also the depth of understanding of both catalytic chemistry and structure-reactivity relationships has shown considerable growth. The origin of activity, shape selectivity as well as various organic transformations using these silica based molecular sieves are briefly discussed below :

1.6.1 Origin of reactivity :

A pure silicalite network is neutral. When Si is replaced by trivalent ions like Al, B, Fe, Ga etc., it leads to anionic framework which is balanced by monovalent cations. When these charge compensating cations are replaced by protons through ammonium ion-exchange followed by calcination at ~ 773 K, the M-(OH)-Si (where M = Al, B, Fe, Ga etc. shown as species II, scheme 1.1) moieties are generated, which are equal to the number of Brönsted acid sites. The strength of these acid sites is found

to vary with (i) zeolite structure, (ii) Si / M molar ratio and (iii) the nature of isomorphously substituted metal ions in the zeolite framework. The Lewis acid sites arise at the defect sites where trigonal Al is present either in the framework or at charge compensating sites[99]. Dehydroxylation of Brönsted acid sites [Si-(OH)-Al] can also generate Lewis acidity at very high temperature (>500 ^{0}C). Sometime the extraframework Al^{3+} ions are associated with higher cracking activities, those active sites are called "superacid sites"[100].

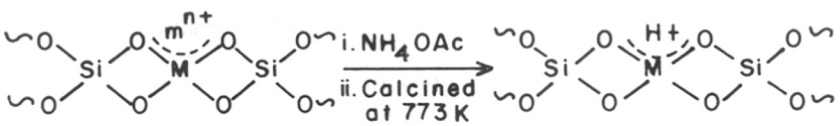

I II

Scheme 1·1

Bronsted basic sites in zeolites are not known. Zeolites may contain Lewis basicity. Alkali and alkaline earth metal ion-exchanged zeolites show Lewis basicity. The number of potential basic sites is equal to the number of alkali / alkaline earth metal ions[101]. Acidity and / or basicity can be determined through many techniques like spectroscopic: IR, UV-VIS, NMR, ESR, XPS etc., calorimetric[101], chromatographic, titration and test reaction methods.

When tetravalent metal ions like Ti^{4+}, V^{4+}, Zr^{4+} etc. are incorporated in the silicate network, the resulting metallo-silicates are neutral in nature. The origin of activity in these metallo-silicates with redox properties under liquid phase reaction conditions in the presence of hydrogen peroxide is believed to be due to the stability of the corresponding metal-peroxo species[102] (IV and V, scheme 1.2). For example, the Ti-peroxo moieties are shown below.

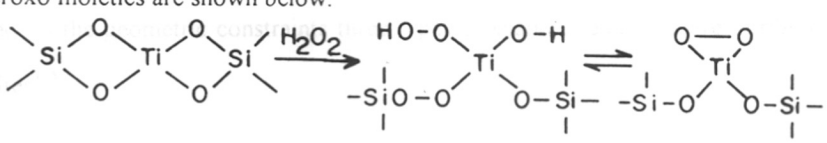

III IV V

Scheme 1·2

1.6.2 Structural / Geometrical phenomenona in catalysis over molecular sieves :

Zeolites and related molecular sieves represent a rich diversity of pore architecture and morphology of their crystallites[103]. Small pore zeolites e.g. Linde A, ZSM-39, etc. having 8-membered ring channels typically sorb linear molecules such as n-parafins or primary alcohols but not branched isomers. Medium pore zeolites e.g. ZSM-5, ZSM-48, EU-1 etc. consisting of 10-membered rings with uniform channel dimensions facilitate the transport of medium sized n- and isoparaffins as well as primary and secondary alcohols. Whereas large pore zeolites like Y, ZSM-12, Beta, having 12 or more membered rings can allow somewhat bulkier organic substrates to transport through channels.

Transport processes, occurring when the reactant arrives near the surface of zeolite crystallite, have profound effect on chemical reaction as well as observed selectivities. Following events must occur during transport[104] :

1. Transfer of reactant molecules to the external surface of the zeolite crystallites.
2. Entry of the reactant into zeolite pore channel system and diffuse to an active site.
3. Adsorption of the reactant at the active site.
4. Chemical reaction of adsorbed reactant to form adsorbed product(s).
5. Desorption of the adsorbed product(s).
6. Diffusion of products from interior active site to the outer surface of the crystallites.
7. Transfer of product(s) away from the zeolite surface.

1.6.3 Shape selectivity :

Shape selectivity is an unique property of zeolites & related molecular sieves. Based on the geometric constraints three types of shape selectivities are attributed to zeolites[105].

* *Reactant selectivity* :

When in a mixture of two or more organic molecules with different size and shape come in contact with zeolite, smaller molecules are allowed to diffuse in the channels while the other larger molecules are hindered (or sieved out), this phenomenon is called reactant shape selectivity. This type of selectivity is used in cracking of linear alkanes by protecting the branched chain ones particularly in petrochemical industry.

* *Product selectivity* :

This is a consequence of the products that are formed within the zeolitic pores or cavities and diffuse faster, leaving behind bulkier molecules which are either converted into less bulky molecules that can diffuse out easily or subsequently deactivate the catalyst.

* *Restricted transition state selectivity* :

This type of selectivity depends upon the size and shape of the transition state complex required vis-à-vis to the void space available in the cavities of the zeolite. The products which result from less bulky transition states are preferentially formed.

However, apart from these geometric factors effecting regiosleceivity, Corma[106], based on the Pearson's concept of hard and soft acid and bases and Perturbation theory, has interpreted the role of chemical nature in directing the selectivities in zeolites. Additionally the hydrophobic / hydrophilic nature of reactants vis-à-vis zeolites may also influences the observed selectivities.

However, almost all the selectivity patterns studied over zeolites are concerned with regio-selectivity only. Other type of selectivities like chemo-selectivity, stereo-selectivity, etc. are rarely addressed over zeolite catalysts. Now, when zeolite and related molecular sieves are being increasingly used in fine chemical

transformations such issues like chemo-selectivity, stereo-selectivity etc. have to be addressed. In this dissertation some initial steps are being taken to study the chemo-selective (selective transformation at one functional group only when two or more functional groups are present in the reactant molecule) behavior of TS-1 in oxidation reaction.

1.6.4 Catalytic reactions :

The application of FAU and MFI type materials has revolutionized the petroleum refining, petrochemical and fine chemical processing[107,108]. A variety of exciting chemical transformations with remarkable contribution of shape selective oxidations came through titanium silicate[20] molecular sieves using dilute hydrogen peroxide under liquid phase[22-30,36,108]. Basically three types of reactions are reported over zeolite based molecular sieve catalysts :

1.6.4.1 Brönsted and Lewis Acid catalyzed reactions :

Zeolites are traditionally used as Brönsted acid catalysts in a variety of organic transformations like alkylation, isomerization, cracking, aromatization, rearrangement and condensation reactions. Venuto[108] has recently reviewed such applications. Electrophilic aromatic substitution catalyzed by large and medium pore zeolites include alkylation (and dialkylation), acylation (and Fries rearrangement), benzoylation, nitration, sulphonation and halogenation using wide range of alkylating agents[109-110]. These reactions are illustrated in Fig. 1.1.

1.6.4.2 Lewis Base Catalyzed Reactions :

Alkali metal exchanged zeolites (viz., Na, K or Cs-FAU, K-L) are also used in Lewis Base catalyzed transformations, like selective halogenation of aromatics[111,112], side chain alkylation[109], etc.

1.6.4.3 Redox reactions :

However, with the incorporation of transition metal ions (Ti, V, Cr, Fe, etc.) with redox behavior in zeolitic network, an increasing attention is being paid to

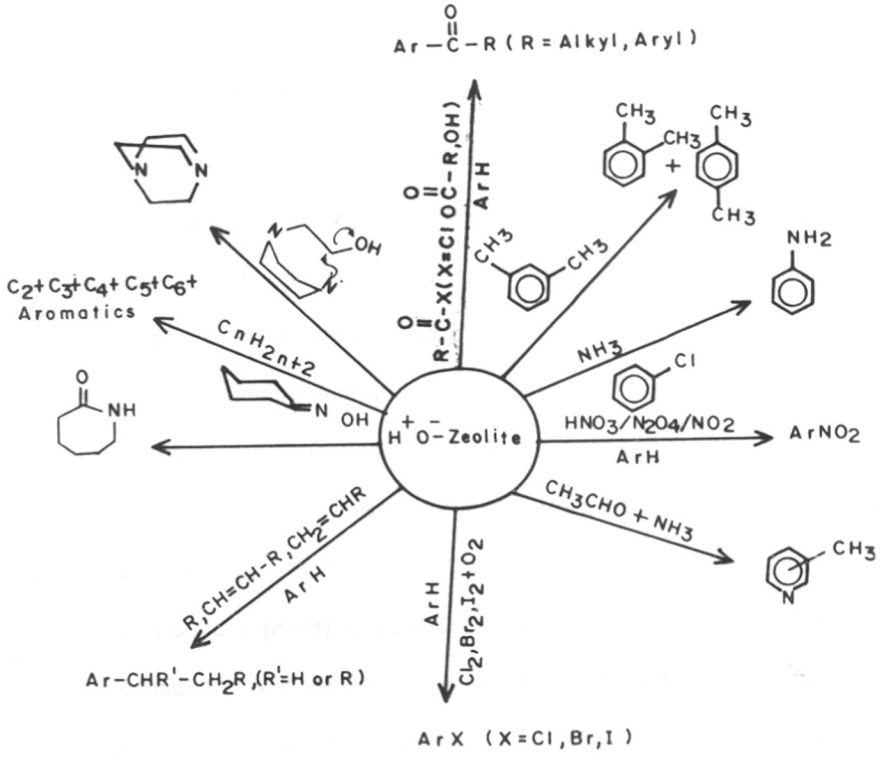

Fig. I.1 : Broad Spectrum of acid Catalyzed reactions Over Zeolites.

oxidation reactions[113]. Ammoxidation of aldehydes with ammonia and oxygen to form nitrile, ammoximation of carbonyls to corresponding oxime, oxyfunctionalization of various aliphatic C-H, N-H and S-H bonds, hydroxylation of aromatics, epoxidations of olefins, aromatic amines to azo and nitroso compounds are the common examples of redox reactions carried out over Ti-silicate molecular sieves using dilute H_2O_2 as oxidizing agent as shown in Fig. 1.2.

In the oxidation reactions using TS-1 / H_2O_2 system, a co-solvent (like acetone, acetonitrile, methanol etc.) is added to homogenize the organic and aqueous layers. However, the use of solvent not only influences the activity and the product selectivities, but also poses the problem of tedious work-up. Further, the use of eco-hazardous solvent is highly undesirable. Use of a cosolvent is quite common in such liquid phase organic transformations where the substrate and the reagents are not freely miscible so that phase barriers disappear leading to a contact between substrates and reagents. Alternatively, a phase transfer catalyst[114] (either in homogeneous state or anchored with solid support) is used to overcome this problem. Hence, concerted efforts were made to avoid the use of organic solvent in chemical transformations using TS-1 / H_2O_2 system. These efforts have resulted in the development of a new methodology (described in chapter 5 and 6 of the present disertation) using TS-1, under heterogeneous three phase (solid-organic-aqueous) conditions, which can avoid the use of organic cosolvent in chemical transformations of hydrophobic organic substrates in the presence of aqueous reagents.

Both in gas phase fixed bed and liquid phase batch reactions over zeolites and related materials, products obtained at various interval of times are usually analyzed and identified by gas chromatography (GC) and mass spectroscopy (GCMS). In gas chromatography when a sample is injected, injecter vaporizes it and vapors pass through the column by carrier gas. Different components of the sample are sorbed on

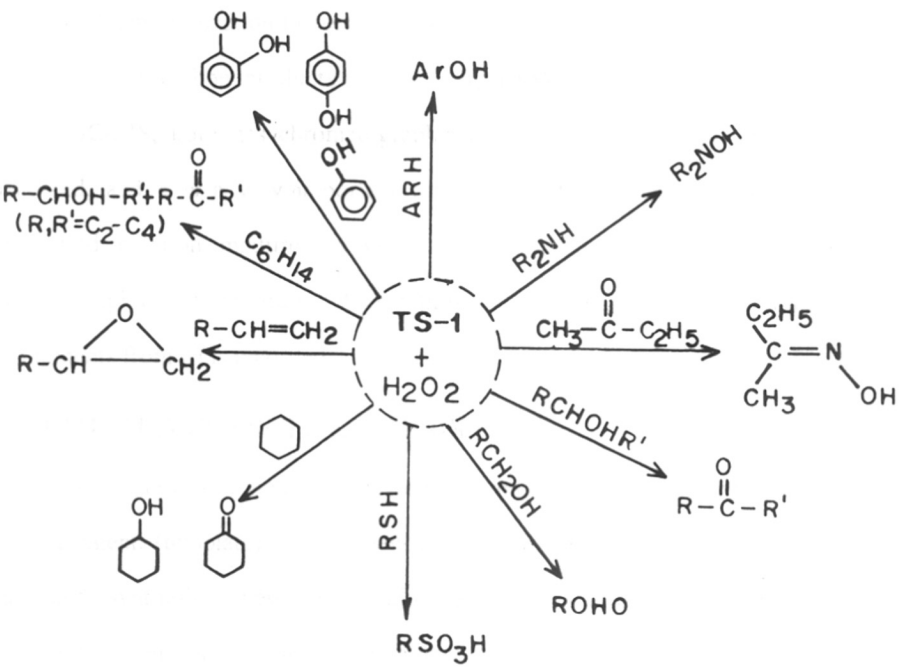

Fig. 1.2 : A broad Spectrum of Selective Oxidation over TS-1.

the stationary phase residing in the column of GC and are separated depending upon their distribution coefficient, affinities and / or boiling points. These separated components are then desorbed by the carrier gas and enter into a suitable detector which analyzes them and the chromatographs are recorded on the chart paper. Commonly Flame Ionization Detector (FID) is used for most of the hydrocarbon, and substituted hydrocarbon products. In chemical derivatization of organic compounds through GC-MS, both gas chromatographic and mass spectroscopic properties are considered, and it is a very important tool in identifying several components in a complicated reaction mixture. In GC-MS, mass of various components of the chromatograph in the mixture together with their fragmentation pattern (i.e. masses of the fragments from it) is recorded.

1.7 OBJECTIVES OF THE THESIS :

Use of various mono and di-quaternary ammonium cations as organic structure directing agent (template) in the synthesis of different zeolite structures is well established. Synthesis of new organic additives provides an opportunity to study their uses in zeolite synthesis. In this context a new diquaternary ammonium salt is prepared and used for the first time in zeolite synthesis. Interestingly, varying its concentration in the hydrogel different zeolite structures namely ZSM-12, ZSM-39 and ZSM-48 are synthesized.

Similarly, isomorphous substitution of various elements in zeolite network to prepare new materials and study of their catalytic properties is an interesting objective and understanding in this field is growing very fast in the recent years. In this context incorporation of arsenic (both As^{3+} and As^{5+}) in the zeolite network is studied. Interestingly, low temperature and very fast synthesis of these arsenosilicates (faster than that of pure silicalites) is a new phenomenon in zeolite synthesis.

Although, the nature of surface and catalytic properties of zeolites and related molecular sieves are relatively better understood, the chemistry governing their hydrothermal synthesis continues to be intriguing and challenging. Various parameters for their hydrothermal synthesis contributes to the understanding of zeolitization in specific ways only. Inui[62] has listed the problems encountered due to very long crystallization times needed for zeolite crystallization. In this context a general method of using *'promoters'* (viz. chlorate, phosphate, nitrate, sulfate, carbonate, arsenate, chlorate etc.) for highly efficient and fast synthesis (five fold or more time saving) of zeolites and related materials compared to those obtained by conventional method has been developed which opens up a new arena in zeolite synthesis. High resolution liquid state NMR spectroscopy, a very important tool in the understanding of zeolitization at the molecular level was used to understand the role of promoters.

Chemoselective oxidation of organic compounds containing more than one functionizable group is an important objective in synthetic organic chemistry. Titanium silicates are used for the fulfillment of this purpose in the present study for the first time. Conventional process of liquid phase oxidation of organics over solid catalyst suffers from the serious drawbacks of use and disposal of hazardous organic solvents and complicated work-up process. Under this circumstances a novel and versatile method is developed in the oxidation of hydrophobic organic compounds. The problem of solvent disposal and work-up is largely overcome by carring out the organic transformations under solvent-free triphase (solid catalyst with organic reactant and aqueous H_2O_2 in absence of any cosolvent) conditions. Not only increase in activity and reversal of selectivity, present method offers a distinct utility by facilitating new routes of organic transformations which are not possible in presence of cosolvents in an eco-friendly way.

1.8 OUTLINE OF THE THESIS :

Chapter I : This Chapter provides general introduction to zeolite chemistry, its developments over the years, main features of synthesis, characterization and selective catalysis and finally the scope of the thesis.

Chapter II : This chapter consists of two parts:

Part A : Synthesis of a new diquaternary ammonium salt, 1,6-hexamethylene bis[benzyl dimethyl ammonium bromide / hydroxide], and its use in the synthesis of MTW, MTN and ZSM-48 zeolites.

Part B : Synthesis of New Materials : In this section, synthesis procedures for metallosilicates (As^{3+}, Ti^{4+}, V^{4+}/V^{5+}, As^{5+} etc.) of ZSM-5, ZSM-11, ZSM-12 and ZSM-48 are described. Incorporation of various heteroelements are investigated by varying the mode of addition of the constituents, changing the synthesis temperature, aging, pH of the synthesis gel, changing the alkali and template concentrations and water content of the medium. Low temperature synthesis of new arsenosilicates (both As^{3+} and As^{5+}) are described. The details of characterization of the above mentioned metallosilicates by spectroscopic (XRD, FT IR, ^{1}H, ^{13}C, ^{29}Si, ^{31}P NMR, SEM/EDX, ESCA, XPS, thermal TG/DTA), ion-exchange and surface area measurements are given. New arsenosilicates (As^{3+}, As^{5+} etc.) were characterized by XRD unit cell volume expansion, shift in framework IR frequencies, XPS, SEM, K^{+}/M exchange capacities etc. The activity of the catalysts were evaluated by n-hexane cracking / aromatization and oxidation reactions.

Chapter III : This chapter deals with the use of a new concept of addition of various promoters in the zeolite crystallization. Enhancement of the crystallization rate of zeolite and related molecular sieves are reviewed by using various oxyanions. Relative role of these promoters, crystallinity, yield, incorporation of heteroelements in the

silicate matrix, morphology of the crystal (particle size and its distribution), ion-exchange and catalytic properties of the zeolites synthesized in presence of these promoters are analyzed. Role of promoters during the course of the synthesis was monitored through the change in nature of soluble silicate species (Q^0-Q^4) using sensitivity enhanced liquid state ^{29}Si NMR experiments.

Chapter IV : This chapter consists of two parts:

Part A : Chemoselective oxidation / epoxidation of organic molecules containing two or more functional groups has been studied over TS-1 molecular sieves using dilute H_2O_2 as oxidant. Electronic and steric effect of the substituent groups on chemoselectivity were studied in detail using organic solvents under biphase conditions.

Part B : Ammoximation of different carbonyl compounds with dilute H_2O_2 and liquid / gaseous NH_3 over MFI type titanium silicate, TS-1, was studied. Electronic and steric effects of the substituent groups along with temperature, solvent and mechanistic aspects of ammoximation have been studied.

Chapter V : In this chapter the use of TS-1 in oxidation catalysis under *triphase condition* (solid catalyst along with two immiscible liquid phases) is described for the first time. Significant enhancement in activity and para selectivity was observed in the hydroxylation / oxidation of various hydrophobic organic compounds (viz. benzene, chlorobenzene, toluene, anisole, benzyl alcohol, cyclohexanol etc.) over crystalline, microporous, titanium silicate, TS-1, using dilute H_2O_2 under triphase system compared to that obtained under commonly used biphase (solid catalyst and immiscible liquid reactants in presence of an organic cosolvent to homogenize the liquid layers).

Chapter VI : In this chapter some novel oxidation reactions are studied under solvent-free conditions over TS-1 using dilute H_2O_2 as oxidant. In addition to new

routes in solvent-free conditions which does not follow in the presence of solvents, present method offers a distinct advantage in easier work up, economy and the development of eco-safer technology / process. Reactions studied are :

a) Oxidation of aliphatic, allylic and aromatic halides.

b) Oxidation (mainly Baeyer-Villiger oxidation) of cyclic and aromatic ketones.

c) Oxidation / hydroxylation of aromatic esters.

Chapter VII : The outcome of the work reported in chapters II to VI is summarized in this chapter. The salient features are as follows:

1) First report of arsenosilicate molecular sieves (As in both, III and V oxidation state).

2) Synthesis of the above mentioned materials at lower temperature and at much reduced crystallization time compared to their silicalite and aluminosilicate analogues.

3) Development of new concept of using promoters (oxyanions of group IV, V, VI and VIIA) in zeolite synthesis with tremendous enhancement in crystallization rate, relatively better yield, crystallinity, morphology and metastability of the solid material in the mother liquor.

4) Application of triphase catalysis over high silica zeolite TS-1 for the first time - with much better reactivity and paraselectivity over conventional biphase one.

5) Solvent-less chemistry, one of the most enchanting objective in the present day chemical research, over high silica zeolite catalyst leading to some new oxidative transformations, is discussed.

1.9 REFERENCES :

1. Barrer, R.M., "*Hydrothermal Chemistry of Zeolites*" Academic Press, New York, (1982).
2. Barrer, R.M., *J.Chem.Soc.*, 971 (1961).
3. Breck, D.W., "Zeolite Molecular Sieves", Wiley, New York (1974)
4. Chen, N.Y., Kaeding, W.W. & Dwyer, F.G., *J.Am.Chem.Soc.*, **101**, 6783 (1979).
5. Liebau, F., *Zeolites*, **3**, 191 (1983).
6. Szostak, R., "*Molecular Sieves : Principles of Synthesis and Identifications*", Van Nostrand Reinhold, New York (1989).
7. Rees, LV.C., *Nature*, **296**, 491 (1992).
8. McBain, J.W., "*The Sorption of Gases and Vapours by Solids*", Ritledge and Sons, London, Ch-1 (1932).
9. Schultz,P.G, *Angew.Chem.Int.Ed.Engl.*, **28**, 1283 (1989).
10. Davis, M.E., *Acc.Chem.Res.*, **26**, 111 (1993).
11. Schlenker, J.L., Dwyer, F.G., Jenkins, E.E., Rohrbaugh, W.J. & Kokotaile, G.T., *Nature,* **294**, 341 (1981).
12. Flanigen, E.M., Kokotailo, G.T., Lowton, S.L. & Olson, D.H., *Nature,* **272**, 437 (1978).
13. LaPierre, R.B., Rohrman Jr, A.C., Schlenker, J.L., Wood, J.D., Rubin, M.K. & Rohrbaugh, W.J., *Zeolites,* **5**, 347 (1985).
14. Treacy, M.M.J. & Newsam, J.M., *Nature,* **332**, 249 (1988).
15. Freyhardt, C.C., Tsapatsis, M., Lobo, R.F., Balkus Jr, K.J. & Davis, M.E., *Nature,* **381**, 295 (1996).
16. Snamprogetti, *U.S.Pat.* 2023562 (1974).
17. Meyers, B.L., Ely, S.R., Kutz, N.A., Kudak, J.A. & Van den Bossche, E., *J.Catal.,* **91**, 352 (1985).
18. McNicol, B.D. & Pott, G.T., *J.Catal.*, **25**, 223 (1972).
19. Gabelica, Z. & Guth, J.L., *Stud.Surf.Sci.Catal.*, **49 A**, 421 (1994).
20. Taramaso, M., Perego, G. & Notari, B., *U.S.Pat.*, 4410501 (1983).
21. Thangaraj. A., Kumar, R., Mirajkar, S.P. & Ratnasamy, P., *J.Catal.*, **130**, 1, (1990).
22. Tatsumi, T., Nakamura, M., Negishi, S. & Tominaga, H., *J.Chem.Soc.Chem.Commun.* 476 (1990).
23. Huybrechts, D.R.C., DeBruyker, L. & Jacobs, P.A., *Nature*, **345**, 240 (1990).
24. Thangaraj. A., Kumar, R. & Ratnasamy, P., *Appl.Catal.*, **57**, L1, (1990).
25. Thangaraj, A., Sivasanker, S. & Ratnasamy. P., *J.Catal.*, **131**, 394 (1991).
26. Reddy, J.S. & Jacobs, P.A., *J.Chem.Soc.Parkin Trans. I*, 2665 (1993).

27. Reddy, R., Reddy, J.S., Kumar, R. & Kumar, P., J.Chem.Soc.Chem.Commun., 84 (1992).

28. Ramasawamy, A.V., Sivasanker, S. & Ratnasamy, P., *Catal.Lett.*, **22**, 236 (1993).

29. Kumar, P., Kumar, R. & Panday, B., *SYNLETT.*, 295 (1995).

30. Camblor, M.A., Corma, A. & Perez-Pariente, J., *J.Chem.Soc.Chem. Commun.*, 589 (1992).

31. Blasco, T, Camblor, M.A., Corma, A. & Perez-Pariente, J., *J.Am.Chem.Soc.*, **115**, 11806 (1993).

32. Tanev, P.T., Chibwe, M. & Pinnavaia, J., *Nature*, **368**, 321 (1994).

33. Tatsumi, T, *J.Chem.Soc.Chem.Commun.*, 156 (1996)

34. Sato,T., Dakka, J. & Sheldon, R.A., *Stud.Surf.Sci.Catal.*, **84C**, 1853 (1994).

35. Bellussi, G., Carati, A., Clerici, M.G., Maddinelli, G. & Millini, R., *J.Catal.*, **133**, 220 (1992).

36. Ratnasamy, P. & Kumar, R., *Stud.Surf.Sci.Catal.*, **95**, 240 (1995).

37. Flanigen, E.M., Bennet, J.M., Grosse, R.W., Patton, R.L., Kirchner, R.M. & Smith, J.V., *Nature*, **271**, 512 (1978).

38. Szostak, R., "Handbook of Molecular Sieves", Van nostrand Reinhold New york (1992).

39. Casci, J.L., *Stud.Surf.Sci.Catal.*, **28**, 215 (1986).

40. Valyocsik, E.W., *U.S Pat.*, 4 585 789 (1986).

41. Whittam, T.V., *E.Pat.*, Appl. 54 363 (1982).

42. Rollmann, L.D. & Valyocsik, E.W., *E.Pat.*, Appl. 15 132 (1980).

43. Casci, J.L., Lowe, B.M. & Whittam, T.V., U.K.Pat., Appl. 2 077 709 (1982).

44. Valyocsik, E.W., *U.S Pat.* 4 481 177 (1884).

45. *U.S. Pat.* 4 623 527 (1987).

46. Szostak, R., *U.S. Pat.* 4 585 639 (1986).

47. *E.Pat.* 1 74 121 (1986).

48. Kumar R., Reddy, K.R., & Ratnasmay, P., *U.S. Pat.* 5 219 813 (1993).

49. Reddy, K.R., Kumar, R., Ramaswamy, V., & Ramaswamy, A.V., *Zeolites,* 14, 326 (1994).

50. Behrens, P.,Stucky, G.D., *Angew.Chem.Int.Ed.Engl.*, **105**, 729 (1993).

51. Guth, J.L., Kessler, H., Higel, J.M., Lamberlin, J.M., Paterin, J., Sieve, A., Chezeau, J.M., & Wey. R., A.C.S.Symp.Ser., **398**, Washington D.C., pg176 (1989).

52. Barrer, R.M. & Sieber, W., *J.Chem.Soc.Dult.Trans.*, 1020 (1977).

53. Dwyer, J., Karim, K., Smith, W.J., Thompson, N.E., Harris, R.K. & Apperley, D.C., *J.Phys.Chem.*, **95**, 8826 (1991).

54. Feijen, E.J.P., Martens, J.A. & Jecobs, P.A., *Stud.Surf.Sci.Catal.*, **84A**, 3 (1994).

55. Guth, J.L., Caullet, P., Seive, A., Patarin, J. & Delprato, F., "*Guidlines for Mastering the Properties of Molecular Sieves*", Eds. Barthomeuf et al., Plenum Press, New York, p.69,

(1990)

56. Lok, B.M., Cannan, T.R. & Massina, C.A., *Zeolites*, **3**, 282 (1983).

57. Barrer, R.M., *Zeolites*, **1**, 130 (1981).

58. Davis, M.E., Stud.Surf.Sci.Catal., **97**, 35 (1995).

59. Engelhardt, G. & Michel, D., "*High-Resolution Solid-State NMR of Silicates and Zeolites*", Ch3, pp75, Wiley, New York (1987).

60. McCorimick, A.V., & Bell, A., *Catal.Rev.-Sci.Eng.*, 31 (**1&2**) 97 (1989).

61. Thangaraj, A. & Kumar, R., *Zeolites*, **10**, 117 (1991).

62. Inui, T., *Synthetic Zeolites*, A.C.S. Symp. Ser., 398, Washington D.C., p.421 (1989).

63. Ratnasamy, P. & Kumar, R., *Catalysis Today*, **9**, 329 (1990).

64. Ratnasamy, P. & Kumar, R., *Catal.Lett.*, **22**, 227 (1993).

65. Kumar, R., Raj, A., Kumar, S.B. & Ratnasamy, P., *Stud.Surf.Sci.Catal.*, **84A**, 109 (1994).

66. Skeels, G.W., & Flanigen, E.M., A.C.S. Symp.Ser. 398, Washington D.C., p 420 (1989).

67. Carati, A., Contarini, S., Millini, R. & Bellussi, G., *Pro.Mat.Res.,Soc.*, Extended Abstract, EA 24 (1990).

68. Reddy, J.S. & Sayari, A., *J.Chem.Soc.Chem.Commun.*, 23 (1995).

69. Reddy, J.S. & Sayari, A., *Stud.Surf.Sci.Catal.*, **94**, 309 (1995).

70. Van Hoff., J.H.C. & Roelofsen, J.W., *Stud.Surf.Sci.Catal.*, **58**, 242 (1991).

71. Flanigen, E.M., Khatami, H. & Szymanski, H.A., A.C.S.Symp.Ser. 101, Washington D.C., p.201, (1971).

72. Flanigen, E.M., A.C.S.Symp.Ser. 171, Washington D.C., p.80, (1976).

73. Whyte, Jr T.E. & Dulla Betta, R.A., *Catal.Rev.Sci.Eng.*, **24** (4) 567 (1982).

74. Boccuti, M.R., Rao, K.M., Zecchina, A., Leofanti, G. & Petrini, G., *Stud.Surf.Sci.Catal.*, **48** 133 (1989).

75. Ward, J.W., A.C.S.Symp.Ser. 171, Washington D.C., (1976).

76. Kutz, N.A., "*Heterogeneous Catalysis - II*", (Ed. Shapiro, B.L., et al.,) p.121 (1984).

77. Szostak, R. & Thomas, T.L., *J.Catal.*, **101**, 549 (1986).

78. Notari, B., *Stud.Surf.Sci.Catal.*, **37**, 413 (1988).

79. Lippamaa, E., Magi, M., Samoson, P. & Engelhardt, G., *J.Am.Chem.Soc.*, **103**, 4992 (1981).

80. Fyfe, C.A., Thomas, J.M., Klinowski, J. & Gobbi, G.C., *Angew.Chem.Int.Ed.Engl.*, **95**, 257 (1983).

81. Nagy, J.B., Gabelica, Z. & Derouane, E.G.,*Chem.Lett.*, **7**, 1105 (1982).

82. Cavell, R.A., Masters, A.F. & Wilshier, K.G., *Zeolites*, **2**, 244 (1982).

83. Derouane, E.G., Nugy, J.B., Gabelica, Z. & Blom, N., *Zeolites*, **2**, 299 (1982).

84. Luan, Z., Cheng, C.F., Zhou, W. & Klinowski, J., *J.Phys.Chem.*, **99**, 1018 (1995).

85. Anderson, M.W., Terasaki, O., Ohsuna, T., Philliou, A., Mackay, S.P., Ferreira, A., Rochca, J. & Lidin, S., *Nature*, **367**, 347 (1994).

86. Kinrade, S.D. & Swaddle, T.W., *Inorg.Chem.*, **27**, 4253 (1988).

87. Barthomeuf, D., *J.Phys.Chem.*, **88**, 42 (1984).

88. Rao, P.R.H.P., Ramaswamy, A.V. & Ratnasamy, P., *J.Catal.*, (1992).

89. Hong-Xim, L., Martenes, J.A. & Jacobs, P.A., "*Innovation in zeolite materials science*", (Ed., Grobet, P.J.), 75 (1987).

90. Olson, D.H., Haag, W.O. & Lago, R.M., *J.Catal.*, **61**, 390 (1980).

91. Derouane, E.G., Detremmeria, S., Gabelica, Z. & Blom, N., *Appl.Catal.*, **1**, 201 (1981).

92. Barrer, R.M. & Langley, D.V., *J.Chem.Soc.*, 1817, 3804 & 3811 (1958).

93. Nakamato, H. & Takahashi, H., *Chemistry Letters*, 1013 (1981).

94. Gal, I.G., Tankocic, O., Malcis, S., Raovanov, P. & Tadorovic, M., *J.Chem.Soc.Far.Trans.*, **67**, 999 (1971).

95. Bremer, H., Morke, W., Schodel, R. & Vogt, F., *Adv.Chem.Ser.*, **121**, 249 (1973).

96. Roland, E., *Stud.Surf.Sci.Catal.*, **46**, 645 (1989).

97. Ono, Y., *Stud.Surf.Sci.Catal.*, **5**, 19 (1980).

98. Van Bekkum, H. & Kouwenhoven, H. W., *Stud.Surf.Sci.Catal.*, **41**, 45 (1988).

99. Barthomeuf, D., *Stud.Surf.Sci.Catal.*, **37**, 157 (1992).

100. Mirodatos, C. & Barthomeuf, D., *J.Chem.Soc.Chem.Commun.*, 39 (1981).

101. Hathaway, I.E. & Davis, M.E., *J.Catal.*, **116**, 263 (1989).

102. Bellussi, G. & Fattore, V., *Stud.Surf.Sci.Catal.*, **69**, 79 (1991).

103. Haag, W.O. & Chen, N.Y., (Ed. Hegedus, L.L.), *Catalysis Design-Process & Prospectives*, John Wiley & Sons, New York, NY, Ch 6, (1987).

104. Smith, J.M., *Chemical Engineering Kinetics,* McGraw-Hill, New York, NY, 2nd Ed.,p.274 (1974).

105. Csicsery, S.M., *Zeolites*, **4**, 220 (1984).

106. Corma, A., "*Guidelines to Mastering the Properties of Molecular Sieves", NATO Ser., 221 : Physics B*, (Eds., Barthomeuf, D. et al.) Plenum Press, New York, p.299 (1990).

107. Chen, N.Y., Garwood, W.E. & Duyer, F.G., "*Shape Selective Catalysis in Industrial Application*", Marcel Dekker, New York, NY, Basel, p.1-303 (1989).

108. Venuto, P.B., *Microporous Materials*, **2**, 294 (1994).

109. Smith, K., & Bahzad, D., *J.Chem.Soc.Chem.Commun.*, 469 (1996).

110. Smith, K., Butters, M., & Nay, B., *Synthesis,* 1157 (1995).

111. Smith, K., Musson, A. & DeBoss, G.A., *J.Catal.*, 469 (1996).

112. Ratnasamy, P., Singh, A.P. & Sharma, S., *Appl.Catal.* A : General, **135**, 25 (1995).

113. Sheldon, R.A., *Stud.Surf.Sci.Catal.*, **66**, 573 (1991).

114. Dehmlow, E.V., *Angew.Chem.Int.Ed.Engl.*, **13**, 170 (1974).

CHAPTER 2

NEW MOLECULAR SIEVES : SYNTHESIS, CHARACTERIZATION AND CATALYTIC PROPERTIES

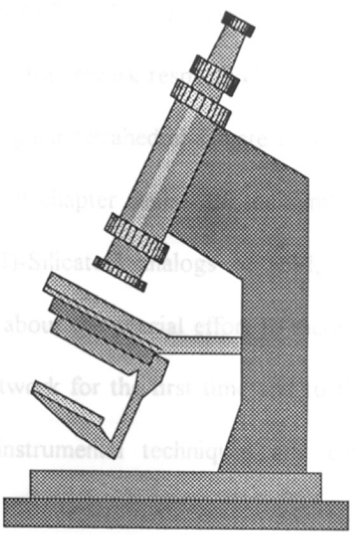

2.1 INTRODUCTION :

Ever since the discovery of the templating role of organic amines and quaternary ammonium cations in the synthesis of high silica zeolites[1], research activities in the area of synthesis and use of various templates have developed tremendously over the past years with the outcome of a large number of new high silica synthetic zeolites. Similarly, the use of diquaternary ammonium salts has also resulted in a variety of interesting high silica zeolite structures[2-5]. The effect of the substituent hydrocarbon group in the diquaternary ammonium skeleton in guiding various zeolite topologies are of special interest[6-8]. Here, the synthesis of a new organic diquaternary template and its use in the synthesis of MTW, MTN, and ZSM-48-type structures are described in detail.

Isomorphous substitution in zeolites has been the object of intensive investigation over a decade[9-11]. While, the incorporation of tri-(Al^{3+}, Fe^{3+}, Ga^{3+})[12,13] and tetravalent metal ions (Ti^{4+}, V^{4+}, Ge^{4+} etc.)[14-17] in zeolitic tetrahedral network leads to anionic and neutral framework respectively, the successful incorporation of a pentavelent element in a regular tetrahedral silicate framework is expected to lead to an cationic network. Present chapter deals with the synthesis and characterization of new arsenosilicate [As(III)-Silicates] analogs of MFI, MEL, MTW and ZSM-48 topology. Further, details about the special effort to incorporate pentavelent element like As^{5+} in the silicate network for the first time and to find out its environments in silicate matrix through instrumental techniques and catalytic test reactions are discussed.

2.2 EXPERIMENTAL :

2.2.1 Materials :

Materials used for the synthesis of metallosilicate analogs of ZSM-5, ZSM-11, ZSM-12 and ZSM-48 are tabulated in Table 2.1, below.

Table 2.1 : Chemicals used in synthesizing various metallosilicates:

Structures	Silica Source	Template	Metal Salt
ZSM-5 (MFI)	Fumed Silica, Sigma, USA. Tetraethyl othosilicate, Aldrich (TEOS), USA.	Tetra propyl ammonium hydroxide, (20 % aqueous) Aldrich, USA.	As_2O_3 Na_2HAsO_4, 10 H_2O, Loba Chemie India.
ZSM-11 (MEL)	TEOS	Tetra butyl ammonium hydroxide, 26% in Methanol	-do-
ZSM-12 (MTW)	TEOS Fumed silica, Sigma, USA.	1,6-Hexamethylene bis [benzyl dimethyl ammonium hydroxide], 15 % aqueous[18]	$Al_2(SO_4)_3$, 16 H_2O, Loba. Tetrabutyl orthotitanate, Aldrich, Vanadyl Sulfate, Aldrich
ZSM-48	Fumed silica	-do-	-do-

2.2.2 Methods :

2.2.2.1 Synthesis :

2.2.2.1.1 Synthesis and use of new template :

Generally, the diquates used in the zeolite synthesis were having same alkyl groups attached to the nitrogen atoms. Here, the synthesis and use of a new diquaternary ammonium cation, where both the quaternary nitrogen are attached with two methyl and one benzyl groups, is given below :

1,6- Hexamethylene bis [benzyl dimethyl ammonium bromide / hydroxide] :-

In a typical synthesis of the title compound, 48.8 g (0.2 mole) of 1,6-dibromo hexane was reacted with 59.4 g (0.44 mole) of benzyl dimethyl amine in 80 g acetone at 333 K under reflux for 6 h. The white solid thus obtained was dried and purified under vacuum. The material was characterized by chemical analysis (experimental: 56.2 % C, 7.4 % H, 5.4 % N and 31.0 % Br; theoratical: 56.0 % C, 7.5 % H, 5.4 % N, 31.1 % Br), mass spectrometry [molecular ion peaks assinged to m/e: 354 (M^+-2Br), 219 (354-$PhCH_2N(CH_3)_2$) , 160, 135 and 91], and ^1H and ^{13}C nuclear magnetic resonance (NMR). Fig. 2.1 shows the ^1H NMR spectra (in D_2O, δ = 4.8 PPM). The chemical shifts δ 1.45-1.6 (2N-CH_2-CH_2-$C\underline{H}_2$, 4H), 1.9-2.0 (2N-CH_2-$C\underline{H}_2$,- 4H), 3.1-3.2 (4N-$C\underline{H}_3$, 12H), 3.3-3.4 (2N-$C\underline{H}_2$-, 4H), 4.5-4.6 (2N-$C\underline{H}_2$Ph, 4H) and 7.5-7.6 (2N-CH_2-$C_6\underline{H}_5$, 10H). Thus ^1H NMR data clearly suggested that the resulting sample is 1,6-hexamethylene bis (benzyl dimethyl ammonium bromide) given by the structural formula :

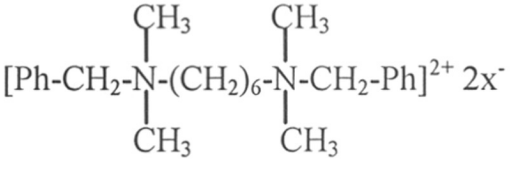

(Where x = Br or OH ; Ph = phenyl)

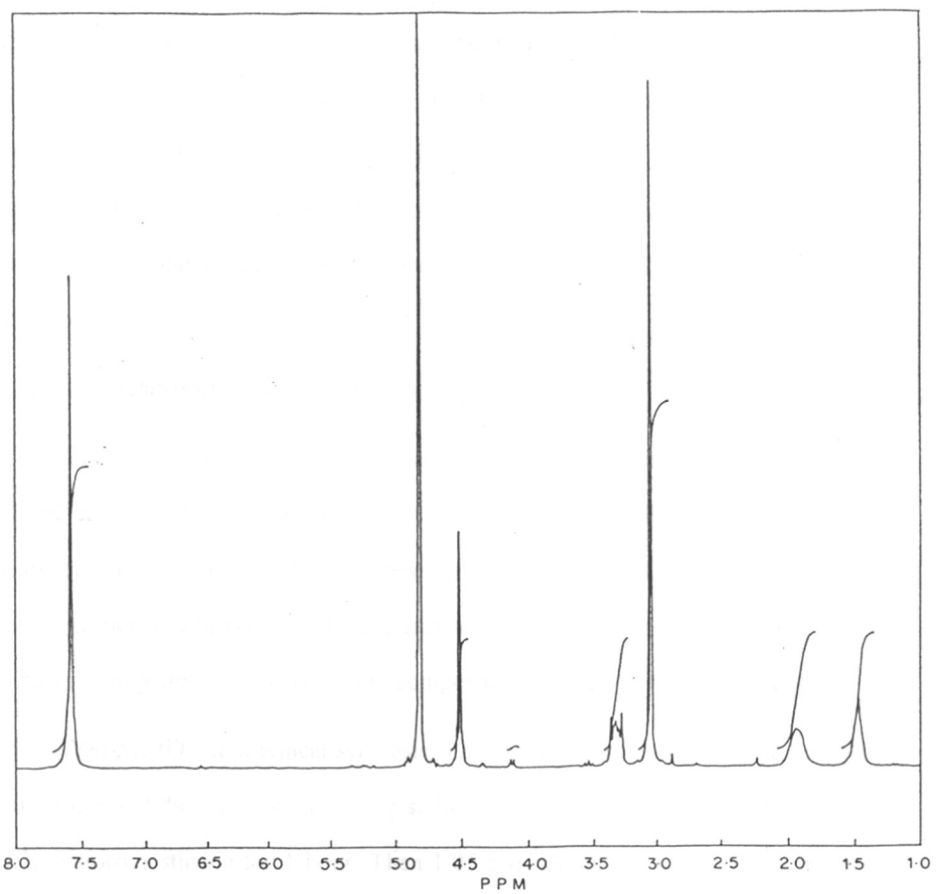

Fig. 2.1 **^{1}H NMR Spectrum of 1,6-hexamethylene bis(benzyl dimethyl ammonium bromide) in D_2O.**

The bromide salt thus obtained was converted into the corresponding hydroxide solution (15 % aqueous) electrochemically using a two compartment cell separated with an anion-exchange membrane (typically Br selective membrane). The electrochemical reaction was carried out at 298 K by taking a 30 wt % aqueous solution of the bromide salt as catholite and 10 wt % aqueous solution of ammonium hydroxide as anolite, and by passing a direct current (DC) till complete conversion of bromide to hydroxide (conversion % was determined by removing aliquots at different reaction hours and titrating it with standard silver nitrate solution using ferric alum indicator).

2.2.2.1.2 Synthesis of Zeolites using new DIQ-6 :

All the hydrothermal syntheses were carried out in stainless steel autoclaves of 150 ml capacity. Autoclaves were thoroughly cleaned with HF before use to remove seeds/impurities of previous batch. Interestingly, three zeolite structures, namely ZSM-12 (large pore), ZSM-48 (medium pore) and ZSM-39 (small pore) were obtained using this template, by varying the gel compositions (Si/Al, Si/Na or Si/DIQ-6).

ZSM-12(Al-MTW) : In a typical synthesis, 12 g of fumed silica was slurried with 51.8 g of DIQ-6 (15 % aqueous) and 0.8 g sodium hydroxide taken in 25 g distilled water under vigorous stirring for 1 hour. Then 1.05 g of aluminum sulfate taken in 38 g of water was added into it and the stirring was continued for another one hour. The crystallization was carried out in a stainless steel autoclave of 250 ml capacity at 433 $\pm$ 1 K under static condition for 6 days. After the crystallization, the solid product was filtered, thoroughly washed with distilled water, dried at 373 K and calcined in flowing air at 823 K for 16 hours. Gel composition in terms of moles of oxides was :

$$SiO_2 : x\ Al_2O_3 : 0.1\ DIQ\text{-}6 : 0.1\ NaOH : 30\ H_2O.$$

where x = 0.00833, 0.00625 and 0.0025 corresponding to SiO_2 / Al_2O_3 molar ratios 120 and 160 and 400 respectively.

When the Si/Na and Si/DIQ-6 mole ratios were varied, ZSM-48 and ZSM-39 zeolites were obtained. In Table 2.2, the gel composition, pH, crystallization time and temperature along with the corresponding product obtained are given.

The as-synthesized samples (C/N form) of ZSM-12, ZSM-48 and ZSM-39 were calcined at 823 K for 16 h in flowing air and were subjected to ammonium exchange treatment. 5 g of the zeolite sample was slurried in 50 ml of 1 M ammonium acetate solution. pH of this solution was maintained at around 7.0 to 8.0 by adding few drops of 25 % aqueous solution of ammonium hydroxide solution. The mixture was stirred at 353 K for 4 h and the procedure was repeated twice to ensure complete exchange. The ammonium form of zeolite (NH_4^+ exchanged) thus obtained was then calcined at 773 K (to remove NH_3) to get the proton form of the corresponding zeolite (i.e. H-Zeolite).

2.2.2.1.3 Synthesis of MTW type Ti- and V-Silicates :

Ti-MTW : Titanium silicate analog of ZSM-12 was synthesized according to the modified procedure described by Thangaraj et al[17]. for titanium silicate analog of ZSM-5 (TS-1). In a typical synthesis, 84 g of tetraethyl orthosilicate were hydrolyzed with 103.5 g of DIQ-6 with vigorous stirring for 2 h. Then 2.3 g of tetrabutyl orthotitanate (TBOT) taken in 10 g of isopropyl alcohol was slowly added into the resulting clear liquid with constant stirring. The stirring was continued for another 1 hour, 92 g water was added and the final clear liquid was charged into stainless steel Parr (USA) autoclave (300 ml) at 433 K with stirring rate of 200 rpm. The pH of the hydrogel before and after crystallization was 11.8 and 12.3 respectively. After 5 days the resulting milky solution was centrifuged. Solid obtained was washed thoroughly with distilled water and dried at 373 K. The material thus obtained was calcined at 823 K for 16 hours in flowing air. Gel composition in terms of moles of oxides was :

$$60\ SiO_2 : TiO_2 : 6.0\ DIQ\text{-}6 : 1500\ H_2O.$$

Table 2.2 : Effect of gel composition on the formation of various zeolite :

Molar gel composition $SiO_2 : Al_2O_3 : DIQ\text{-}6 : NaOH : H_2O$	pH	Time, d	Product
1 : 0.00333 : 0.08 : 0.10 : 30	11.2	5.0	ZSM-12
1 : 0.00333 : 0.10 : 0.10 : 30	11.4	5.0	ZSM-12
1 : 0.00833 : 0.10 : 0.10 : 30	11.0	6.5	ZSM-12
1 : 0.00833 : 0.10 : 0.07 : 30	10.8	9.0	ZSM-12
1 : 0.00833 : 0.10 : 0.04 : 30	10.6	9.0	Amorphous
1 : 0.01111 : 0.10 : 0.10 : 30	10.9	4.0	Amorphous
1 : 0.01111 : 0.10 : 0.15 : 30	11.4	4.0	b + ZSM-12
1 : 0.00833 : 0.10 : 0.15 : 30	11.5	4.0	b
1 : 0.0111 : 0.13 : 0.15 : 35	12.1	5.0	ZSM-48
1 : 0.00833 : 0.12 : 0.15 : 35	12.2	4.5	ZSM-48
1 : 0.00625 : 0.12 : 0.1 : 35	12.4	4.5	ZSM-48
1 : 0.00833 : 0.15 : 0.16 : 35	12.6	4.0	ZSM-48 + ZSM-39
1 : 0.0250 : 0.17 : 0.10 : 30	11.7	4.5	ZSM-39
1 : 0.01111 : 0.17 : 0.05 : 30	11.5	4.0	ZSM-39
1 : 0.00833 : 0.17 : 0.05 : 30	11.6	4.0	ZSM-39

a: Crystallization temperature for ZSM-12 was 433 K whereas that for ZSM-48 and ZSM-39 was 443 K, all under static condition.

b: Crystobalite

V-ZSM-12[18] *(VS-12*[19]*)* : In a typical hydrothermal synthesis of vanadium silicate analog of ZSM-12 (with MTW topology[26]), 6 g of highly reactive fumed silica was slurried in 25.8 g of DIQ-6 under vigorous stirring for 1 hour before adding to it a solution of 0.36 g of vanadyl sulfate [$V(O)SO_4$, 3 H_2O] in 10 g of distilled water. Finally an alkaline solution containing 0.4 g of sodium hydroxide in 10 g of water was added into it. The resultant mixture was stirred for about 1 hour after adding to it the remaining 12 g of water. The pH of the gel before crystallization was 11.2 to 11.4. The crystallization was carried out at 433 $\pm$ 1 K under static condition. After crystallization the solid product was separated (pH of the final hydrogel ranges between 11.7 to 11.8), thoroughly washed with hot water, dried at 393 K and calcined at 843 K (heating rate 2^0 min^{-1}) in flowing air for 18 hours. Gel compositions in terms of moles of oxides were :

$$SiO_2 : x\ VO_2 : 0.1\ DIQ\text{-}6 : 0.1\ NaOH : 30\ H_2O.$$

where x = 0.016, 0.01 and 0.00625 corresponding to Si / V = 60, 100 and 160, respectively.

2.2.2.1.4 Synthesis of new As(III)-silicates[20] :

Although As^{3+} can be incorporated in MFI, MEL, MTW and ZSM-48 structures, the detailed studies were made on As(III)-MFI molecular sieve taken as representative. This is mainly, to avoid extensive handling of these potentially toxic materials.

As(III)-MFI (As-ZSM-5) was synthesized by first hydrolyzing 21 g of TEOS with 33.8 g TPAOH solution with constant stirring for 1 h at room temperature. Then 0.99 g of As_2O_3 dissolved in 0.4 g of sodium hydroxide solution in 10 g of distilled water was added into the mixture very slowly under vigorous stirring. The stirring was continued for another 1 h. Then remaining 17 g water was added to the mixture, stirred for 0.5 h

and finally the mixture was transferred into autoclave (below 373 K polypropylene air tight bottles were used) in the temperature range 358 K to 433 K for 6 hours to 3 days. Crystallization time at various temperature and at various SiO_2 / As_2O_3 ratios are given in Table 2.3, pH of the final gel ranged from 11.5 to 12.5 depending upon the As content in the hydrogel. The gel composition of the starting reaction mixture in terms of moles of oxides were :

$$SiO_2 : x\ As_2O_3 : 0.33\ TPAOH : 0.1\ NaOH : 30\ H_2O.$$

where x = 0.05 (A), 0.025 (B), 0.0125 (C) and 0.00 (Silicalite-1).

Gel composition of various As(III)-silicates analogs along with crystallization time and temperature are given in Table 2.4.

2.2.2.1.5 As(V)-Silicates of MFI, MEL, MTW and ZSM-48 topology :

Although As^{5+} can be incorporated in MFI, MEL, MTW and ZSM-48 structures, the detailed studies were made on As(V)-MFI molecular sieve taken as representative.

As(V)-MFI[21] : In a typical synthesis, 21 g tetraethyl orthosilicate was hydrolyzed with 33.8 g of TPAOH solution under vigorous stirring for 1 hour. Then an aqueous solution of disodium hydrogen arsenate (1.56 g Na_2HAsO_4, 7 H_2O in 10 g water) was added very slowly into it with vigorous stirring. The clear liquid thus obtained was stirred for another 1 hour and then remaining 17 g water was added into it. The pH of the final clear liquid ranged between 11.0 to 12.5 depending upon the As content of the hydrogel. Then the solution was put into polypropylene bottle and heated in the temperature range 333 K to 363 K. After complete crystallization, the product was centrifuged, washed thoroughly with distilled water, dried at 373 K and calcined at

Table 2.3 : Physico-chemical properties of As(III)-MFI :

Sample	Si/As molar ratio		Ion-exchange capacity,	Cryst. time, h[b]	BET surface	Unit cell volume
	gel	product	K / As		area, m^2g^{-1}	
As(III)-MFI A	10	17	0.82	24	512	5360
As(III)-MFI B	20	27	0.80	32	499	5354
As(III)-MFI C	40	50	0.83	46	497	5349
Silicalite-1 D	∝	-	-	72	439	5339

a: T = 358 K, static conditions.

b: Calcined, organic free samples A - C were subjected to ion exchange with a 1 mol dm^{-1} solution of KCl at 353 K for 3 hours. This treatment was repeated twice. The samples were then recovered, washed thoroughly and analyzed for K and As.

Table 2.4 : Synthesis of various As(III)-Silicates :

Molar gel composition $SiO_2 : As_2O_3 : ROH^a : NaOH : H_2O$	Silica source	Cryst. temp (K)	Cryst. time	Product
1 : 0.02500 : 0.333 : 0.10 : 30	TEOS	343	72	As(III)-MFI
1 : 0.02500 : 0.333 : 0.10 : 30	TEOS	373	12	As(III)-MEL
1 : 0.01250 : 0.333 : 0.05 : 30	TEOS	373	16	As(III)-MEL
1 : 0.00833 : 0.333 : 0.034 : 30	TEOS	373	18	As(III)-MEL
1 : 0.00000 : 0.333 : 0.050 : 30	TEOS	373	48	Si-MEL
1 : 0.01666 : 0.100 : 0.050 : 30	SiO_2	413	36	As(III)-MTW
1 : 0.01250 : 0.100 : 0.100 : 30	SiO_2	413	36	As(III)-MTW
1 : 0.00000 : 0.100 : 0.100 : 30	SiO_2	413	72	Si-MTW
1 : 0.01250 : 0.150 : 0.054 : 30	SiO_2	393	48	As-ZSM-48
1 : 0.00625 : 0.150 : 0.040 : 30	SiO_2	393	48	As-ZSM-48
1 : 0.00000 : 0.150 : 0.050 : 30	SiO_2	393	96	Si-ZSM-48

a : R = tetrapropyl ammonium for MFI, tetrabutyl ammonium for MEL and 1,6-hexamethylene bis (menzyl dimethyl ammonium) for MTW and ZSM-48 structures.

773 K for 16 hours in flowing air. The yield was 75 to 80 % (on the basis of SiO_2). Four such As(V)-S-1 samples with Si / As input molar ratios 15, 20, 40 and 80 were prepared (samples a, b, c and d, respectively). Corresponding crystallization time and temperature are shown in Table 2.5. The molar gel compositions were :

$$SiO_2 : x\ As_2O_5 : 0.4\ TPAOH : 4x\ NaOH : 30\ H_2O.$$

where x = 0.066 (a), 0.05 (b), 0.025 (c) and 0.0125 (d).

Other As(V)-Silicates were synthesized in an identical way by varying the gel compositions. Table 2.6 depicts the gel composition, crystallization temperature, crystallization time as well as corresponding product.

2.2.2.2 Characterization techniques :

2.2.2.2.1 Chemical Analysis :

A known weight (say 0.5 g) of the zeolite sample was taken in a platinum crucible with lid and ignited for 1 hour. Then the crucible was transferred to a dessicator and cooled. The anhydrous weight of the sample was noted. The solid was then saturated with few drops of concentrated sulfuric acid (96 %) and 10 ml of aqueous (48 %) hydrofluoric acid was added to dissolve it. The solution was then evaporated to dryness and the procedure was repeated twice more to ensure that all SiO_2 is evaporated as H_2SiF_6. The remaining sample was then ignited again and the final weight was taken after cooling it in a dessicator. The difference in weight of the residue and the original weight gave the weight of SiO_2 in the sample. To the solid obtained after cooling, 2-3 drops of HCl was added and then the content was dissolved in a known volume of water. This solution was analyzed separately by Inductively Coupled Plasma emission spectroscopy (ICP, JOBIN YVON 38) and Atomic Absorption Spectroscopy (Hitachi Z-8000) for As, Al, Ti and V.

2.2.2.2.2 Ion-Exchange Capacities :

Ion-exchange capacity measurements were performed by treating 1 g of H-form of the zeolite with 10 g of 1 M solution of KNO_3 (together with few drops of

Table 2.5 : Physico-chemical properties of As(V)-MFI:

Sample	Si / As ratio		Cryst. time[a]	BET surface	Unit cell
	gel	product	(h)	area (m^2g^{-1})	volume (A^{03})
As(V)-MFI-a	15	37	18	488	5352
As(V)-MFI-b	20	44	26	483	5349
As(V)-MFI-c	40	72	36	472	5346
As(V)-MFI-d	80	145	44	460	5342
As(V)-MFI-e[b]	20	84	3	449	5345
Si-MFI	∞	-	72	439	5340

a: Temperature = 358 K, static conditions (under stirring / agitation, crystallization becomes slightly faster).

b: Synthesis temperature = 443 K.

Table 2.6 : Synthesis of various As(V)-Silicates :

Molar gel composition SiO_2 : As_2O_5 : ROH : Na_2O : H_2O	Silica source	Cryst. temp, K	Cryst. time	Product
1 : 0.02500 : 0.333 : 0.050 : 30	TEOS	343	72	As(V)-MFI
1 : 0.02500 : 0.333 : 0.050 : 30	TEOS	373	12	As(V)-MEL
1 : 0.01250 : 0.333 : 0.025 : 30	TEOS	373	16	As(V)-MEL
1 : 0.00833 : 0.333 : 0.017 : 30	TEOS	373	18	As(V)-MEL
1 : 0.00000 : 0.333 : 0.025 : 30	TEOS	373	48	Si-MEL
1 : 0.01666 : 0.100 : 0.050 : 30	SiO_2	413	36	As(V)-MTW
1 : 0.01250 : 0.100 : 0.050 : 30	SiO_2	413	36	As(V)-MTW
1 : 0.00000 : 0.100 : 0.050 : 30	SiO_2	413	72	Si-MTW
1 : 0.01250 : 0.150 : 0.027 : 30	SiO_2	393	48	As(V)-ZSM-48
1 : 0.00625 : 0.150 : 0.020 : 30	SiO_2	393	48	As(V)-ZSM-48
1 : 0.00000 : 0.150 : 0.025 : 30	SiO_2	393	96	Si-ZSM-48

a : R = tetrapropyl ammonium for MFI, tetrabutyl ammonium for MEL and DIQ-6 for MTW and ZSM-48 topologies.

dilute KOH solution to maintain pH at around 8) and then stirring for 4 hours at 373 K, washing thoroughly the product and drying to obtain the K-form of the zeolite. The K-form of the zeolite was analyzed by chemical analysis procedure which gave the ion exchange capacity (K^+ / MO_2^- molar ratio where M = Al, As etc.). By chemical analysis of the K-form of the zeolite K^+ / SiO_2 molar ratio also can be determined.

2.2.2.2.3 Powder X-Ray Diffraction (PXRD) :

The samples at each stage during the study were analyzed by PXRD in Rigaku D MAX III VC diffractometer using Ni filtered Cu K_α radiation (λ = 1.5404 A^0). The integrated area of the PXRD patterns in 2θ range between 18 - 25 ^{0} were used to determine the relative crystallinity during the course and of various metallosilicate analogs of particular zeolite topology. The samples exhibiting maximum area were taken as reference samples. Unit cell calculations were made by indexing the peaks with known h, k and l values, and refining them using PDP11 and HOCT softwares.

2.2.2.2.4 Infrared Spectroscopy (IR) :

The infrared spectra were recorded through a FTIR spectrometer (Parkin Elmer Series 1600) in the range of 450 - 4000 cm^{-1} wavenumbers using nujol mull or KBr technique. 20 mg of the powdered sample was taken, mulled with nujol / KBr to form a homogeneous mixture. This was then kept on KBr plates before recording the spectra.

2.2.2.2.5 Electron Spin Resonance Spectroscopy (ESR) :

ESR spectra of vanadium silicate analog of ZSM-12 (V-MTW) samples were recorded in Bruker ER 200D at 9.7 MHz (x-band) with a rectangular cavity (ST 8424). Frequency modulation was carried out at 9.7 KHz (intensity at GPP) and a time constant of 10^3 msec was used. The spectra were scanned both at room temperature (298 K) and liquid N_2 temperature (78 K). A constant weight of (0.1 g) sample was used to record all the ESR specctra.

2.2.2.2.6 UV-VIS spectroscopy :

UV-VIS spectra were recorded on a Shimadzu UV-VIS scanning spectrometer (UV-2101 PC) using solid sample holder. The baseline correction was made using barium sulphate standard. Ti, V and As substituted silicalite show strong UV-VIS adsorption band at 220-210 nm[22,23]. Whereas TiO_2, V_2O_5, As_2O_3 and As_2O_5 shows adsorption at 330, 380, 300 and 390 nm respectively.

2.2.2.2.7 SEM / EDX studies :

Scanning electron micrographs were obtained by JEOL, JSM 5200, operated at 20 KV. Elemental analysis was performed through electron probe microanalysis on a EDX detector KEVEX 7000 system. SEM coupled with EDX analysis allows to determine Si and other heteroelement distribution among the different crystalline phases. Samples were mounted over the probe and sputtered with thin film of gold before scanning.

***2.2.2.3 Catalysis* :**

Gas phase catlytic test reactions were carried out in a fixed bed downflow quartz reactor with 10 mm i.d.. 1 g of binder free catalyst was loaded in it and the reactant was fed at a rate of 4 ml h^{-1} in presence of carrier gas N_2. Liquid phase reactions were carried out in a two neck batch reactor fitted with water condenser and oil bath to maintain the reaction temperature. Required amount of catalyst, reactants and solvent were taken in the two neck batch reactor and the mixture was stirred vigorously at the required temperature. At various intervals the products were collected and analyzed by gas chromatography (HP 5880 and Shimadzu R17A equipped with capillary column and Flame Ionization Detector), gas chromatography coupled with mass spectrometry (Shimadzu, 14A QP-2000A), infrared spectroscopy, ^1H and ^{13}C NMR spectroscopy. FTIR measurements were carried out on Perkin Elmer Series 1600, FTIR using KBr and Nujol as standard for solid and liquid sample

respectively. ^{1}H and ^{13}C NMR measurements were carried out using Bruker MSL 200 (internal reference as trimethyl selane). $CDCl_3$ and D_2O were used as solvents for ^{1}H NMR of water immiscible and water miscible substances respectively.

2.3 RESULTS AND DISCUSSION :

2.3.1 Synthesis :

2.3.1.1 Synthesis of MTW type Al, Ti and V-silicates :

1, 6-Hexamethylene bis [benzyl dimethyl ammonium bromide / hydroxide] has been found to be an interesting organic structure directing agent giving three structures ZSM-12, ZSM-39 and ZSM-48 by varying its concentration (along with pH) in the hydrogel. In a typical synthesis of large pore ZSM-12, the SiO_2 / template and SiO_2 / Na molar ratios are kept at about 10. Within 10 - 6 value of SiO_2 / template molar ratio, it gives medium pore zeolite ZSM-48 and below 6 small pore ZSM-39 is obtained. In the synthesis of Ti-MTW proper precaution was taken in the synthesis to avoid the precipitation of TiO_2. Template (DIQ-6) thus obtained through electrochemical exchange was made ammonia free by passing hot N_2. Since, VO_2 / V_2O_5 is highly soluble in presence of alkali, such precaution is not necessary in the synthesis of V-MTW samples.

2.3.1.2 Synthesis of As(III)-silicates [As(III)-MFI] :

A remarkable feature of the synthesis of arsenosilicates is the requirement of relatively low hydrothermal crystallization temperature, and these can be crystallized faster than other metal substituted MFI silicates as well as pure silica polymorph (As-free silicalite-1[24]). Interestingly, the crystallization of silicalite-1, compared to all other high silica zeolites, is commonly known to be fastest among all high silica molecular sieves[25,26]. This may be due to greater solubility[27] of As^{3+} under hydrothermal conditions. However, contrary to the common observation that the incorporation of hetero metal / element in the silicate network is a relatively difficult process[25], in the

present case with increasing the As^{3+} content of the gel, a simultaneous decrease (almost proportional) in the crystallization time was observed.

2.3.1.3 Synthesis of As(V)-Silicates [As(V)-MFI] :

In general non-metal based molecular sieves (viz. beryllo / zinco-arsenates[27]) crystallize at much lower temperature (below 373 K), while metallo-silicate molecular sieves (particularly high silica[25,26] ones) requires higher temperature. The difference is attributed to higher solubility of the former under hydrothermal synthesis conditions[27]. These materials can be prepared from the reaction mixtures at much lower temperature and at far shorter synthesis time than that required for synthesizing other metal substituted MFI silicates as well as pure silica polymorph (Silicalite-1). This is probably the first report of the synthesis of high silica zeolites at a temperature as low as 343 K within 66 hours. Further, the crystallization becomes faster with the increase in As(V) content in the gel, i.e., decrease in Si / As molar ratio. These observations are contrary to the common experience of in the synthesis of all other high silica metallosilicates, where the incorporation of hetero-element (vis-à-vis silicate ions) is a relatively difficult process. This may be due to (i) greater solubility of the As(V) under hydrothermal conditions, and (ii) an increased charge / ionic radius ratio of As^{5+} (10.6) compared to that of the Si^{4+} (9.7). Apart from solubility and charge / radius ratio, other factors like, pH, concentration of alkali metal ion, template, dilution, etc. also affect the crystallization of these arsenosilicates. Since, As(V)-oxides are soluble under alkaline hydrothermal conditions, it is unlikely that the crystalline solid will contain occluded As-oxides. The uptake of As(V) from the reaction mixture into the solid material was nearly 50 % (Table 2.5, entries 1-4). The incorporation of As(V) in the crystalline solid decreases drastically further to 20 % only at higher temperature (Table 2.5, entry 5). Higher solubility of As(V) at higher temperature may retard its uptake from the solution.

2.3.2 Characterization :

MTW type Al, Ti, V-Silicates : Fig. 2.2 represents the powder X-ray diffraction pattern of (a) Al-MTW (sample A of Table 2.7), (b) Ti-MTW (sample C, Table 2.7) and (b) V-MTW (sample D, Table 2.7). Three such V-MTW samples (D, E and F with SiO_2 / VO_2 mole ratio 60, 100 and 160, respectively) were synthesized and characterized (Table 2.7). From Table 2.7 it is clear that with an increase in vanadium content of V-MTW samples a parallel increase in unit cell volume occurs.

In Fig. 2.3 framework IR spectra of Ti-MTW (curve a) and Si-MTW (curve b) are shown. A characteristic absorption band at 960 cm^{-1}, same as that observed for TS-1[28,29] and TS-2[30] which is attributed to the tetrahedral Si-O-Ti linkages, is exhibited by Ti-MTW samples. The intensity of this band increases with the increase in Ti content of Ti-MTW. This band is absent in the IR spectra of titanium free ZSM-12[31] (curve b) and TiO_2. In the case of V-MTW also similar band at 965 - 970 cm^{-1} appeared[18,20]. An identical band with band intensity proportional to the content of vanadium was observed in the case of V-ZSM-48[33] also. Probably, this band is due to Si-O-X (where X = heteroelement, Ti, V, As, etc.) stretching vibration, a characteristic of all metallosilicates. Intensity ratio of this band to that of 550 cm^{-1} was (i.e., I_{960} / I_{550}) 0.54 in the case of Ti-MTW.

Fig. 2.4 depicts the diffuse refractance spectra of Ti-MTW sample (Si/Ti = 62, curve a). Curve b represents the UV-VIS spectra of V-MTW sample (Si/V = 178). A sharp absorbtion band at ~210 nm in both the samples indicates the presence of heteroelement in tetrahedral coordination in silicate framework. Same band is absent in Si-MTW (Curve c) and TiO_2 (Curve d).

Table 2.7 : Physico-chemical properties of MTW type molecular sieves :

Sample	Cryst. time, d	Si / M gel[a]	Si / M product[a]	BET surface area (m^2g^{-1})	Unit cell volume A^0	I_{960}/I_{550}
(A) Al-MTW	6	80	78	256	1452	0.00
(B) Si-MTW	4	∝	-	240	1423	0.00
(C) Ti-MTW[b]	6	80	62	349	1471	0.54
(D) V-MTW	8	75	178	267	1455	0.19
(E) V-MTW	7	100	250	259	1451	0.17
(F) V-MTW	6	160	357	260	1444	0.13
(G) V-MTW[c]	-	-	-	244	1427	0.04

a: M = Al (for sample A), Sample B is Al- free pure silica analog, Ti (for sample C) and V (for samples D - G).

b: Under stirring condition.

c: Sample D after steaming at 773 K for 4 hours.

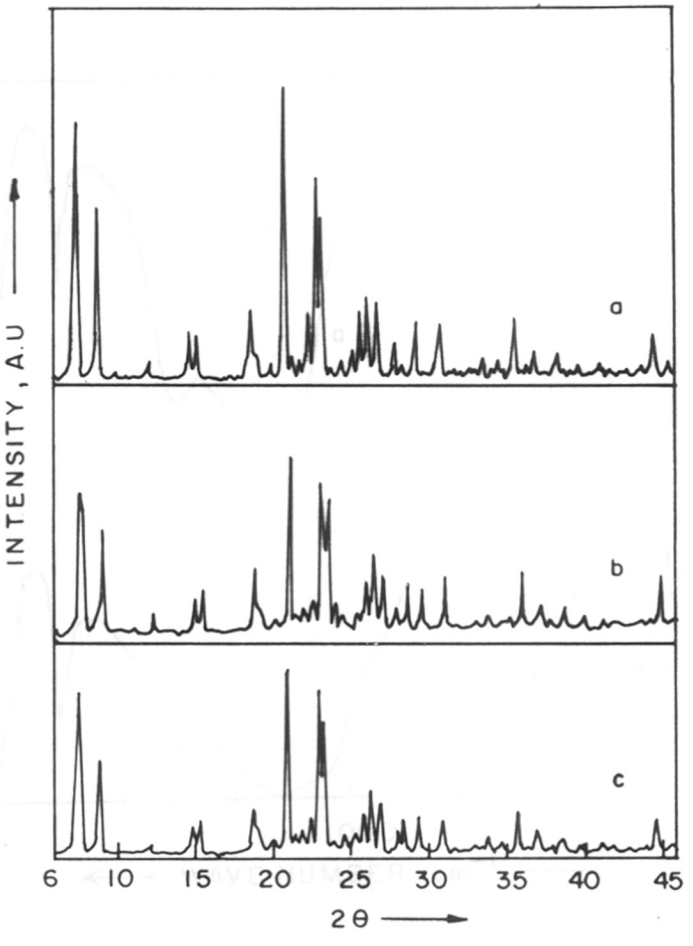

Fig. 2.2 X-ray diffraction pattern of (a) : Al-MTW, (b) : Ti-MTW and (c) : V-MTW.

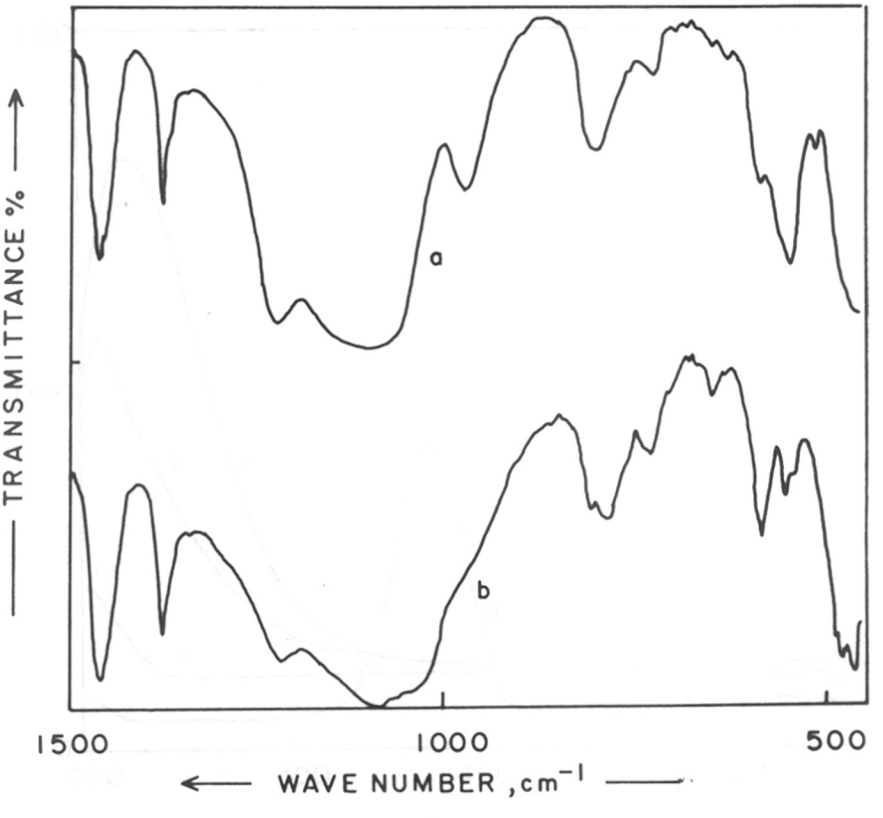

Fig. 2.3 **Framework IR spectra of (a) : Ti-MTW and (b) : Si-MTW.**

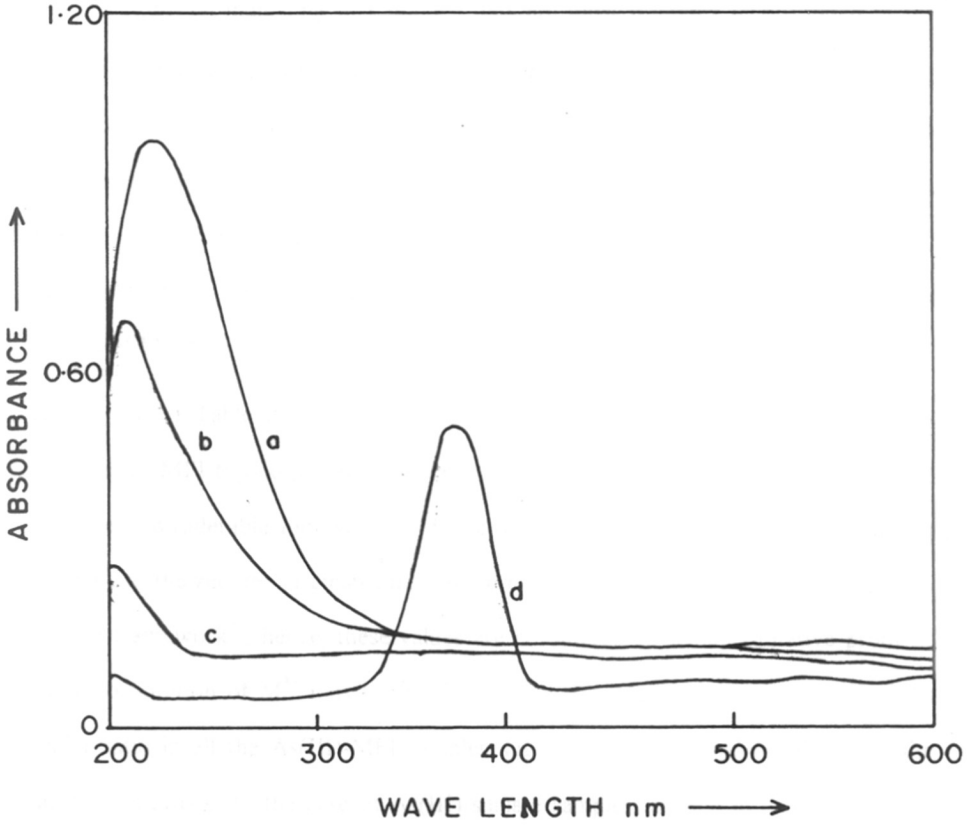

Fig. 2.4 UV-VIS spectra of (a) : Ti-MTW, (b) : V-MTW, (c) : Si-MTW and (d) : TiO_2.

Fig. 2.5 depicts the ESR spectrum of the as-synthesized V-MTW (sample D, Table 2.7) exhibiting eight equally spaced hyperfine splittings, indicating the presence of paramagnetic, atomically dispersed and immobile V^{4+} ions[32]. The g and A parameters calculated from the ESR spectra were $g_{II} = 1.924$, $g_{\perp} = 1.960$, $A_{II} = 195$ G and $A_{\perp} = 69$ G, indicating that the V^{4+} ions are most probably incorporated in the silicate framework. On calcination in flowing air, the ESR signals disappear, indicating the oxidation of V^{4+} to V^{5+} species. The reduction of the calcined samples in hydrogen restored the original spectrum with eight equally spaced hyperfine splitting, indicating that $V^{4+} \rightleftharpoons V^{5+}$ transition is reversible. In Fig. 2.6 SEM micrographs of Al-MTW (a) and V-MTW (b) samples are shown. Both the sample possesses rod type crystals typical of MTW topology.

As(III)-MFI : Table 2.4 exhibits the physico-chemical characterization of As(III)-Silicates of MFI topology. From the table it is clear that As(III)-MFI samples (A-C) exhibited considerable ion-exchange capacity (K^+ / As). Since, the cation exchange capacity in the zeolites originates from the presence of isolated M^{3+} ions in regular T_d silicate framework[26], hence, these values are considered as semiquantitative proof of the incorporation of M^{3+} ions in the silicate network. Quite high values for K / As molar ratio in all the As(III)-MFI samples suggest the incorporation of As^{3+} in the siliate framework. In the case of As(III)-silicate samples, change in unit cell volume corresponds to the change in ionic radii of As^{3+} ions and their loading, as shown in Table 2.4.

As(V)-MFI : Fig. 2.7 shows the UV-VIS spectra of As(V)-MFI (a) and that of amorphous As_2O_5 (b). Strong absorbtion of As(V)-MFI samples at 210 nm indicates the presence of As(V) in lower corodination in silicate network. In the inset framework IR spectra of As(V)-MFI sample is shown. Here also an identical band, as observed in Ti- and V- silicates at 965 - 970 cm^{-1}, appeared[18,20,21].

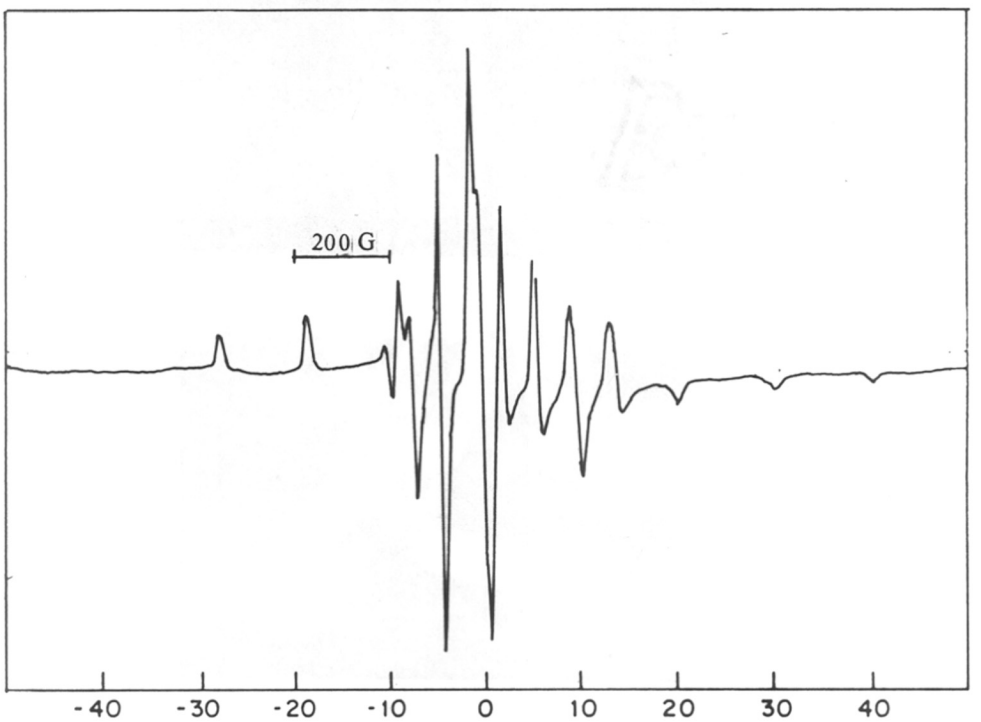

Fig. 2.5 ESR spectrum of as-synthesized V-MTW (Si/V = 178).

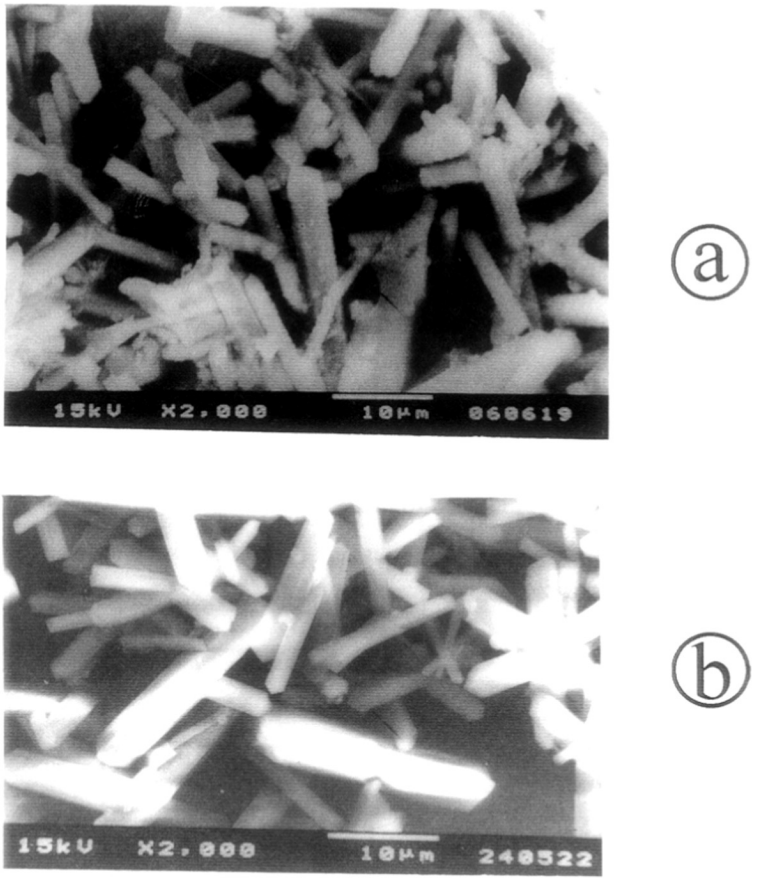

Fig. 2.6 SEM photographs of as-synthesized [Al]-MTW (a) and [V]-MTW (b).

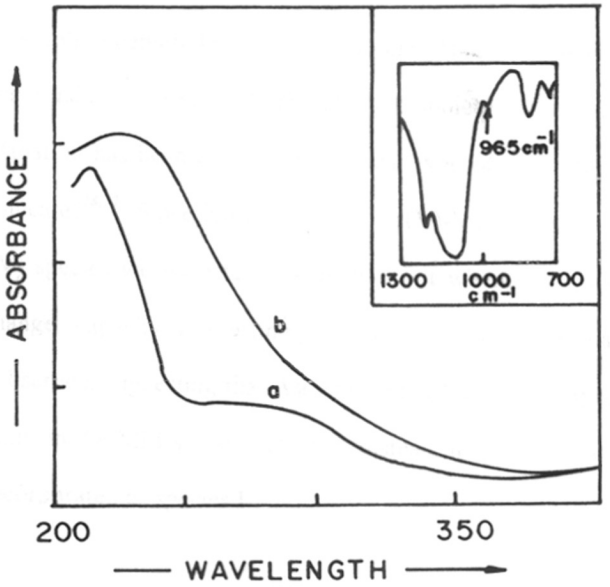

Fig. 2.7 UV-VIS spectrum of a: As(V)-MFIb (calcined), b: As_2O_5; inset : IR spectrum (framework region) of the same sample As(V)-MFI b.

In Fig 2.8 SEM micrographs of aresenosilicate analogs of various zeolite structures are given. As(V)-MFI shows (Fig. 2.8a) cubic shaped crystals of 0.1 - 0.2 μm uniformly distributed crystallites. SEM micrographs of As(V)-MTW shows very sharp needle shaped crystals of 2 - 5 μm length (Fig. 2.8b). Whereas that of As(V)-ZSM-48 shows (Fig. 2.8c) flower like aggregates composed of very fine fibers.

In the hydroxyl region IR spectra of As(V)-MFI exhibits (i) a strong absorption at about 3741 cm^{-1} due to silanol groups, (ii) a weak shoulder at about 3714 cm^{-1}, probably due to silanol groups in the vicinity of As(V) & (iii) a broad, and (iii) very weak absorption centered at around 3646 cm^{-1} (Fig. 2.9), which may be due to some hydrogen bonding between Si-O-H and As=O moiety in the proposed species I. A similar explanation has been reported for similar type of absorbtion observed in pentasil type V-silicates[28,32]. Since XPS spectra of As(V)-MFI samples confirmed the presence of As(V) species we were tempted to find out whether As(V)-MFI exhibit any anion exchange capacity. Interestingly, no significant anion exchange capacity ($Cl \leftrightharpoons OH^-$) was observed, suggesting that As(V) may not be occupying regular corner sharing T_d positions in the MFI silicate network. Instead, it is likely that these As(V) species may be incorporated as species I :

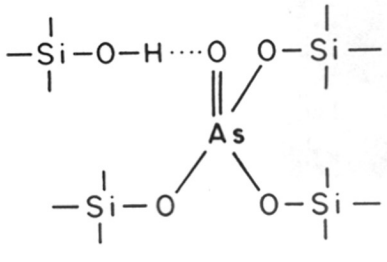

Species I

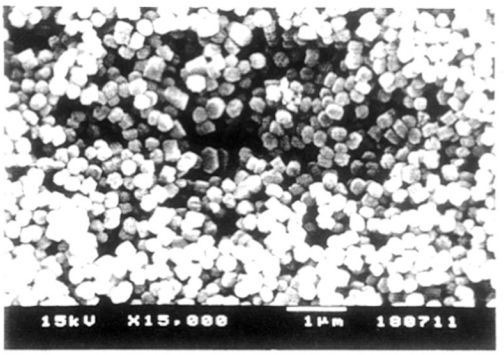

a

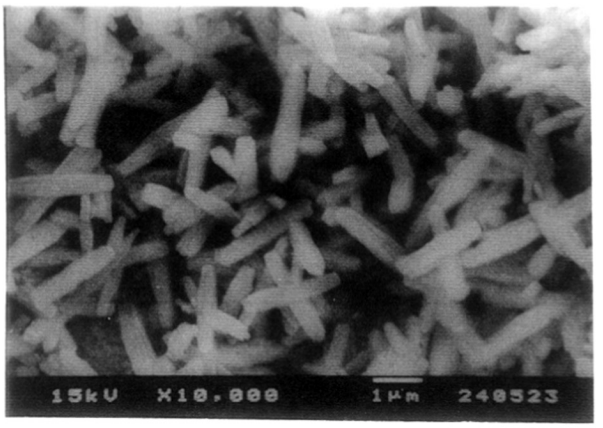

b

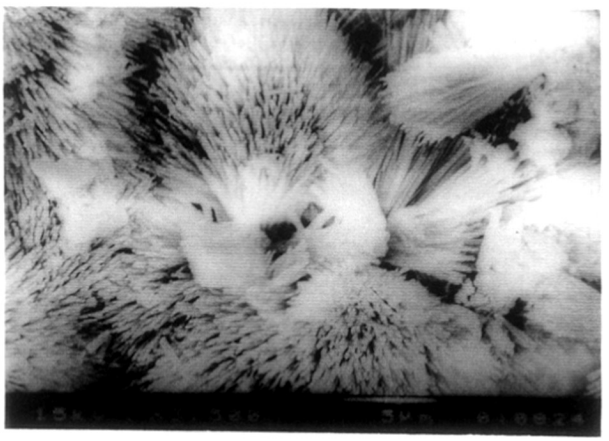

c

Fig. 2.8 SEM photographs of As(V)-MFI (a), As(V)-MTW (b) and As(V)-ZSM-48 (c).

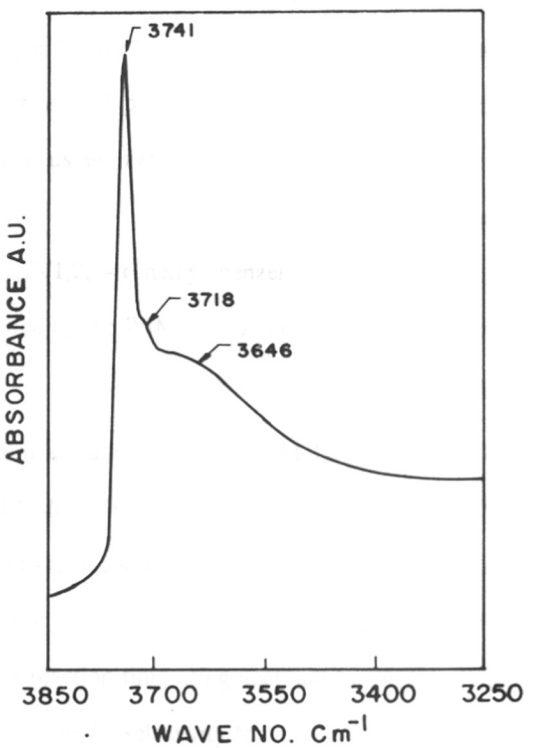

Fig. 2.9 FTIR (Nicolet, 60 SXB) spectrum (hydroxyl region) of As(V)-MFIb obtained using self-supported wafer technique.

2.3.3 Catalysis :

2.3.3.1 Al-, Ti- and V-MTW :

Al-MTW : The catalytic activity and selectivity of Al-MTW (Si/Al = 74) in *m*-xylene isomerization was found to be comparable with the activity exhibited by H-ZSM-12 samples synthesized through known literature procedure[34]. For example at 573 K and at 4.0 WHSV sample A gave 27.6 % conversion and *p-/o-* ratio = 1.3 to be compared to 27.4 % conversion and *p-/o-* ratio = 1.2 exhibited by the sample obtained by literature procedure using methyl triethyl ammmonium bromide as template. The product selectivity [*p- / o*-xylene ratio = 1.1; log(isomerization/disproportionation ratio) = 1.45; 1,3,5-/1,2,4-trimethyl benzene ratio = 0.05 at about 5 % m-xylene conversion] exhibited by the ZSM-12 sample was characteristic of 12-membered ring zeolites[34,35].

Ti-MTW : Titanium silicate analog of ZSM-12 was found to be an active catalyst in phenol hydroxylation reaction (H_2O_2 efficiency 85 %, almost identical to that exhibited by TS-1). However, in allyl alcohol epoxidation reaction whereas TS-1 (Si / Ti = 29) shows ca. 96 % conversion with 95 % selectivity towards epoxide, at 343 K after 4 hour reaction time using acetonitrile solvent, Ti-MTW exhibit only ca. 56 % conversion with 98 % selectivity for epoxide under identical conditions. Lower activity of Ti-MTW compared to TS-1 may be attributed to the lower loading probability of titanium in MTW topology (Si / Ti = 62, output compared with Si / Ti = 29 for TS-1).

V-MTW : In Table 2.8, the results of oxidation of various organic compounds like phenol, n-hexane, cyclohexanol and ethyl benzene over V-MTW (Si / V = 178) are given. V-MTW samples are quite active in various oxidation / oxyfunctionalization reactions. Under similar conditions neither V_2O_5-impregnated Si-MTW, nor pure Si-MTW exhibit any catalytic activity. In phenol hydroxylation, the catechol to

Table 2.8 : Oxidation reactions over V-MTW (sample A)[a] :

Substrate	Conversion	H_2O_2 sel[b]	Products[c] (%)					
			2-OH	4-OH	-al	-ol	-one	other
n-Hexane	14.5	81.8	-	-	3.7	11.8	84.2	0.3
Cyclohexane	14.9	73.0	-	-	-	20.8	76.8	2.5
Phenol	19.4	59.0	58.9	39.5	-	-	-	1.6
Ethylbenzene	12.0	56.6	2.9	9.1	15.5	30.9	41.6	-

a: Si / V = 178; reaction conditions : substrate (5 g) : H_2O_2 mole ratio = 3 : 1; solvent (25 g) acetonitrile and water (for phenol); catalyst, 1.0 g; temperature, 353 K; reaction time, 12 h; stirred parr or batch (for phenol) reactor.

b: Utilization of H_2O_2 for hydroxy / oxy products, referred below (see footnote c)

c: 2-OH = catechol or 2-hydroxy ethylbenzene;

4-OH = hydroquinone or 4-hydroxy ethylbenzene;

-al = aldehyde;

-ol = alcohol;

-one = ketone;

others = some unidentified higher boiling compounds.

hydroquinone ratio was about 60 : 40, the phenol conversion being 19 % (theoretical maximum ~ 33 % at phenol / H_2O_2 molar ratio 3). In order to check whether any vanadium leached out during the reaction, the following control experiment was carried out. The catalyst was filtered-off, the products were analyzed by GC, then additional amount of H_2O_2 [1 : 1 (mole / mole) with respect to remaining phenol] was added to the reaction mixture (filtrate) and the reaction was further carried out under same conditions for 12 hours, exhibiting only ca. 1 % increase in phenol conversion (20 % compared to 19 % in first operation). Further, the used catalyst was calcined and reused in the same way giving a comparable phenol conversion (19.5 % vis-à-vis 19 % in the first cycle) suggesting that the catalytic activity of V-MTW (sample D, Table 2.7) is retained after use.

Like other vanadium silicate molecular sieves[22,32], V-MTW samples are found to be active in *n*-hexane oxidation, oxyfunctionalizing 2- and 3- positions (Table 2.8). The regioselectivity with respect to carbon position in *n*-hexane was 1- (6.1 %) << 2-(42.7 %) < 3- (51.2 %). In medium pore vanadium silicate zeolites, e.g., VS-1, the regio-isomer distribution in *n*-hexane oxidation has been observed as : 1- (13.0 %) < 2- (45.0 %) > 3- (42 %)[22]. In medium pore VS-1 / VS-2 zeolites the diffusion of hex-3-ol / one (vis-à-vis hex-2-ol / one) may be hindered. Such diffusional constraints are not expected in large pore V-MTW resulting in higher selectivity for hex-3-ol / one. However, the secondary reaction (i.e., formation of ketone from secondary alcohol and aldehyde from primary alcohol) was predominant over primary reaction (i.e., formation of alcohols). In cyclohexane oxidation over V-MTW, both primary and secondary oxidation products cyclohexanol and cyclohehanone was obtained with ketone to alcohol molar ratio 3.2.

Both ring hydroxylation and side chain oxyfunctionalization were observed when ethylbenzene was reacted over V-MTW in presence of dilute H_2O_2. Among hydroxy ethylbenzenes, *p*- and *o*- mono hydroxy derivatives were obtained with *p*- / *o*- ratio 3.1. Among side chain oxidation products, secondary carbon moiety (61.1 % selectivity) is favored over primary carbon (26.6 % selectivity). However, selectivity towards secondary products, namely acetophenone and phenylacetaldehyde, was significantly higher than that of primary products, i.e., alcohols.

2.3.3.2 As(III)-MFI and As(V)-MFI :

As(III)-MFI : As(III)-silicates are quite active in Bronsted acid catalyzed reactions such as n-hexane-cracking. For example, As(III)-MFI (sample A ,Table 2.4) exhibited 25.3 % n-hexane conversion at 623 K (fixed bed down flow reactor feed rate of n-hexane : 4 ml h^{-1}). Under similar reaction conditions As-free silicalite-1 and ZSM 5 (Si / Al = 20) catalyze ca. 2 and 32 % n-hexane conversion, respectively. These results show that Brönsted acid sites are present on [As^{3+}]-silicates, the strength of which is lower than that of Al-ZSM-5 . As(III)-silicates of ZSM-11, ZSM-12 and ZSM-48 topology also behave in an identical manner.

As(V)-MFI : As(V)-MFI samples (a-d, Table 2.5) are found to be quite active in the hydroxylation of phenol using dilute (30 wt % aqueous) H_2O_2 (Table 2.9). The catechol to hydroquinone ratio ranges between 1.35 to 1.50 (for phenol / H_2O_2 mole ratio = 3). MFI type Ti and V-silicates also exhibit similar product distributions. However, the H_2O_2 selectivity exhibited by As(V)-MFI is less than that reported for TS-1[36]. This may be due to the higher redox potential of As^{3+} / As^{5+} couple (0.55 ev, higher potential facilates H_2O_2 decomposition) compared with that of Ti^{4+} / Ti^{3+} couple (0.06 ev) and lower stability of As-peroxo species[37] compared with Ti-peroxo

Table 2.9 : Hydroxylation of phenol over As(V)-MFI[a] :

Sample	Phenol/H_2O_2 mole ratio	Phenol conv. (mole %)	H_2O_2 sel. (%)[b]	Product sel. (%)		CAT HQ
				HQ	CAT	
As(V)-MFI a	3	17.2	52.0	39.6	60.4	1.52
As(V)-MFI b	3	16.8	51.0	40.0	59.9	1.49
As(V)-MFI b	2	25.4	51.0	37.4	62.6	1.67
As(V)-MFI b	1	48.5	49.0	35.3	64.7	1.83
As(V)-MFI c	3	14.2	43.0	42.6	57.4	1.35
As(V)-MFI d	3	11.5	35.0	41.7	58.3	1.40
As-impregneted Silicalite-1	1	7.6	8.0	14.3	85.7	7.00

a: Conditions : catalyst 0.12 g, 1 g phenol, solvent = water 10 g, reaction temperature = 353 K, reaction time 12 h.

b: H_2O_2 utilized in the formation of hydroquinone (HQ) and catechol (CAT).

species[38]. For the same reason, vanadium silicates also exhibit lower H_2O_2 efficiency compared to that by titanium silicate analogs.

Table 2.10 exhibits the results of vapor phase oxidative dehydrogenation of 2-butanol and benzyl alcohol in the presence of air, reaction being carried out in a fixed bed reactor having catalyst size 20 - 25 mesh. As expected, the conversion increases and selectivity for oxidation products decreases with increase in reaction temperature. However, when 2-butanol was reacted over the same catalyst in the presence of nitrogen, instead of oxygen / air, under otherwise similar reaction conditions, little conversion was observed with almost 90 % selectivity towards butenes among the products (Table 2.10). In the case of benzyl alcohol also the conversion increases with temperature, main product being benzaldehyde.

2.4 CONCLUSION :

A new diquaternary ammonium salt, 1,6- hexamethylene bis [benzyl dimethyl ammonium bromide / hydroxide] has been synthesized which can efficiently produces MTW type alumino-silicate, pure silica polymorph as well as titanium and vanadium-silicate analogs. Same template directs the synthesis of ZSM-39 (MTN) and ZSM-48 topology also.

As-silicate analogs [both As(III) and As(V)-Silicates] of MFI, MEL, MTW and ZSM-48 have been synthesized and the incorporation of heteroelement (As) has found to be relatively good when the synthesis is employed at low temperature. Further, with increasing the As content in the hydrogel, crystallization became faster. These As(III) silicates are quite active in acid catalyzed reactions whereas As(V)-Silicates are found to be good oxidation catalyst using dilute H_2O_2 in liquid phase and using O_2 in vapor phase reactions.

Table 2.10 : Oxidative dehydrogenation of 2-butanol and benzyl alcohol over As(V)-MFI b sample using air[a] :

Temp.	2-butanol (wt %)			Benzyl alcohol (wt %)			
K	Conv.	2-butanone	others[b]	Conv.	ald.	acid	others[c]
623	15.0	90.0	10.0	22.8	87.0	4.0	9.0
623[d]	5.2	5.0	95.0	nd	-	-	-
673	35.2	78.2	21.8	45.7	83.4	5.4	12.2
673[d]	8.6	9.5	90.5	nd	-	-	-
723	55.3	65.4	34.4	74.3	80.2	6.6	13.2

a: O_2 / alcohol = 1 (mole / mole), WHSV (alcohol) = 3.5 h^{-1}

b: Mainly butenes and some dimerized etheric products.

c: Mainly cleaved products like benzene and HCHO.

d: Reactions were carried out in the flow of nitrogen, nd = not done.

2.5 REFERENCES :

1. Casci, J.L., *Stud.Surf.Sci.Catal.*, **84A,** 129 (1994).
2. Perego, G., Bellussi, G., Corus, C., Taramasso, M., Buonomo, F. & Esposito, A., *Stud.Surf.Sci.Catal.*, **28,** 129 (1986).
3. Tuel, A. & Ban Taarit, Y., *Zeolites*, **14**, 18 (1994).
4. Casci, J.L., Lowe, B.M. & Whittam, T.V., *UK.Pat.* Appl., 2 077 709 (1982).
5. Kumar, R., Reddy, K.R. & Ratnasamy, P., *US.Pat.*, 5 219 813 (1993).
6. Reddy, K.R., Kumar, R., Ramaswamy, V., Ramaswamy, A.V., *Zeolites,* **4**, 326 (1994).
7. Barrer, R.M., Pro.Sixth.Int.Zeol.Conf. (Olson,D.,& Bisio, A., Eds.), Butterworths : Surrey, pp. 870 (1984).
8. Rollmann, L.D. & Valyocsik, E.W., *E.Pat.* Appl., 15 132 (1980).
9. Barrer, R.M., "*Hydrothermal Chemistry of Zeolites*", Academic Press, New York, (1982).
10. Meier, W.M., *Pure Appl.Chem.*, **58**, 1323 (1986).
11. Flanigen, E.M., Lok, B.M., Patton, R.L. & Wilson, S.T., *Pure Appl.Chem.*, **58**, 1351 (1986).
12. Chu, C.T.W. & Chang, C.D., *J.Phys.Chem.*, **89**, 1569 (1985).
13. Ione, K.G., Vostrikova, L.A., Petrova, A.V. & Mastikhin, V.M., *Stud.Surf.Sci.Catal.*, **18**, 151 (1984).
14. Fricke, R., Kosslick, H., Tuan, V.A., Grohmann, I., Pilz, W., Storck, W. & Walther, G., *Stud.Surf.Sci.Catal.*, **83**, **57** (1994).
15. Notari, B., *Stud.Surf.Sci.Catal.*, **37**, 413 (1987).
16. Reddy, J.S., Kumar, R. & Ratnasamy, P., *Appl.Catal.*, **58**, L1 (1990).
17. Thangaraj, A., Eapen, M.J., Sivasanker, S. & Ratnasamy, P., *Zeolites*, **12,** 943 (1992).
18. Bhaumik, A., Dongare, M.K. & Kumar, R., *Microporous Materials*, **5,** 173 (1995).
19. Reddy, K.M., Moudrakovski, I. & Sayari, A., *J.Chem.Soc.Chem.Commun.*, 1491 (1994).

20. Bhaumik, A. & Kumar, R., *J.Chem.Soc.Chem.Commun.*, 869 (1995).

21. Bhaumik, A., Hegde, S.G. & Kumar, R., *Catal.Lett.*, **35**, 327 (1995).

22. Rao, P.R.H.P., Belhekar, A.A., Hegde, S.G., Ramaswamy, A.V. & Ratnasamy, P., *J.Catal.*, **141**, 595 (1993).

23. Ratnasamy, P. & Kumar, R., *Catal.Lett.*, **22**, 227 (1993).

24. Flanigen, E.M., Bennet, J.M., Grosse, R.W., Patton, R.L., Kirchner, R.M. & Smith, J.V., *Nature*, **271**, 512 (1978).

25. Jacobs, P.A. & Martens, J.A., *Stud.Surf.Sci.Catal.*, **33**, 58 (1987).

26. Szostak, R, *"Molecular Sieves : Principle of Synthesis and Identification"*, Van Nostrand Reinhold, New York (1989).

27. Gier, T.E. & Stucky, G.D., *Nature*, **349**, 509 (1991).

28. Rao, P.R.H.P., Ramaswamy, A.V. & Ratnasamy, P., *J.Catal.*, **137**, 225 (1992).

29. Thangaraj, A., Kumar, R., Mirajkar, S.P. & Ratnasamy, P., *J.Catal.*, **131**, 1 (1994).

30. Reddy, J.S., Kumar, R. & Sciscery, S.M., *J.Catal.*, **145**, 73 (1995).

31. La Pierre, R.B., Rohrman, A.C., Schlenker, J.L., Wood, J.D., Rubin, M.K. & Rohrbaugh, W.J., *Zeolites*, **5**, 346 (1985).

32. Ramaswamy, A.V. & Sivasanker, S., *Catal.Lett.*, **22**, 239 (1993).

33. U.de Navarro, C., Machado, F., Lopez, M., Maspero, D. & Perez-Pariente, J., *Zeolites*, **15**, 157 (1995).

34. Ernst, S., Jacobs, P.A., Martens, J.A. & Weitkamp, J., *Zeolites*, **7**, 458 (1987).

35. Martens, J.A., Perez-Pariente, J., Sastre, E., Corma, A. & Jacobs, P.A., *Appl.Catal.*, **45**, 85 (1988).

36. Thangaraj, A., Sivasanker, S., Ratnasamy, P., *J.Catal.*, **131**, 394 (1991).

37. Jacobson, S.E., Mares, F. & Zambri, P.M., *J.Am.Chem.Soc.*, **101**, 6938 (1979).

38. Bellussi, G. & Fattore, V., *Stud.Surf.Sci.Catal.*, **69**, 79 (1991).

CHAPTER 3

PROMOTER-INDUCED CRYSTALLIZATION : A NOVEL CONCEPT

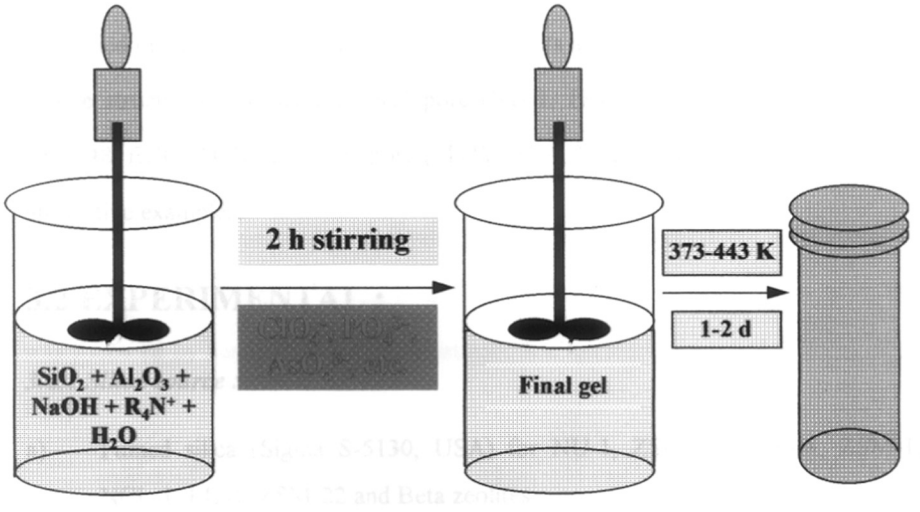

3.1 INTRODUCTION :

Although, the nature of surface and acid catalytic properties of zeolites and related molecular sieves is relatively better understood[1-4], the chemistry governing their hydrothermal synthesis at autogeneous pressure (crystallization temperature = 353 - 473 K, time = few hours to few days) continues to be intriguing and challenging. Inui[5], has suggested various drawbacks to long crystallization process which causes (i) extensive labor coupled with delays and expenses, (ii) poor reproducibility and (iii) formation of larger crystals with inhomogeneous particle size distribution mainly because of secondary crystallization. Further, the optimization of recipes of each structure is done on a case to case basis.

This chapter will describe a novel and general method for significant enhancement in the nucleation and crystallization rates of zeolite and other related silica based molecular sieves using *'promoters'*[6] (oxyanions of group VA, VIA and VIIA elements like nitrate, phosphate, carbonate, perchlorate, chlorate, bromate, iodate etc). Further, in the presence of small amount of a promoter, the synthesis may be carried out at lower temperature (vis-à-vis in its absence) in certain cases. Various zeolite structures representing small pore (NU-1, FER, LTA), medium pore (MFI, ZSM-48, EUO, TON) and large pore (MTW, BEA, NCL-1 and FAU) were chosen as illustrative examples.

3.2 EXPERIMENTAL :

3.2.1 Silica source :

a) Fumed silica (Sigma S-5130, USA) for NU-1, ZSM-5, ZSM-48, ZSM-12, NCL-1, EU-1, ZSM-22 and Beta zeolites.

b) Sodium silicate (28 % SiO_2, 8.5 % Na_2O) for Ferrierite and Y zeolite.

c) Tetraethyl orthosilicate (TEOS, Aldrich, USA) for Si-ZSM-5 and TS-1.

3.2.2 Synthesis Procedure :

Depending upon the silica source, the synthesis is classified into following categories :

3.2.2.1 NU-1, ZSM-5, ZSM-48, ZSM-12, NCL-1, EU-1, ZSM-22 and Beta zeolites :

The molar gel composition of all the zeolites studied during this work, is given in Table 3.1. However, following general procedure was used for preparing the gels. The silica source was first slurried with required amount of alkali (NaOH / or KOH) and template (as given in Table 3.1) in deionized water for 2 hours. Then the aluminum source [$NaAlO_2$ (43 % Al_2O_3, 39 % Na_2O) in most cases except in the case of ZSM-12, NCL-1 and EU-1 where the source was aluminum sulfate] taken in water was added to the reaction mixture with vigorous stirring. Finally, an aqueous solution of promoter (in the form of oxyacid, or their sodium / potassium salt depending upon the choice and need in keeping the molar gel composition constant) was added into the gel and stirring was continued for another 1 hour at room temperature. The pH of the final gel was measured (given in Table 3.1) and the gel was transferred into teflon lined stainless steel autoclave at elevated temperature required for particular structure (caption of Table 3.1). After the crystallization, pH of the mother gel was measured, products were separated (filtered / centrifuged), washed thoroughly with deionized water, dried at 373 K and calcined to get Na-form of the corresponding zeolites. This was followed by ammonium acetate treatment and calcination to yield H-form of the zeolite.

Although the above mentioned procedure was employed for most of the cases, following specific method was used for FAU, Si-MFI and TS-1.

Table 3.1 : Starting molar gel composition of various zeolites :

Zeolite	Molar gel composition	pH
NU-1	40 SiO_2 : Al_2O_3 : 5.0 NaOH : 20 TMAOH : 1000 H_2O : 4*P*	12.0 ± 2
FER	60 SiO_2 : Al_2O_3 : 36 NaOH : 7.5 Pyrrolidine : 2400 H_2O : 6*P*	11.8 ± 2
ZSM-5	40 SiO_2 : Al_2O_3 : 8 NaOH : 5 TPABr : 1200 H_2O : 4*P*[a]	11.0 ± 2
ZSM-22	60 SiO_2 : Al_2O_3 : 15 NaOH : 10 Et-PyBr : 1200 H_2O : 6*P*	11.7 ± 2
ZSM-48	90 SiO_2 : Al_2O_3 : 18 NaOH : 15 DIQ-6 : 2700 H_2O : 9*P*	12.0 ± 2
EU-1	60 SiO_2 : Al_2O_3 : 10 NaOH : 8 DIQ-6[1] : 1500 H_2O : 6*P*	11.4 ± 2
ZSM-12	120 SiO_2 : Al_2O_3 : 20 NaOH : 10 DIQ-6 : 3600 H_2O : 12*P*	10.9 ± 2
Beta	30 SiO_2 : Al_2O_3 : 2 NaOH : KOH : 15 TEAOH : 600 H_2O : 3*P*[a]	12.4 ± 2
Si-NCL-1	120 SiO_2 : 12 NaOH : 10 DIQ-6[2] : 3600 H_2O : 12*P*	11.2 ± 2
FAU	9 SiO_2 : Al_2O_3 : 8.4 NaOH : 270 H_2O : *P*	13.2 ± 2
Si-MFI	3 SiO_2 : TPAOH : 75 H_2O : 0.3 NaH_2PO_4	11.3 ± 2
Ti-MFI	30 SiO_2 : TiO_2 : 15TPAOH : 750 H_2O : 3 H_3PO_4	11.0 ± 2

Where *P* = promoter chosen from $HClO_4$, Na_2HPO_4 and Na_2HAsO_4.

a : In addition to the above promoters, $NaClO_4$, Na_3PO_4, $NaNO_3$, Na_2SO_4 were used.

TMAOH = tetramethyl ammonium hydroxide.

TEAOH = tetraethyl ammonium hydroxide.

TPAOH = tetrapropyl ammonium hydroxide.

Et-PyBr = N-ethyl pyridinium bromide.

DIQ-6 = 1,6-hexamethylene bis [benzel dimethyl ammonium], if otherwise not stated.

DIQ-6[1] = 1,6-hexamethonium bromide.

DIQ-6[2] = 1,6-hexamethalene bis (triethyl ammonium bromide).

Crystallization temperature (K) was 443 for NU-1, ZSM-22, ZSM-48, EU-1 and NCL-1, 433 for FER, ZSM-5, ZSM-12 and Ti-MFI (TS-1), 413 for Beta, 373 for FAU and 358 for Silicalite-1 (Si-MFI).

3.2.2.2 FAU :

Synthesis of zeolite Y was carried out in an usual two step process[7] adding promoter in the second step. First, a seed solution (20 g) consisting of sodium silicate (12.0 g), sodium aluminate (0.66 g) and sodium hydroxide (2.7 g) taken in water (5 g) was prepared and aged for 1 day. In the second phase, the seed solution was added to another clear solution obtained by mixing sodium silicate solution (24.5 g), sodium aluminate (2.6 g) and sodium hydroxide (0.8 g) mixture in water (30 g). To this resultant solution, a mixture of 3.3 g aluminum sulfate in 33 g water and the required amount of promoter (Table 3.1) was added under vigorous stirring. The stirring was continued for another 2 hours before autoclaving at 373 K. Crystallization kinetics was carried out by removing samples from various autoclaves of identical size at different interval of time.

3.2.2.3 Si-MFI (Silicalite-1) :

21 g of tetraethyl orthosilicate was first hydrolyzed with 33.9 g of tetrapropyl ammonium hydroxide (20 % aqueous, Aldrich) under vigorous stirring. After 2 hours a solution of 1.38 g of sodium dihydrogen phosphate (s.d.fine Chem., India) in 17.9 g of deionized water was added into the mixture slowly and the stirring was continued for another 1 hour. Crystallization was carried out at 358 K in polypropylene bottles. Initial molar composition of the reaction mixture is given in Table 3.1.

3.2.2.4 Titanium silicate-1 (TS-1) :

35 g of tetraethyl orthosilicate was hydrolyzed with 84.6 g of tetrapropyl ammonium hydroxide solution under vigorous stirring for 2 h. Then 1.9 g of tetrabutyl orthotitanate (E.Mark, Germany) in 10 g of dry isopropyl alcohol (s.d.fine chem., India) was added into the resulting hydrolyzed gel very slowly. While adding titanium source proper precaution was taken in order to avoid white precipitate of insoluble

TiO_2. Stirring was continued for another 1 h. Finally to the clear liquid thus obtained, 1.92 g of promoter orthophosphoric acid (85 %, s.d.fine chem. India) taken in 7.5 g of water were added very slowly. After vigorous stirring for 1 h, pH of the solution was 11.2 and the resulting clear solution was transferred into teflon lined stainless parr autoclave at an elevated temperature (Table 3.1). After the crystallization at 433 K, pH of the mother solution was 11.8. Then the solid was separated by centrifugation, dried and calcined.

In all the cases a blank experiment in the absence of promoter was carried out.

3.2.3 Liquid state NMR experiments:

Silicalite-1 sample was chosen for these NMR studies. The samples were removed at various interval of time, quenched and immediately used for NMR experiments. Liquid state ^{29}Si and ^{31}P NMR experiments was carried out taking this sample in a leak-proof sealed plastic tube (8 mm i.d., length 40 mm) devoid of any background ^{29}Si signal. The spectra were obtained on a Bruker MSL-300 FT-NMR spectrometer by co-addition of 8 successive spin-echoes, generated in a CPMG[8,9] pulse sequence and a magnitude mode Furrier Transform of the resultant time domain signal. Number of transients = 5120, $\pi/2$ pulse width = 10.5 μsec.; pulse sequence recycle time = 20 sec.; total accumulation time = 3.5 h. In order to improve the detection sensitivity, a home made selenoidal coil assembly (silver plated R.F. coil having Q of 120) was used.

3.3 RESULTS AND DISCUSSION :

3.3.1 Synthesis :

3.3.1.1 Effect of different promoters :

Addition of a small amount of various promoter (ClO_4^-, NO_3^-, PO_4^{3-}, SO_4^{2-}, CO_3^{2-}, AsO_4^{3-}, ClO_3^-, BrO_3^- and IO_3^-), significantly enhances the crystallization process

of a variety of zeolite structures. Fig. 3.1 exhibits the results on the crystallization time of different zeolite structures representing small (NU-1 and FER), medium (ZSM-5 and ZSM-48) and large pore (Beta and ZSM-12) high silica zeolites, with and without adding promoters (ClO_4^-, PO_4^{3-}, AsO_4^{3-} and none). Similar effects are also observed in the synthesis of other zeolites (Table 3.2) like EU-1 (promoter $HClO_4$), ZSM-22 (promoter $HClO_4$), Si-NCL-1 (promoter Na_2HAsO_4), FAU, LTA, Si-MFI and TS-1. The effect is also appreciable in the case of aluminous / low silica molecular sieves (Si / Al = 1 - 5, zeolite LTA and FAU). For example, in the synthesis of zeolite Y[7] the crystallization time was 4 hours using Na_2HPO_4 as promoter and 11 hours in the absence of it at 373 K (Table 3.2). Furthermore, the stability of the fully crystalline material in the mother liquor was found to increase in the presence of promoter. While following the conventional method (without the use of promoter) zeolite P, a common impurity in Y synthesis[7,8] was detected within 30 - 60 min after the fully crystalline zeolite Y was obtained, following the present method with promoters zeolite P was not observed up to 2 hours after the complete crystallization of zeolite Y (Fig. 3.2). Similarly, zeolite A was obtained in 2 h and 4 h, respectively, with and without the use of promoter (Na_3PO_4, Table 3.2). Crystallization kinetics of zeolite Y is shown in Fig. 3.2. Decrease in crystallinity for sample without promoter (curve c, Fig. 3.2) after the complete crystallization accompanied with the appearance of zeolite P.

Apart from the representative promoters used above, other oxyanions (acid or salt) like NO_3^-, CO_3^{2-}, SO_4^{2-}, ClO_3^-, BrO_3^- and IO_3^- also enhance the crystallization process to a varying extent. As typical example, in the synthesis of zeolite ZSM-5 and Beta, the time needed to obtain fully crystalline material using these promoters (*P*),

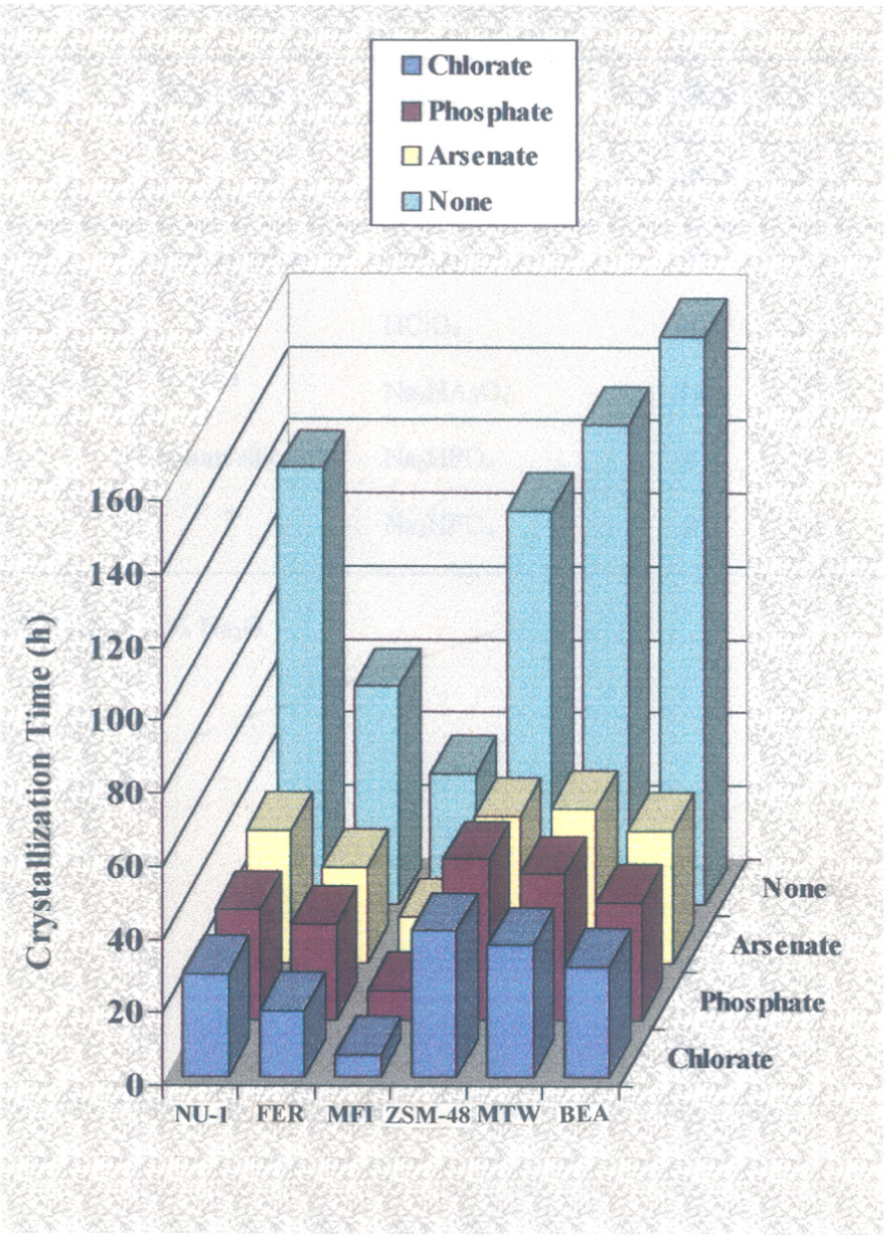

Fig. 3.1: Crystallization time (hours) of fully crystalline sample of various zeolites with and without using promoter.

Table 3.2 : Effect of various promoters in zeolite synthesis :

Zeolite	Silica source	Promoter, *P*	Crystallization time, h	
			With *P*	No *P*
ZSM-22	Fumed silica	$HClO_4$	24	80
EU-1	"	$HClO_4$	40	144
Si-NCL-1	"	Na_2HAsO_4	18	56
FAU	Sodium silicate[a]	Na_2HPO_4	4	11
LTA	"	Na_2HPO_4	2	4

a: 28 % SiO_2, 8.3 % Na_2O.

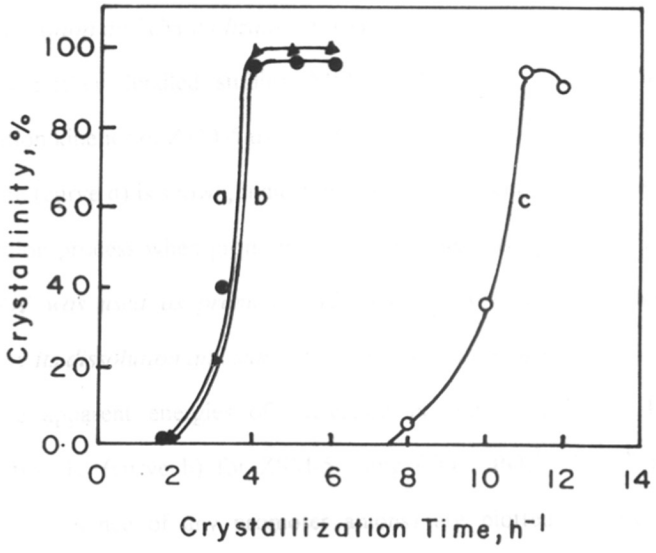

Fig. 3.2 Crystallization kinetics of zeolite Y (curve a with $HClO_4$, b with Na_2HPO_4 and c with no promoter).

under otherwise similar condition is given in Table 3.3.

Table 3.3 : Effect of promoter in the crystallization time of ZSM-5 and Beta

Structure	Crystallization time (h) using								
	$HClO_4$	$NaNO_3$	Na_2HPO_4	$NaHCO_3$	Na_2SO_4	$NaClO_3$	$KBrO_3$	KIO_3	No *P*
ZSM-5	6.0	7.5	8.0	10.0	10.0	12.0	14.0	18.0	48
Beta	30.0	40.0	36.0	44.0	48.0	48.0	60.0	96.0	156

3.3.1.2 Nucleation and Crystallization Energies :

For further detailed studies, MFI topology was chosen. In Fig. 3.3 the crystallization kinetics of ZSM-5 using ClO_4^- (curve a), PO_4^{3-} (curve b), AsO_4^{3-} (curve c) and none (curve d) is shown, indicating the enhancement of both the nucleation and crystallization process when promoters are used. *Here it is pertinent to mention that while ClO_4^- was used as promoter, TPA-ClO_4 was first crystallized immediately followed by its dissolution and subsequent crystallization of ZSM-5.*

The apparent energies of nucleation E_n (curve a, Fig. 3.4) and that of crystallization E_c (curve b) for ZSM-5 using ClO_4^-, PO_4^{3-}, AsO_4^{3-} and none (i.e., standard, in absence of any promoter anions) are plotted against the inverse of crystallization time, exhibiting E_n and E_c increases in the following order :

$$ClO_4^- < PO_4^{3-} < AsO_4^{3-} << \text{None}.$$

and thereby reducing the overall synthesis time in the reverse order. E_n and E_c were calculated according to the equation $\ln(1/\theta) = -E_n/RT$ and $\ln(1/k) = -E_c/RT$, where θ is the induction period, i.e., minimum time required to obtain first crystallites and k is the half crystallization time, i.e., time required to obtain 50 % crystallinity by XRD.

3.3.1.3 Effect of promoter concentration :

Fig. 3.5 illustrates the effect of promoter concentration (PO_4^{3-} taken as representative) on the crystallization time of ZSM-5. As the amount of promoter

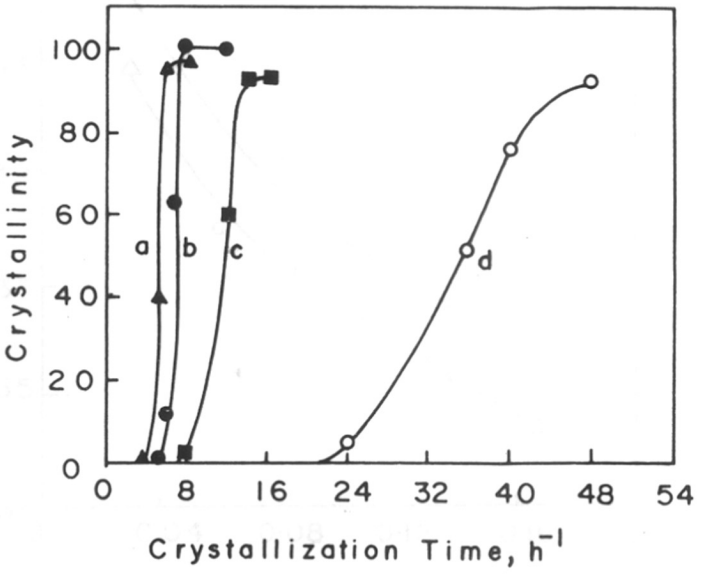

Fig. 3.3 Crystallization kinetics of ZSM-5 (curves a, b, c and d represent the use of $HClO_4$, NaH_2PO_4, Na_2HAsO_4 and no promoter, respectively).

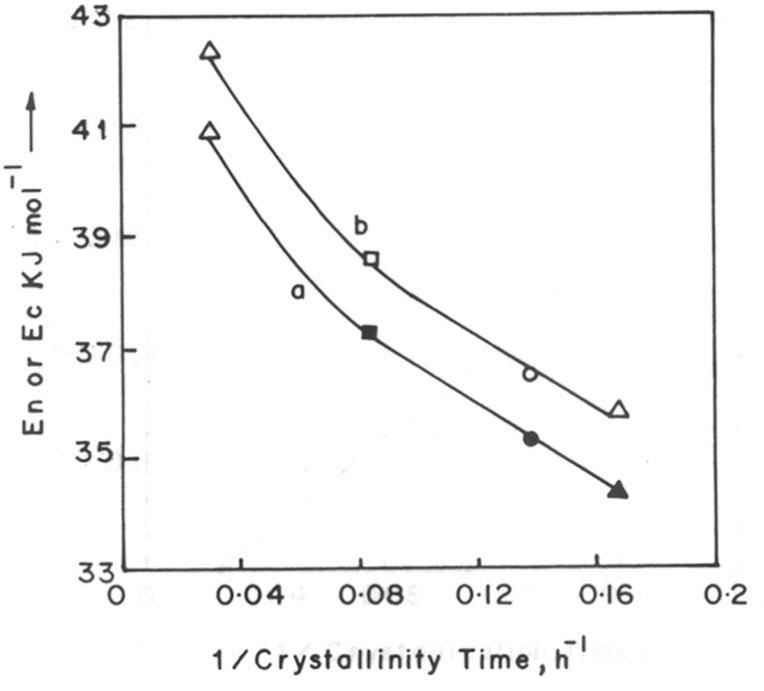

Fig. 3.4 E_n (curve a) and E_c (curve b) vs. (crystallization time)$^{-1}$.

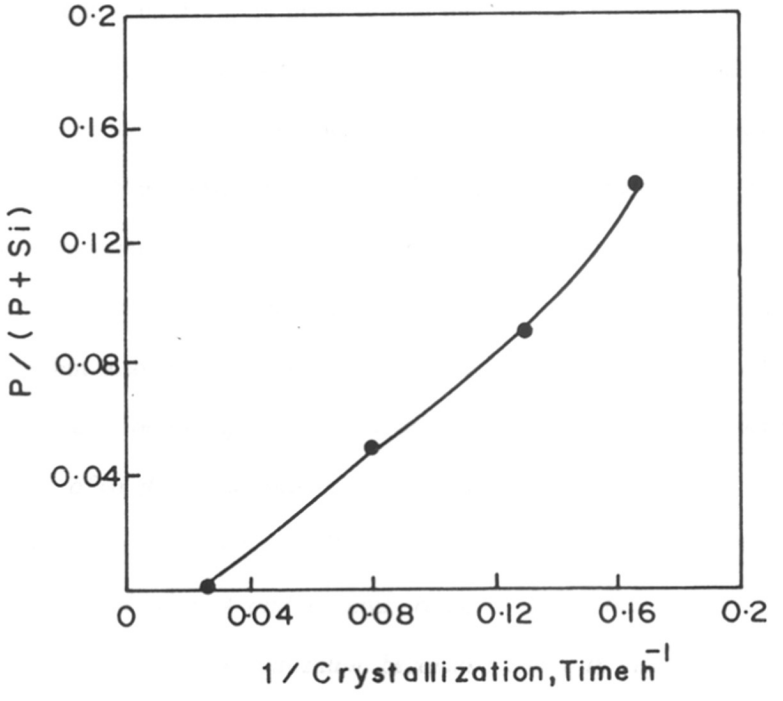

Fig. 3.5 Effect of promoter (PO_4^{3-}) concentration on crystallization time in the crystallization of ZSM-5.

increases in the gel, the crystallization time decreases linearly in the beginning and then remains nearly same after an optimum concentration. This observation suggests that a minimum amount of promoter is needed. Further, there is an optimum range of promoter concentration.

3.3.1.4 Synthesis of Si-MFI (Silicalite-1) : Effect of Temperature :

After establishing that the use of promoter drastically reduces the synthesis time of zeolites, efforts were made to find out whether synthesis temperature can be reduced using these promoters. Si-MFI was chosen as an example because of its simplicity and the requirement of less crystallization time. Fig. 3.6 represents the effect of promoter (NaH_2PO_4) on the crystallization time of Silicalite-1 (Si-ZSM-5[10]) at various temperatures. Not only reduction in the crystallization time was observed, as expected,at a particular temperature in presence of promoter (vis-à-vis in their absence),but also the crystallization could be accomplished at comparatively lower temperatures. *For example at 333 K and 343 K (lowest ever temperature for the synthesis of (high silica) Silicalite-1) Si-MFI crystallizes within 72 and 36 h, respectively, in the presence of PO_4^{3-} promoter, whereas only amorphous materials were recovered after 9 and 6 days, respectively in the absence of promoters. However, as expected crystallization becomes faster with increase in temperature. It is interesting to note that probably this is the first report of the low temperature (333 - 343 K) promoter-induced synthesis of any high silica zeolites in reasonable time.*

3.3.2 General Applicability :

Barrer[11], one of the pioneer of in zeolite synthesis, has pointed out that the observation on the synthesis of zeolites which have some generality are of much interest, mainly because the general / unifying observations can significantly contribute to the growing understanding of the synthesis of these porous materials at the mechanistic level. One of the most fundamental basis of the hydrothermal synthesis of

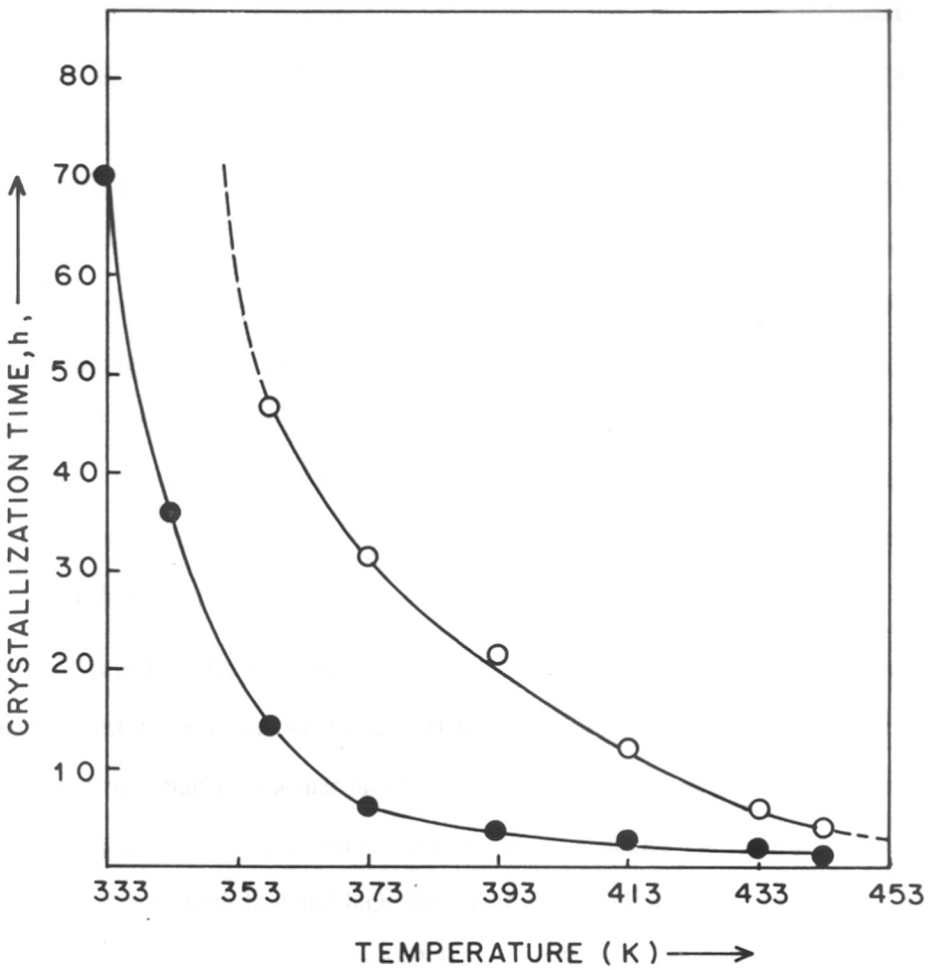

Fig. 3.6 Effect of temperature on the synthesis of Si-ZSM-5 with (●) and without (○) using promoter (NaH_2PO_4).

zeolites is the mineralizing role of water, which is greatly assisted by the free OH^- concentration in the solution / hydrogel. Apart form this basic requirement of mineralizability, other factors like, Si / Al molar ratio, pH of the gel, aging at lower temperature, crystallization temperature and time etc., influence the type and quality of the crystalline material in rather specific ways[1,11,12]. For example, in the crystallization of alumnus zeolites (Si / Al = 1-5, like A, X and Y) the synthesis becomes faster with decreasing Si / Al molar ratio, while for high silica zeolites like ZSM-5, ZSM-12, ZSM-48, Beta etc. reverse is true. Further, low silica zeolites are better obtained at low temperatures (353 - 393 K), while high silica zeolites are generally synthesized at relatively higher temperature (around 393 - 473 K). Similarly, organic bases (i.e. templates) play particularly significant role in the synthesis of high silica zeolites for the reason that with increase in Si / Al ratio, hydrophobicity of the crystalline material also increases, these organic bases then play the stabilizing role like what played by the inorganic bases and water in the case of alumnus / low silica zeolites[11,12].

From Fig. 3.1 it is clear that the enhancement of the crystallization rate is independent of the choice of the acid (H^+), sodium (Na^+) or potassium (K^+) salt from of the corresponding particular promoter, keeping the molar gel composition and pH same. The results of using promoters is very general in nature and equally applicable in a similar way to both low and high silica zeolites as well as more open to less open porous structure. Further, this approach is also applicable to Al-free pure silicalite type and other metallosilicates like titanium silicate (TS-1). In the case of titanium silicate instead of sodium or potassium salt of promoter oxyanions, parent acid i.e., orthophosphoric acid (H_3PO_4) was used. For TS-1 fully crystalline materials with equally good crystallinity, yield and Ti-content in silicate network was observed after 4 h at 443 K, 6 h at 433 K, 12 h at 413 K and 24 h at 393 K using H_3PO_4 promoter under stirring condition. The corresponding time needed in absence of promoter at 443

and 433 K was 24 h and 30 h respectively. At 413 and 393 K synthesis in absence of promoter yields material with very poor crystallinity even after 3 and 4 days, respectively.

Some stabilizing effect of certain neutral sodium salts of some anions (e.g., NaCl, $NaNO_3$, Na_2SO_4, $NaClO_3$ etc.) during the hydrothermal transformation of kaolinite into sodalite and cancrinite[11] has been observed where the inclusion of these salts in the sodalite / cancrinite structure was found to be the main cause of stabilizing a particular phase. In the present case of direct synthesis, no such inclusion of promoters (anions or their salts) in the crystalline molecular sieves was obtained after proper washing of the synthesized solid by hot deionized water. However, in the case of Silicalite-1, an aluminum free all silica MFI analog[10], a small amount of one of the promoter, As(V) was found to be present in the solid when the synthesis was conducted at lower temperature[13] (353 - 358 K, Chapter 2, section 2.3.1.3). Although, at higher temperature very poor As(V) containing material was obtained. It seem that at low temperature synthesis, AsO_4^{3-} acts both as reagent as well as promoter. However, presence of Al^{3+} in the hydrogel and at elevated synthesis temperature not even a minor quantity of this promoter was detected in the crystalline solid.

3.3.3 Characterization :

XRD : The next obvious question is to check the quality of the material obtained by using these promoters. XRD of different structures shows the crystallinity of the materials synthesized in presence of promoters is comparable if not better, than that synthesized in their absence. One of the important aspect of the zeolite synthesis is the yield of the final product. The uptake of Al from the gel to the solid using various promoters was quantitative and yield was above 90 % (on the basis of silica and alumna in the gel) in most of the cases leading to comparable SiO_2 / Al_2O_3 molar ratio in the solid (vis-à-vis in the gel) crystalline product. For example, in the case of zeolite

beta final solid using Na_2HPO_4 was 90.2 %, whereas under conventional procedure (in absence of promoter) yield was only 75 %.

SEM : Scanning electron micrographs of ZSM-5 (Fig. 3.8) and zeolite Y (Fig. 3.7), taken as representatives, synthesized in the presence and absence of promoter demonstrate that the crystallite size of samples is smaller and more uniform when the synthesis employs a promoter. The crystallite size of ZSM-5 was 0.8 - 1.0 μm and 1.2 - 2.0 in the presence and absence of Na_2HPO_4, respectively. Corresponding values for zeolite Y were 0.6 - 0.7 μm and 1.0 - 1.5 μm, respectively. From the figure it is clear that crystallite size of the samples synthesized in the presence of promoter (e.g., PO_4^{3-} Fig. 3.7a and 3.8a) vis-à-vis its absence (Fig. 3.8b and 3.9b) is smaller coupled with better uniformity of the particle size distribution. Same observations are obtained for other topologies also. In Fig 3.9 SEM photographs of TS-1 samples synthesized with (Fig. 3.9a) and without (Fig. 3.9b) promoter, H_3PO_4, are shown. From the catalytic point of view, homogeneous distribution of smaller particles are of paramount interest. It is quite expected that the enhanced nucleation and crystallization rates will result in smaller particles with more uniform distribution.

UV-VIS, IR and Ion-exchange : TS-1 material thus obtained was characterized[14,15] by UV-VIS (strong charge-transfer band at ~ 210 nm and no hump or broad peak at 280 - 380 nm) and framework IR (sharp band at ~ 960 cm^{-1} along with other framework vibrations, as depicted in Fig 3.10, curve a with promoter H_3PO_4 and curve b without promoter). Ratio of I_{960}/I_{550} band for the TS-1 samples synthesized with and without promoter were 0.58 and 0.60, respectively. The ion-exchange capacity (K / Al molar ratio in the solid after K^+ exchange) of the ZSM-5 (Si / Al = 20) samples (represented by the curves b and d of Fig. 3.3) was 0.93 and 0.91 respectively.

3.3.4 Catalysis :

The n-hexane cracking was taken as standard reaction for checking the

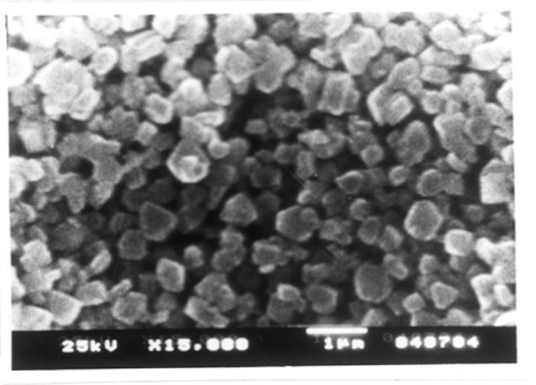

ⓐ

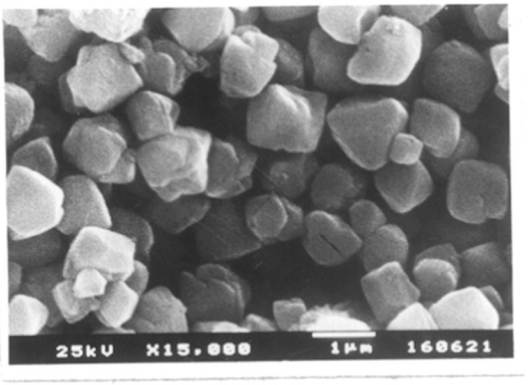

ⓑ

Fig. 3.7 SEM photographs of zeolite Y : (a) with Na_2HPO_4 and (b) no promoter.

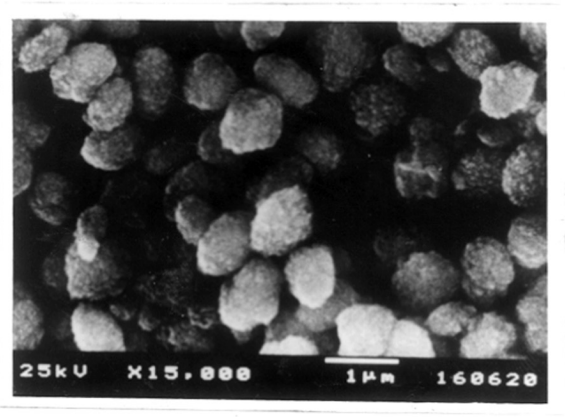

ⓐ

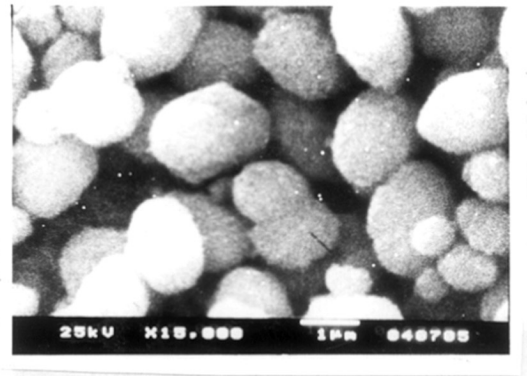

ⓑ

Fig. 3.8 SEM photographs of zeolite ZSM-5 : (a) with NaH_2PO_4 and (b) no promoter.

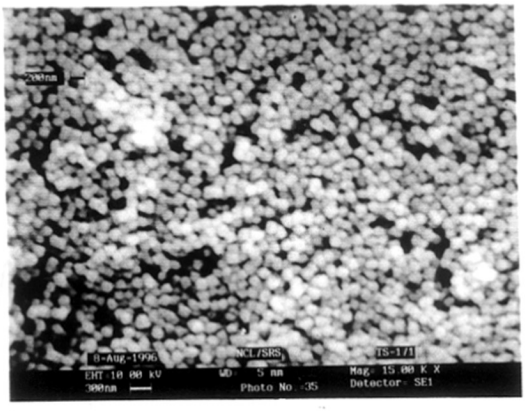

ⓐ

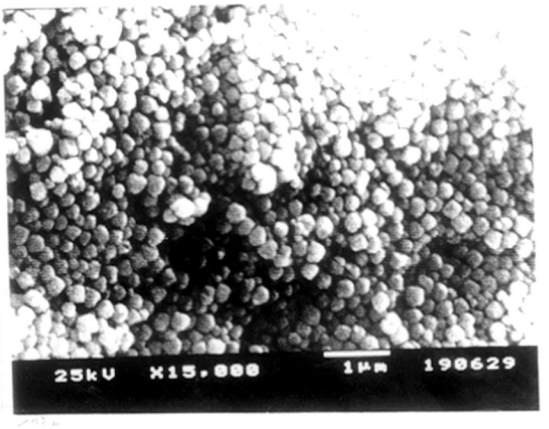

ⓑ

Fig. 3.9 SEM photographs of TS-1 : (a) with H_3PO_4 and (b) no promoter.

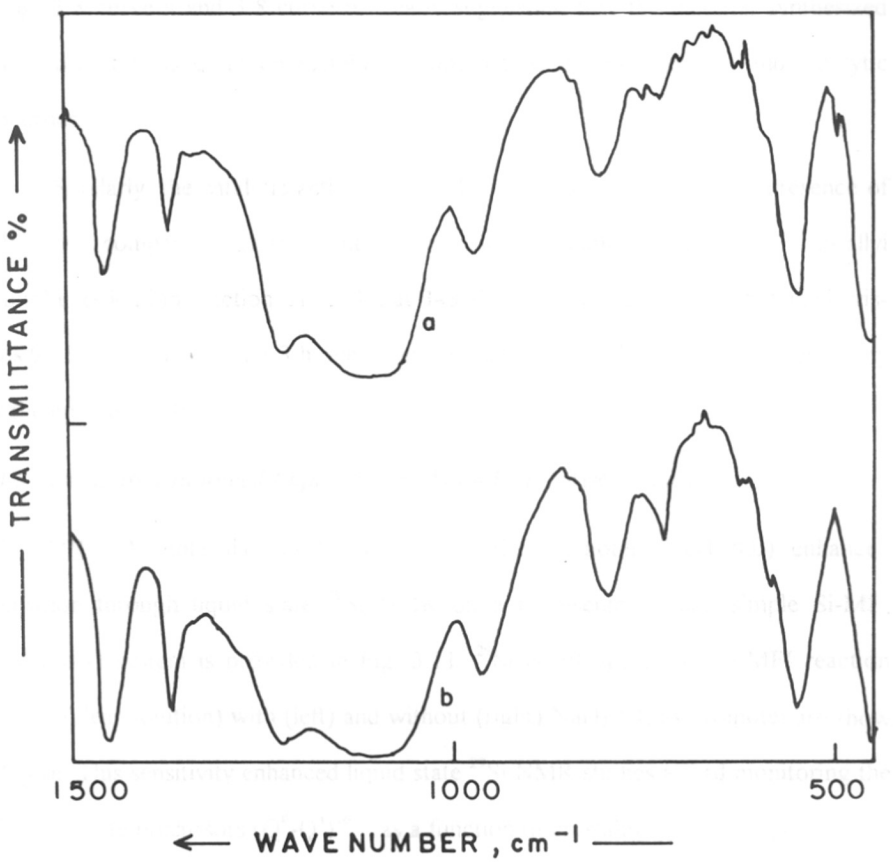

Fig. 3.10 Framework IR Spectra of TS-1 (a) with H_3PO_4 promoter and (b) no promoter.

catalytic activity of the ZSM-5 (Si /Al ≈ 20) samples synthesized with and without using promoters. The *n*-hexane cracking activity (moles of *n*-hexane converted per mole of Al per h) was 18.0 and 17.2 respectively at 623 K for the samples represented in Fig. 3.8 curve a and 3.8 curve b, clearly suggesting that the material synthesized using promoters is quite comparable, if not better, in both textural and catalytic properties.

Similarly, the catalytic activity of the TS-1 samples synthesized in presence of H_3PO_4 was compared with that synthesized under conventional procedure[14,15] in allyl alcohol epoxidation reaction. After 3 h at 343 K, 98 % conversion was obtained (vis-à-vis 95 % conversion after 3 h over conventional TS-1) with equally good selectivity for the epoxide (>95 %).

3.3.5 Sensitivity Enhanced Liquid State ^{29}Si and ^{31}P NMR Studies :

^{29}Si NMR : A molecular level evidence for the promoter (NaH_2PO_4) enhanced nucleation through liquid state ^{29}Si NMR on a representative and simple Si-MFI (Silicalite-1) system is provided in Fig. 3.11. ^{29}Si NMR spectra of Si-MFI reaction mixture (clear solution) with (left) and without (right) NaH_2PO_4 as promoter are shown in figure. This sensitivity enhanced liquid state ^{29}Si NMR studies afford monitoring the soluble silicate precursors (Q^0-Q^4)[16-19] as a function of crystallization time spent during hydrothermal synthesis at 358 K. In Fig. 3.12 the relative concentration of Q^0 - Q^4 silicate species[19] is plotted against the crystallization time of Silicalite-1 in the presence (Fig. 3.12 curve a) and absence (Fig. 3.12 curve c) of promoter. The relative concentration of Q^4 among the total soluble silicate species decreases sharply at the onset of crystallization and vanishes after crystallization. The corresponding crystallinity (as shown by XRD) is also plotted as a function of time (curve b and d). There is a striking correspondence between the increasing crystallinity of Si-MFI, as shown by the corresponding sample through XRD, and the decreasing intensity for the

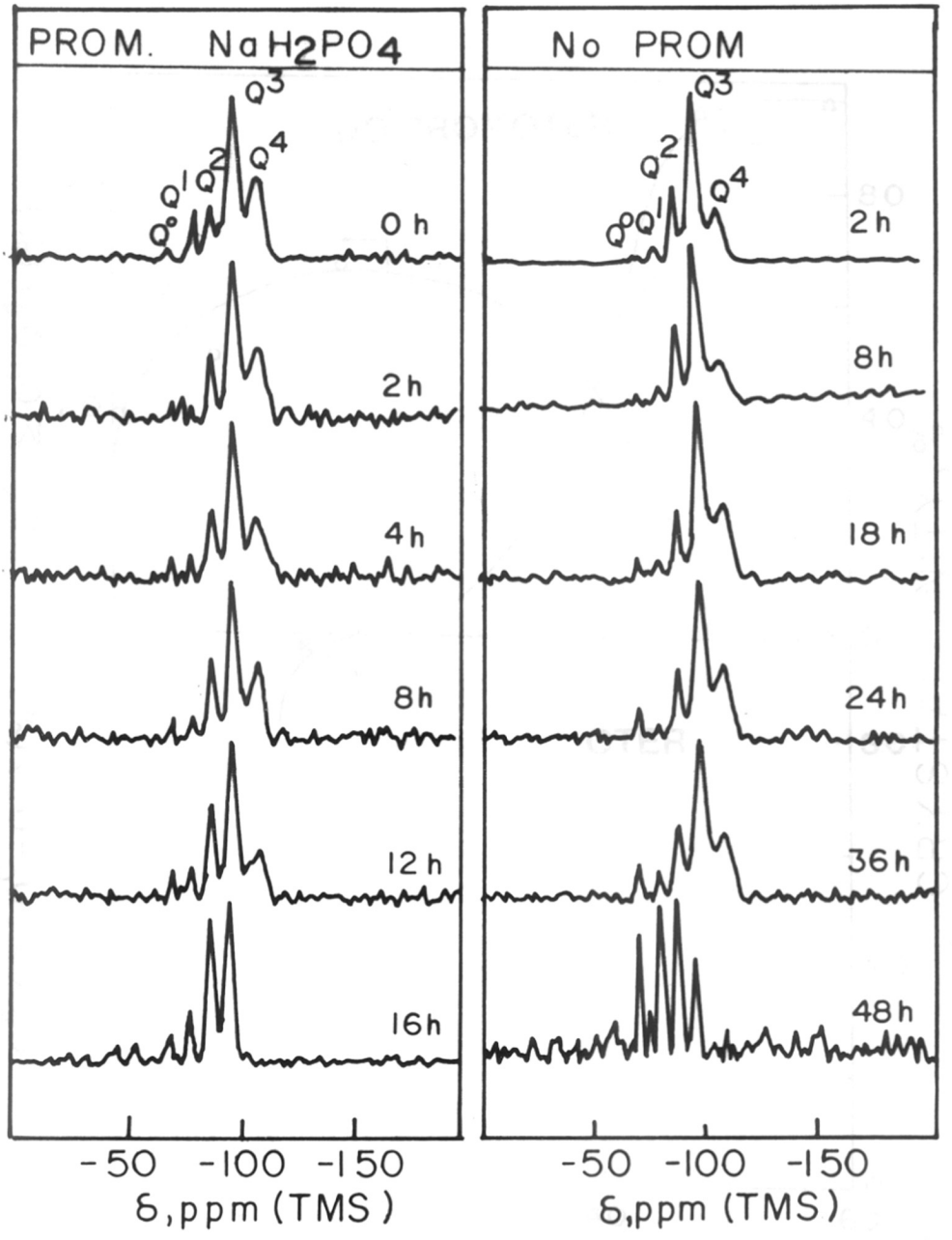

Fig. 3.11 ^{29}Si NMR spectra of Si-ZSM-5 reaction mixture with (left) and without (right) NaH_2PO_4 as promoter. Reaction hours (at 358 K) are given along with each spectrum.

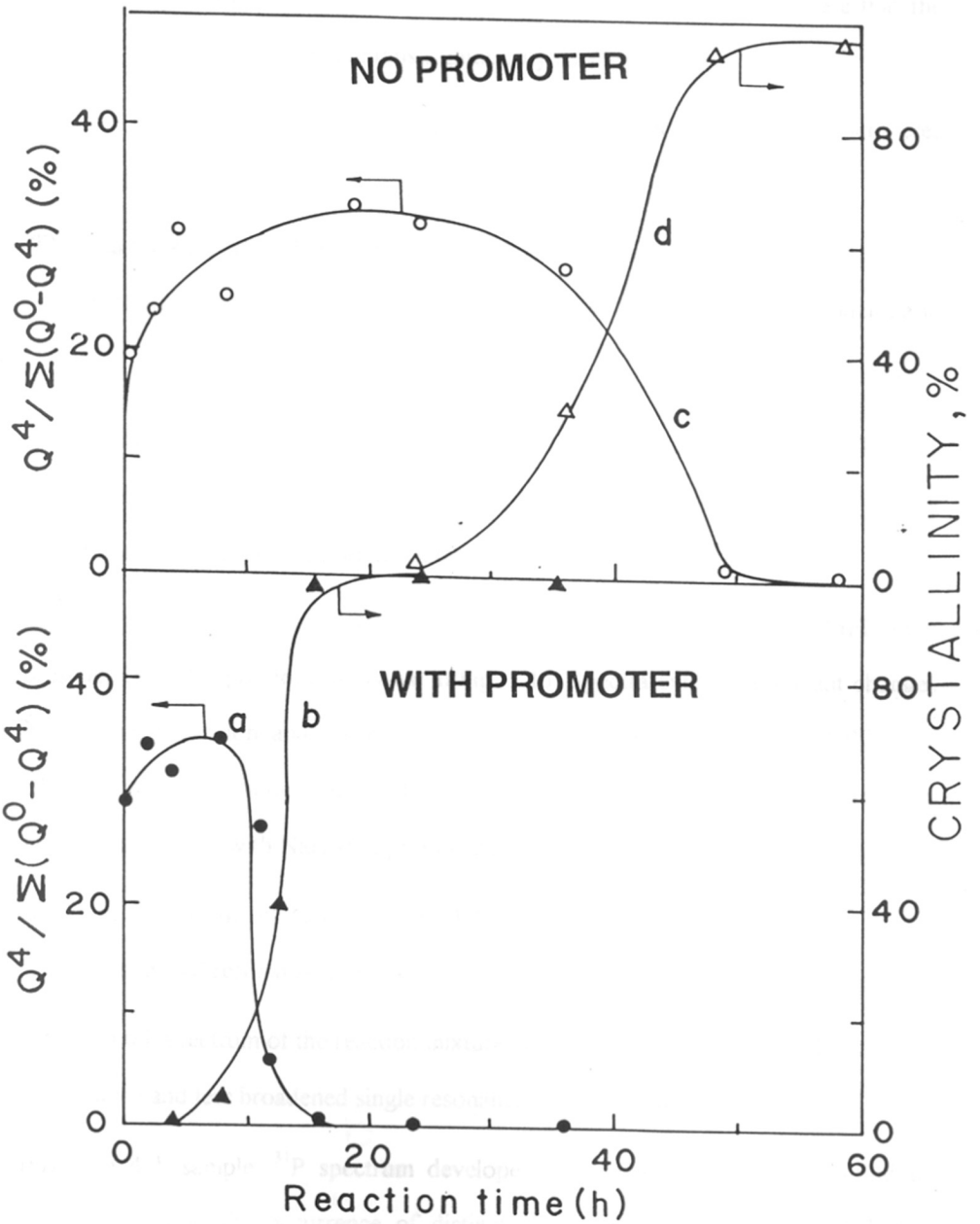

Fig. 3.12 **Reaction time dependence of relative concentration of Q^4 species (from ^{29}Si NMR; left hand ordinate) and percentage crystallinity of the same samples (from XRD; right hand ordinate).**

soluble Q^4 species measured by ^{29}Si NMR, the effect being dramatically fast in the presence of promoter vis-à-vis its absence. These results indeed demonstrate that the presence of promoter phosphate ions significantly accelerates :

(i) the formation of soluble Q^4 species (probably double 3, 4 and 5- membered rings),

(ii) and their rapid condensation into crystalline silicate units in the form of cage and channel structures, which are not detected by liquid state NMR under static conditions.

The longer condensation period observed in hydrogel of Si-ZSM-5 (Fig. 11 and Fig 12) in the absence of promoter is as a result of relative stabilization of soluble Q^4 silicate species in the reaction mixture.

^{31}P NMR : Independent liquid state ^{31}P NMR experiments conducted on Si-MFI in the presence of PO_4^{3-} promoter is shown in Fig. 3.13. Spectra exhibit significant changes in ^{31}P signal position and resolution. ^{31}P NMR (121.443 MHz) of NaH_2PO_4 and TPAOH mixture in water, and 0, 4, 8, 12 and 16 h samples of Si-ZSM-5 reaction mixture (at 358 K) with NaH_2PO_4 promoter exhibit the following spectral features :

(i) In ^{31}P spectra of NaH_2PO_4 and TPAOH mixture (pH = 13.4, high) a single broadened resonance appears.

(ii) In 0 h spectrum of the reaction mixture, an upfield shift occurs (pH = 11.2, low) and less broadened single resonance was detected.

(iii) In 4 h sample, ^{31}P spectrum developed a shoulder with partial resolution, suggesting the occurrence of distinct ^{31}P environments with the exchange occuring between them at a rate that is slow on the NMR time scale.

(iv) In 8 h and 12 h samples, ^{31}P signal does not shift further, but exhibits an

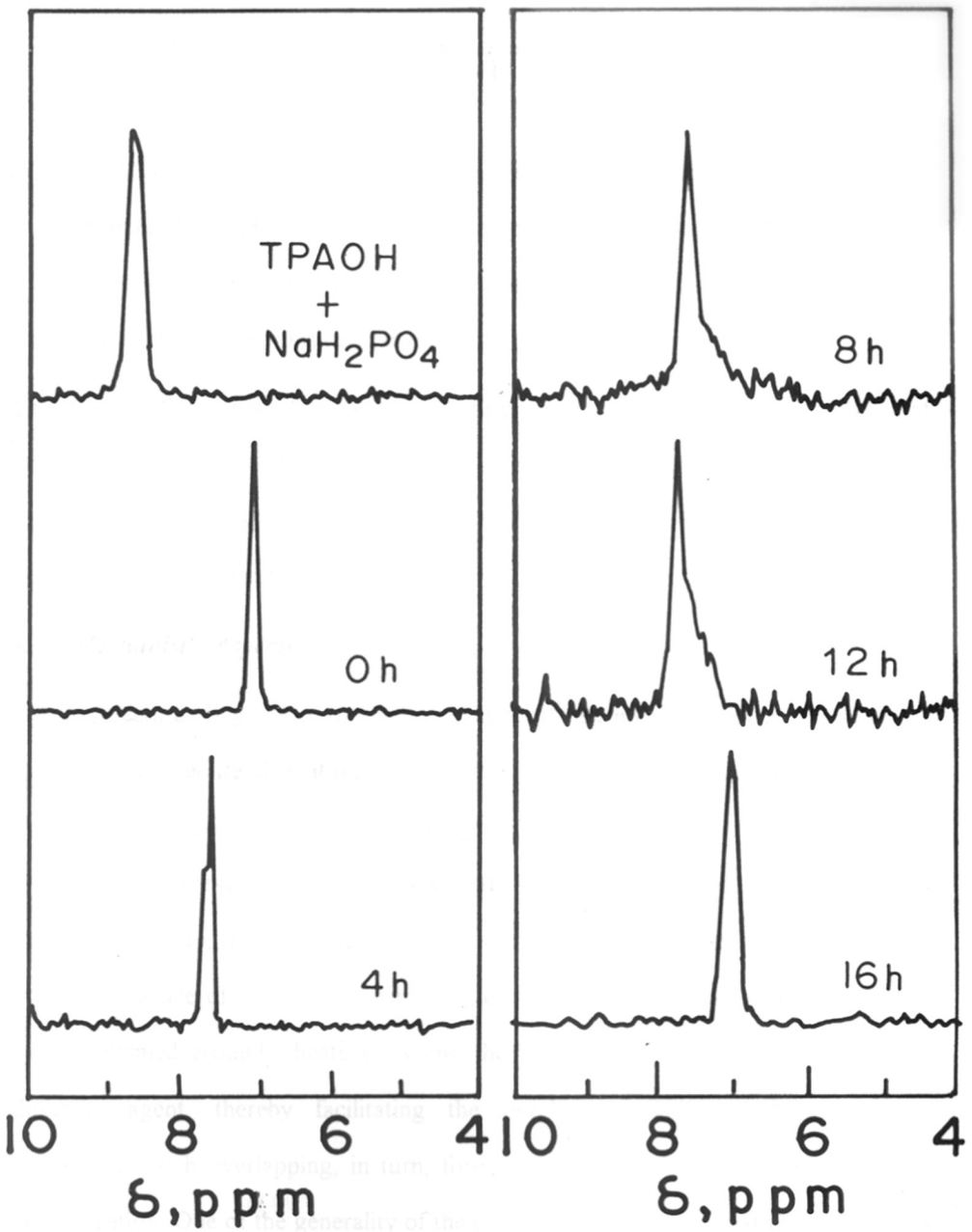

Fig. 3.13 ^{31}P NMR spectra of NaH_2PO_4 + TPAOH and Si-ZSM-5 reaction mixtures (at 358 K) of 0 h, 2 h, 4 h, 8 h, 12 h and 16 h.

asymmetric broad feature. This is not due to shiming problems as the experiments were conducted in a high resolution liquids broad band probe on a well shimmed magnet. These observations are suggestive of an association of promoter with the silicate polyanions - template - water structure.

(V) In 16 h sample, where ^{29}Si NMR shows that all condensable Q^4 species have formed the solid, a reassociation of the promoter with water is thought to lead to the observation of a broadened ^{31}P resonance as at that of very beginning (0 h), except for its position (pH effect).

Thus the significant change in ^{31}P signal position and resolution as well as retention of original ^{31}P structure after crystallization indicates a catalytic role played by the promoter in enhancing zeolite crystallization. Phosphate was taken as representative example due to its abundance.

3.3.6 Mechanistic Aspects :

Recent findings of Davis[20] and Knight et al[21]. strongly support the clathration - hypothesis of zeolite formation where the silicate polyanions (mainly Q^4 species) clathrate the organic structure directing agent (TPA in Si-ZSM-5 system). Davis has proposed that these clathrated TPA-silicate hydrophobic hydration spheres come closer and overlap, thus forming composite species leading to crystal growth. It seems that the presence of promoter oxyanions greatly polarizes the hydrophobic hydration spheres formed around silicate units and the alkyl groups of the organic structure directing agent, thereby facilitating the overlap of TPA-enclathrated silicate polyanions. Such overlapping, in turn, forms the composite species at the onset of crystallization. One of the generality of the promoter oxyanions is that they all possess central element of very high oxidation state. Thus their Z / r (i.e., charge / radius ratio or charge density) is very high, which, in turn, is proportional to the polarizing ability of the central cation. Supporting the above proposition, a good correlation was

observed between the Z/r of central element of the promoter oxyanions and the corresponding crystallization time of ZSM-5 synthesized in the presence of such promoters (Fig. 3.14). From the figure it is clear that, as the polarizing ability (greater Z/r value) of oxyanions increases, crystallization becomes faster.

One of the fundamental requirement of network formation between two heteroelement oxides is their relative hardness. According to Pearson's Hard-Soft-Acid-Base principle Hard acid - Hard base will give stable network only when both component parts have matchable hardness, e.g., hard acid SiO_2 binds with hard base Al_2O_3 to give stable zeolite network. Further, the ionic size of Si^{4+} should also match with that of heterometal ion, as far as possible for better connnectivity and incorporation. Now, promoter oxyanions chosen, posses higher hardness and acidity than SiO_2 and Al_2O_3. Thus when competition arises between Al^{3+} and these promoter central element to incorporate in the silicate network, preferentially it is Al^{3+} which is expected to form bonding with silicate units. Probably, this is the reason, along with smallar or larger ionic sizes of the promoters (vis-à-vis Si^{4+} and Al^{3+}) for non-incorporation of the promoters. Higher solubility of these promoter oxyanioons in the synthesis medium may also be responsible for their non-incorporation.

3.4 CONCLUSION :

Oxyanions and their corresponding oxyacids of Gr IV, V, VI and VII elements (viz. ClO_4^-, SO_4^{2-}, PO_4^{3-}, CO_3^{2-} etc.) enhances the nucleation and crystallization of zeolites and related molecular sieves to varying extent. The effect is very general in nature and equally applicable, independent of zeolite structure (viz. small, medium or large pore) and composition (low silica, high silica, pure silica or metallosilicates). Liquid state ^{29}Si and ^{31}P NMR experiments indicate the interaction of these promoter oxyanions with template enclathrated silicate-water structure at the onset of crystallization, in enhancing the crystallization rate.

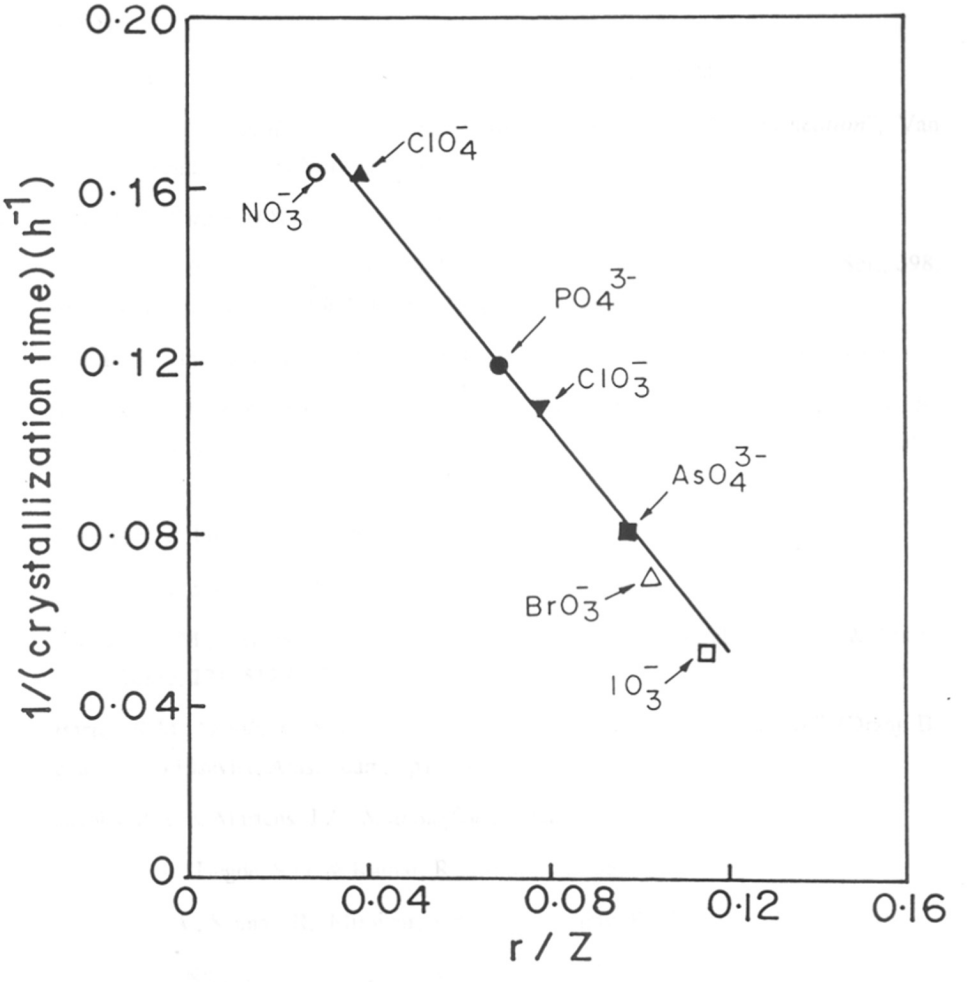

Fig. 3.14 Plot of crystallization time against charge / radius ratio of the central cation in promoter NO_3^- (○) ClO_4^- (▲), PO_4^{3-} (●), ClO_3^- (▼), AsO_4^{3-} (■), BrO_3^- (Δ) and IO_3^- (□) in the synthesis of zeolite ZSM-5.

3.5 REFERENCES :

1. Barrer, R.M., "*Hydrothermal Chemistry of Zeolites*", Academic Press, New York, (1982).
2. Break, D.W., "*Zeolite Molecular Sieves*", Wiley, New York (1974).
3. Szostak, R., "*Molceular Sieves : Principals of Synthesis and Identification*", Van Nostrand Reinhold, New York (1989).
4. Roland, E., *Stud.Surf.Sci.Catal.*, **46**, 645 (1989)..
5. Inui, T., "*Zeolite Synthesis*", (Occelli, M. & Robson, H.E., Eds.) ACS Symp. Ser., **398**, Am.Chem. Soc., Washington D.C., Ch.33, pp 479 (1989).
6. Kumar, R., Bhaumik, A., Ahedi, R.K. & Ganapathy, S., *Nature*, **381**, 298 (1996).
7. Ratnasamy, P., Kotasthane, A.N., Shiralkar, V.P., Thangaraj, A. & Ganapathy, S., "*Zeolite Synthesis*", (Occelli, M. & Robson, H.E., Eds.) ACS Symp. Ser., **398**, Am.Chem. Soc., Washington D.C., Ch.28, pp 405 (1989).
8. Carr, H.Y. & Purcell, E.M., *Phys. Rev.*, **94**, 630 (1954).
9. Meiboom, S. & Gill, D., *Rev.Sci.Instrum.*, **29**, 688 (1958).
10. Flanigen, E.M., Bennet, J.M., Grosse, R.W., Patton, R.L., Kirchner, R.M. & Smith, J.V., *Nature*, **271**, 512 (1978).
11. Barrer, R.M., "*Zeolites : Synthesis, Structure, Technology and Application*", (Drzaj, B., et al., Eds.) Elsevier, Amsterdam, pp1 (1985).
12. Jacobs, P.A. & Martens, J.A., *Stud.Surf.Sci.Catal.*, **33**, 58 (1987).
13. Bhaumik, A., Hegde, S.G. & Kumar, R., *Catal.Lett.*, **35**, 327 (1995).
14. Thangaraj, A., Kumar, R., Mirajkar, S.P. & Ratnasamy, P., *J.Catal.*, **130**, 1 (1990).
15. Reddy, J.S., Kumar, R. & Scisery, S.M.,.*J.Catal.*, **145**, 73 (1994).
16. Knight, C.T.G., Kirkpatrick, R.J. & Oldfield, E., *J.Am.Chem.Soc.*, **108**, 33 (1986).
17. Knight, C.T.G., Kirkpatrick, R.J. & Oldfield, E., *J.Am.Chem.Soc.*, **109**, 1632 (1987).
18. Thangaraj, A., Sivasanker, S. & Ratnasamy, P., *Zeolites*, **130**, 1 (1991).
19. Engelhardt, G. & Michel, D., "*High-Resolution Solid-State NMR of Silicates and Zeolites*", Ch3, pp75, Wiley, New York (1987).
20. Davis, M.E., *Stud.Surf.Sci.Catal.*, **97**, 35 (1995).
21. Knight, C.T.G., Syvitski, R.T. & Kinrade, S.D., *Stud.Surf.Sci.Catal.*, **97**, 483 (1995).

CHAPTER 4

SELECTIVE LIQUID PHASE OXIDATION CATALYSIS UNDER BIPHASE USING SOLVENTS

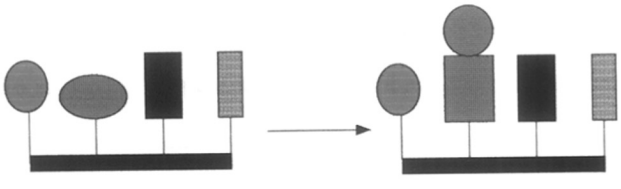

4.1 INTRODUCTION :

Among all the metal containing molecular sieves, titanium-containing silica-based materials, particularly, TS-1[1,2], TS-2[3] are extensively studied in selective oxidation reactions in liquid phase using dilute hydrogen peroxide as oxidant[2-5]. Vanadium silicates are also used in oxidation catalysis. Although these catalysts are used extensively, the main emphasis has been made on the regio-selectivity and no information is available on chemo-selectivity. The chemoselective oxidation of organic compounds involves selective oxidation of one functional group among two or more reactive moieties / functional groups present in the same molecule. Present chapter deals with chemoselective oxidation of allylic alcohols and aldehydes over TS-1 catalyst under biphase (one solid phase, i.e. catalyst and another liquid phase consisting of organic substrate, aqueous hydrogen peroxide in presence of a cosolvent to homogenize the liquid layers) condition. The substrates used are allyl- and methallyl-alcohols, allyl- and methallyl-chlorides, acrolein and methacrolein.

Oximes are very important raw materials in various industries - from polymer to paints and petrochemicals. Although the ammoximation[6,7] of cyclohexanone to its oxime over TS-1 has been reported[8], little is known about the ammoximation of other carbonyls (specially of aldehydes). Moreover, the reaction conditions vary largely from the substrate to substrate. This chapter also describes an generalized methodology for the liquid phase ammoximation of various carbonyls in a simple way using TS-1, H_2O_2 and liquid or gaseous ammonia in presence of organic cosolvent without any significant co-production of by-products.

4.2 EXPERIMENTAL :

TS-1 (Ti-MFI, Si / Ti = 27) was synthesized and characterized by well known published procedures[4,5]. The details are described in Chapter 2 (conventional

method) and Chapter 3 (using promoter[9]). The liquid phase chemoselective oxidation reactions were carried out in a three neck (100 ml capacity) glass batch reactor (Fig. 4.1); one neck was fitted to condenser and remaining two were fitted to rubber septum. The temperature of the reaction vessel was maintained by using an oil bath. The reaction condition were : temperature 323 - 353 K, catalyst 20 wt % with respect to substrate, substrate : H_2O_2 mole ratio = 1 : 1, solvent acetone, acetonitrile or methanol. In ammoximation reaction,the substrate : H_2O_2 : NH_3 molar ratio was kept at 1 : 1.2 : 2.0. Hydrogen peroxide (30 % aqueous) as well as liquid ammonia were injected dropwise through the rubber septum using feed pump (Sage instruments, USA) through two syringes simultaneously, for a period of 0.5 h to 3 h depending upon the substrate and the rate of the reaction. At different time intervals small aliquots were taken out from the reaction mixture and were analyzed by high resolution capillary gas chromatography (HP 5880, HP 5890 and Shimadzu R-17A using Flame Ionization Detector).

4.3 RESULTS AND DISCUSSION :

4.3.1 Characterization :

The physico-chemical characteristics of TS-1 sample are given in Chapter 3 (Section 3.3.3, Fig. 3.9 and Fig. 3.10). The samples were highly crystalline and free from crystalline and amorphous impurities. Scanning electron micrograph revealed that the TS-1 crystals consists of uniform cuboid crystallites of 0.1 - 0.2 μm (Fig 3.10).

4.3.2 Catalysis :

4.3.2.1. Chemoselective Oxidation :

4.3.2.1.1 Effect of Substrate :

Fig. 4.2 depicts the conversion (I) and product selectivity (II) in the oxidation of allyl alcohol (A) and methallyl alcohol (B), with H_2O_2 over TS-1. Allyl alcohol is

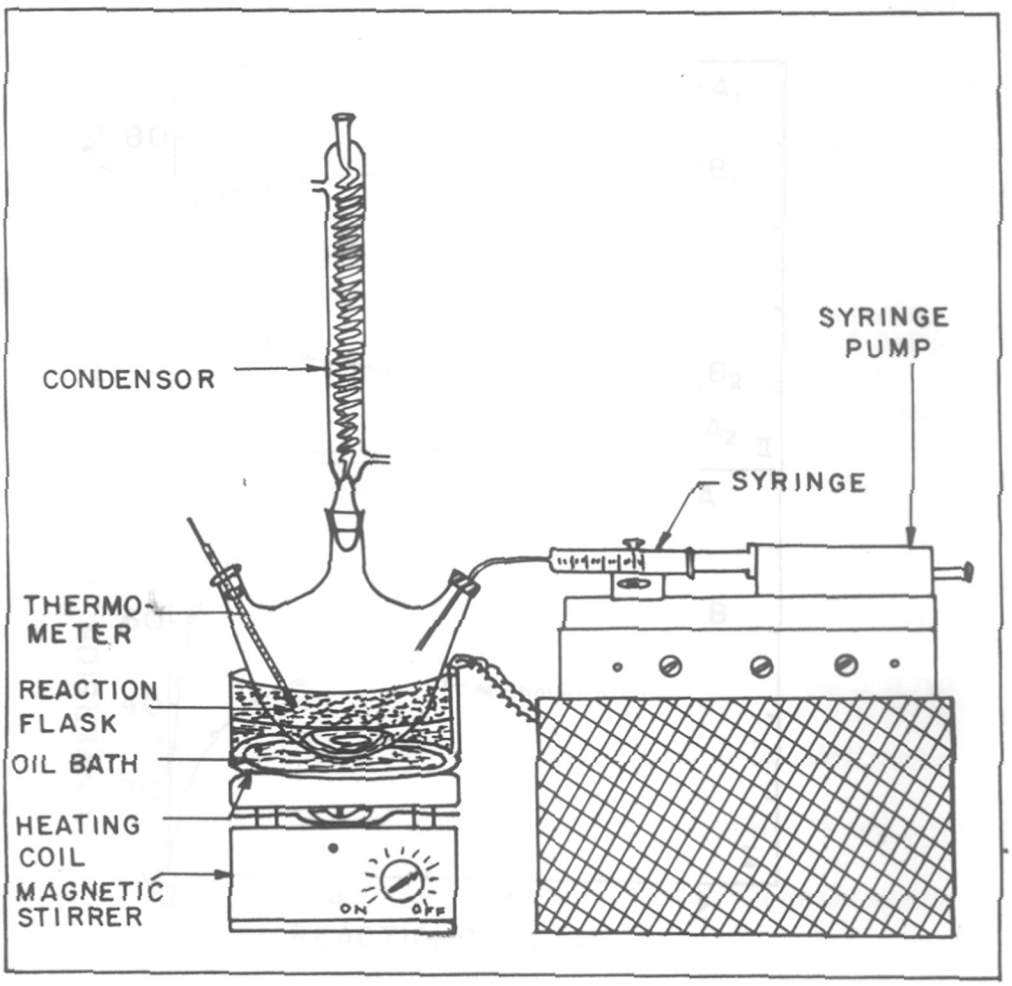

Fig. 4.1 : Schematic diagram of liquid phase batch reactor.

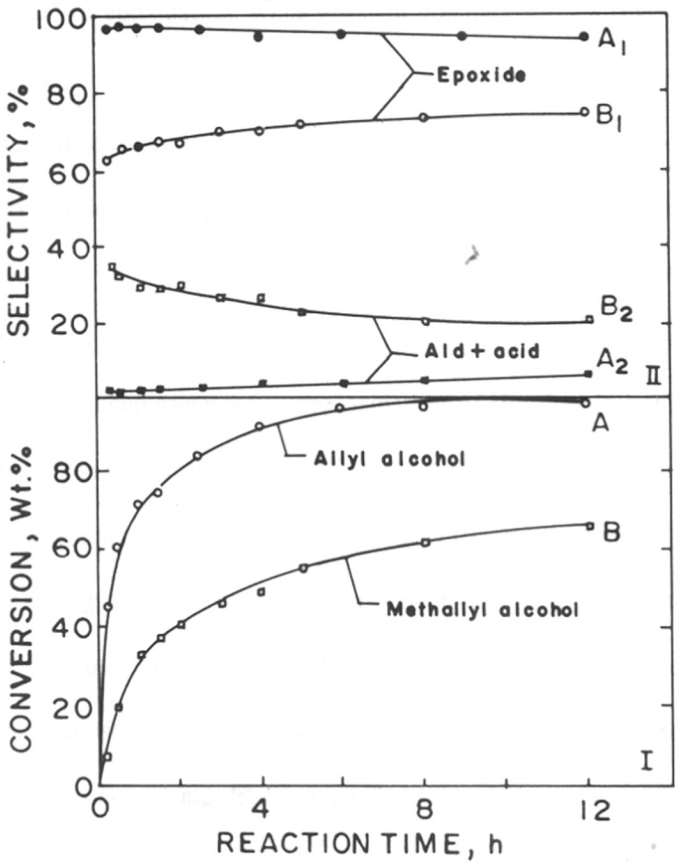

Fig. 4.2 : **Conversion (I) and selectivity (II) as a function of reaction time in the oxidation of allyl alcohol. Curves A, A_1 and A_2 represent allyl alcohol, glycidol and acrolein + acrilic acid, respectively. Curves B, B_1 and B_2 represent methallyl alcohol, methyl glycidol, methacrolein + methacrylic acid, respectively.**

converted faster than the methallyl alcohol. Using soluble Ti (IV) complexes as catalyst under homogeneous conditions it has been found during alkene epoxidation reaction that the electron withdrawing groups attached to the alkene double bond decrease the rate of epoxidation, while electron donating groups (like $-CH_3$ group in methallyl alcohol) increase the rate[10]. The higher reactivity of allyl alcohol vis-à-vis metahllyl alcohol observed in the present case (Fig. 4.2I) in contrast to the homogeneous solution[11,12], is probably a manifestation of the reactant shape selectivity exhibited by the TS-1 molecular sieve in retarding the diffusion of bulkier methallylalcohol to the Ti (IV) active sites located inside the channel system. Regarding product chemoselectivity, the oxidation of the double bond (to yield the epoxide) rather than that of the $-CH_2OH$ group (to yield the corresponding aldehyde / acid) is more prominent in the case of allyl alcohol (95 %) than methallyl alcohol (75 %) as shown in Fig. 4.2II. The higher chemoselectivity for oxidation of the $-CH_2OH$ group (vis-à-vis epoxidation) in methallyl alcohol, compared to the allyl alcohol (aldehyde / acid constitute 20 % of the products in the former compared to only 5 % in the latter case) is interesting. Electronic effect of methyl group alone cannot explain this phenomenon. The greater steric crowding at the reaction site (the C=C double bond) in case of methallyl alcohol, relative to allyl alcohol, is perhaps, responsible for the lower relative reactivity of the carbon - carbon double bond vis-à-vis the $-CH_2OH$ group. It is probably an illustration of restricted transition state shape selectivity leading to chemoselectivity in a molecule containing two oxidizable functional groups.

Table 4.1 compares the oxidation of unsaturated alcohols (allyl and methallyl) with the analogous chlorides. Epoxidation is the only oxidation reaction in the case of

Table 4.1 : Oxidation of different substrates over TS-1[a] :

Substrate	Temp.	Conv.	Selectivity %			
	(K)	wt %	epoxide	aldehyde	acid	Others[b]
Allyl alcohol	323	65.0	96.0	4.0	-	-
Allyl chloride	323	90.0	95.0	-	-	5.0
Methallyl alcohol	333	62.0	72.0	12.0	10.0	6.0
Methallyl chloride	333	72.0	90.0	-	-	1 0.0

a: Solvent : acetonitrile (10 g); TS-1 / Substrate (wt / wt) = 0.2; reaction time = 8h.

b: Mainly cleaved products of epoxide.

the allylic chlorides. In agreement with Clerci et al[13]. the conversion with allyl chloride was higher than that with allyl alcohol (90 % compared to 70 %) under similar reaction conditions. The greater electronegativity / electron withdrawing character of oxygen (vis-à-vis chlorine) is expected to lower the rate of epoxidation as observed in homogeneous systems.

Fig. 4.3 depicts the result of allyl alcohol, methallyl alcohol, acrolein and methacrolein oxidation over TS-1 / H_2O_2 system. From the figure following features are observed[14] :

a) In the case of allyl alcohol, the chemoselectivity for epoxidation (rather than oxidation of -CH_2OH group to -CHO group) is higher than that obtained for methallyl alcohol.

b) As expected, the chemoselectivity for the oxidation of -CHO (rather than epoxidation) in acrolein and methacrolein is observed.

4.3.2.1.2 Effect of Solvent :

Table 4.2 exhibits the influence of different solvents in the epoxidation of allyl alcohol over TS-1. In the case of acetone and acetonitrile (aprotic solvent) the conversion and epoxide selectivity are quite high. However, in protic solvents like methanol and ethanol epoxide selectivity is low mainly due to the cleavage of epoxide through alcoholysis, in accordance with earlier results in the epoxidation of olefins[13,14]. Interestingly, in epoxidation of allyl- and methallyl chlorides using protic solvents like methanol as cosolvent, reaction occurs at a very high rate, compared to that when aprotic solvents were used, although, the selectivity for epoxide was quite low mainly due to the cleavage of oxyrane ring (Table 4.2).

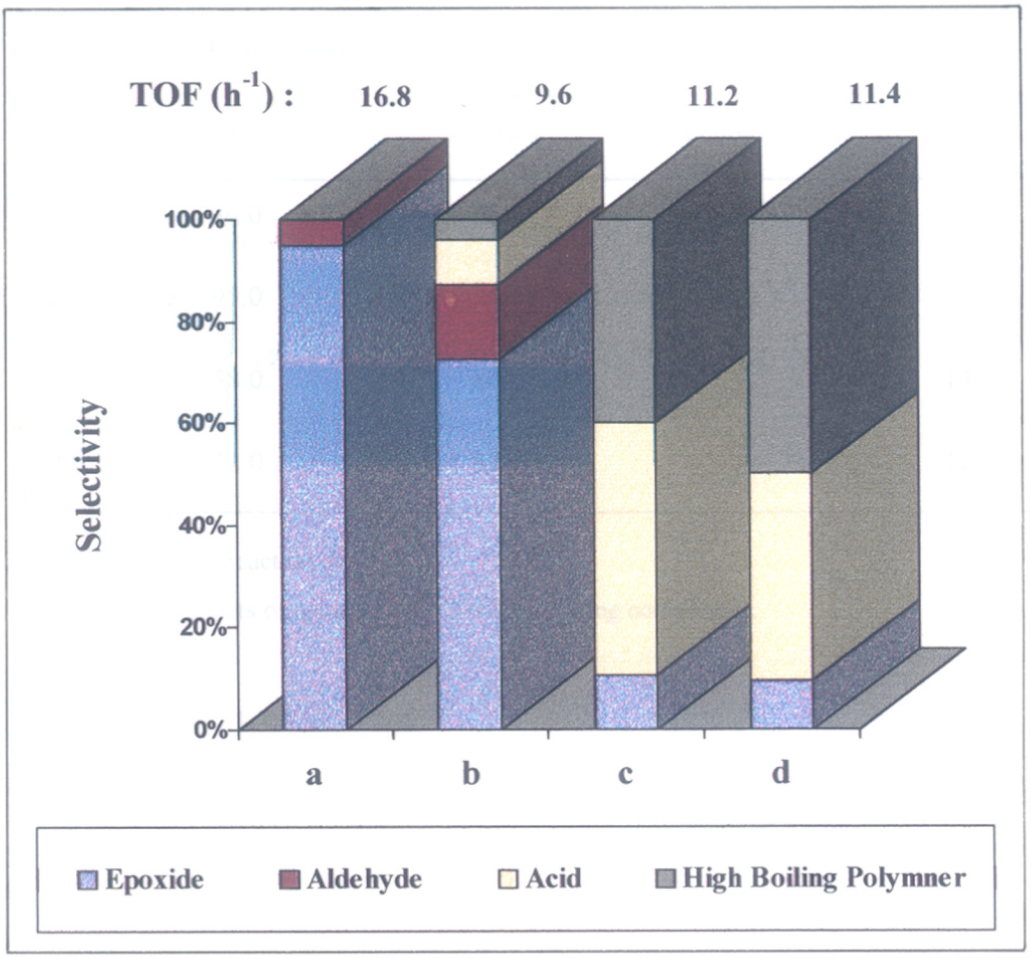

Fig. 4.3 : **Activity (TOF, h^{-1}) and selectivity of TS-1 in oxidation of allyl alcohol (a), methallyl alcohol (b), acrolein (c) and methacrolein (d).**

Table 4.2 : Influence of solvent in epoxidation of allyl alcohol over TS-1 / H_2O_2 system[a] :

Solvent	Conversion	Product selectivity, %		
	wt %	epoxide	aldehyde	others[b]
Acetone	96.0	96.0	4.0	-
Acetonitrile	95.0	95.0	5.0	-
Ethanol	58.0	86.0	-	14.0
Methanol	52.0	82.0	-	18.0

a: Temp. 333 K, reaction time = 8 h.

b: Cleaved products of epoxide and other high boiling compounds.

4.3.2.1.3 Mechanistic Aspects :

Clerici et al[13]. as well as Tatsumi et al[15]. have earlier shown that over TS-1, epoxidation occurs probably by a heterolytic mechanism. A possible mechanism for epoxidation over TS-1 is shown below (Scheme 4.1), which involves the formation of titanium peroxo species (III and IV, Scheme 4.1) at the initial stage followed by its attack selectively to the olefinic double bond to give the corresponding epoxide in a concerted manner. Species II thus formed react with another molecule of H_2O_2 to give back species III or IV, which catalyzes the next substrate and this chain reaction continues until all H_2O_2 get consumed.

4.3.2.2 Ammoximation of Carbonyls :

4.3.2.2.1 Ketones :

Table 4.3 summarizes the conversion and selectivity data of ammoximation of different carbonyls over TS-1 / H_2O_2 / NH_3 system[16]. Corresponding turn over frequencies (TOF) and the time of completion of reaction of various substrates are also given. As the +I effect of the alkyl groups increases in the carbonyls from acetone to isobutyl ketone via 2-butanone, the rate of the reaction as well as % conversion at a given time increases. However, slight increase in TOF in the case of 2-butanone and isobutyl ketone indicates that slightly more bulkiness of the later may also be the contributing factor. Cyclic ketone, like cyclohexanone undergo facile ammoximation, bulkier acetophenone and *p*-hydroxy acetophenone react very slowly resulting in less conversion and TOF.

4.3.2.2.2 Aldehydes :

In the case of aldehydes the ammoximation reaction is vary fast and within 1.5 h to 2.0 h almost 100 % conversion level can be achieved along with 99 % oxime

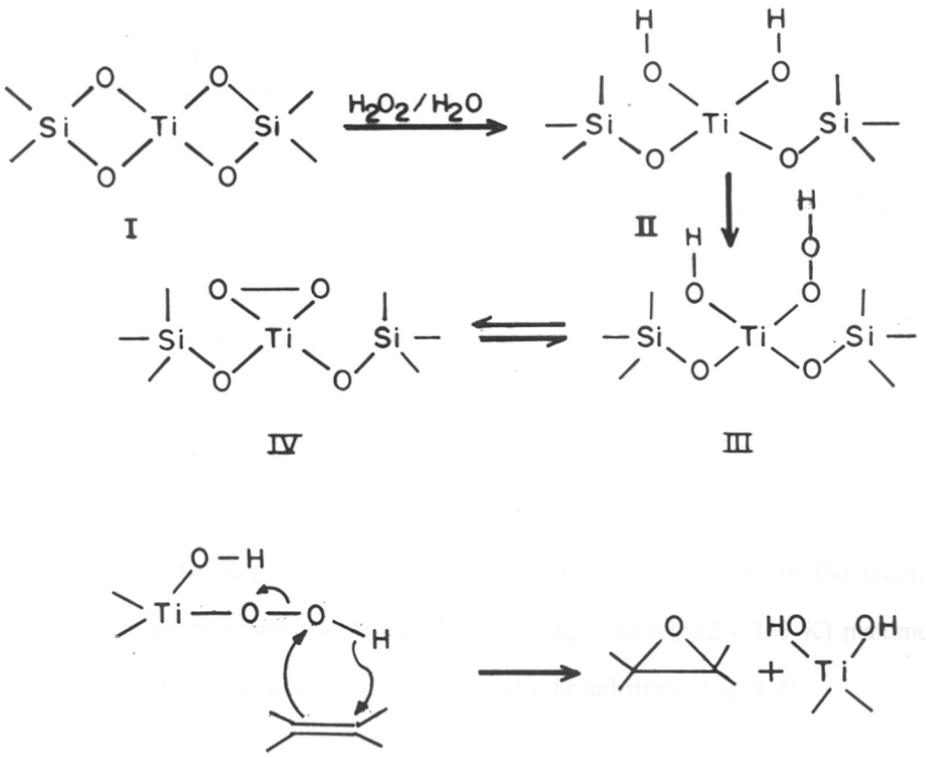

Scheme 4·1

selectivity. If we compare the rate of conversion of carbonyl moiety to the corresponding oxime between acetophenone and benzaldehyde, the mere replacement of $-CH_3$ group of the former by -H of the latter, increases the rate of the reaction as well as yield of the product drastically (Table 4.3, entry 9 vs. 6). Same effect was observed between *p*-hydroxy acetophenone and *p*-tolualdehyde (keeping into consideration that the steric and electronic factors arising due to *para* -OH / $-CH_3$ group remains almost the same), where in the later case the reaction is very fast. Introduction of chloro group (as in the case of *o*-chloro benzaldehyde) does not change the rate of the reaction and product yield to a considerable extent.

In the case of but-2-one, cyclohexanone and acetophenone, some rearrangement products are formed having identical molecular weight (confirmed through GC MS) to that of the oxime. This may be due to oxime - oxamino tautomarism and / Beckman rearrangement. The ease of the formation of these by-products seems to be predominantly controlled by the temperature of the reaction medium for a given cosolvent. At an optimum temperature (333 - 353 K) maximum oxime selectivity can be obtained depending upon the substrate (Fig. 4.4).

4.3.2.2.3 Influence of Temperature :

For all the carbonyls there is an optimum range of reaction temperature at which maximum conversion level as well as oxime selectivity can be achieved. Beyond that temperature range, the decomposition of H_2O_2 as well as evaporation of ammonia from the reaction mixture increases and hence H_2O_2 and NH_3 are less effectively utilized leading to lower yield of the product. At low temperature the rate of ammoximation is very slow leading to lower conversion. However, the increase in reaction temperature beyond the optimum range increases the by-product formation to a large extent. This point is illustrated in Fig. 4.4 where the effect of temperature on

Table 4.3 : Ammoximation of various carbonyls over TS-1 :

Entry	Substrate	TOF, h^{-1}	Time, h	Conversion %	Oxime sel. %.
1.	Acetone	31.0	6.0	83.5	98.2
2.	But-2-one	39.7	4.0	95.0	93.0
3.	Methyl isobutyl ketone	41.9	3.0	98.3	99.5
4.	Cyclohexanone	31.5	4.0	98.7	96.4
5.	Acetophenone	5.4	8.0	41.6	90.8
6.	*p*-Hydroxy acetophenone	1.6	12.0	20.3	100.0
7.	*p*-Tolualdehyde	51.2	2.0	97.5	97.7
8.	Benzaldehyde	46.2	2.5	98.5	99.4
9.	*o*-Chloro benzaldehyde	34.8	2.5	97.5	99.0

a: temperature 343 K, catalyst 15 wt % of the substrate, Substrate : H_2O_2 : NH_3 = 1 : 1.2 : 2.0, Solvent = *t*-butanol.

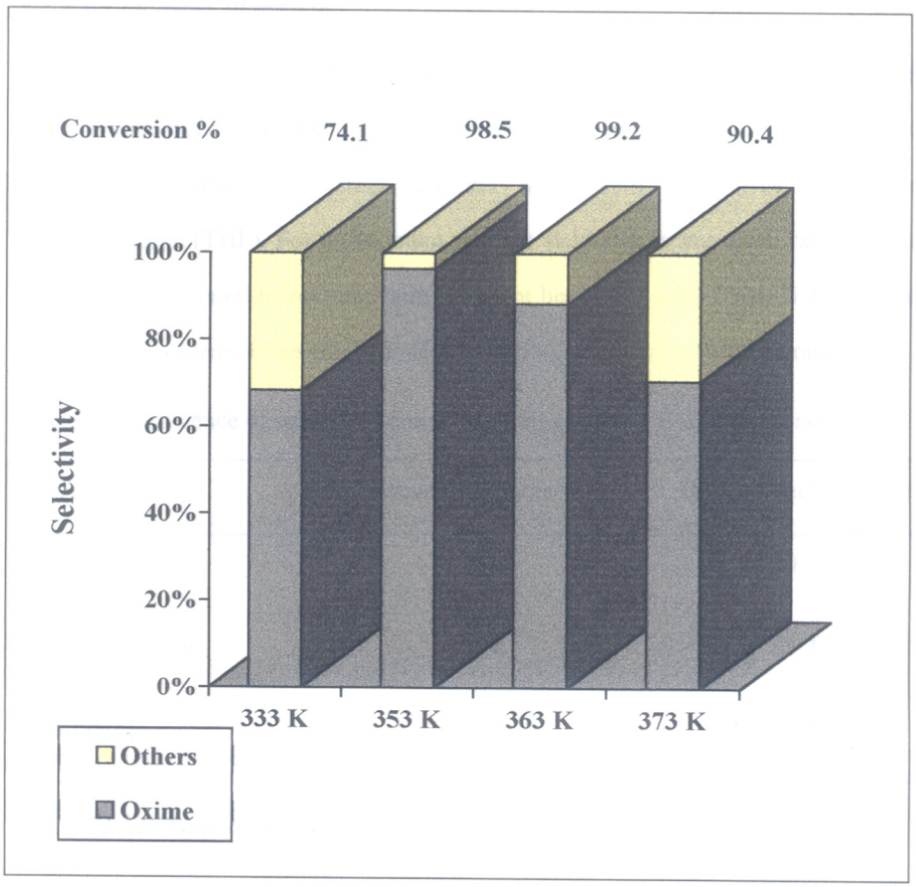

Fig. 4.4 : Effect of temperature in ammoximation of cyclohexanone over TS-1

conversion and oxime selectivity in the ammoximation of cyclohexanone is depicted.

4.3.2.2.4 Influence of Solvent :

Among all the solvents chosen for ammoximation reactions, *t*-butanol - water mixture was found to be most suitable solvent as far as effective utilization of H_2O_2 and NH_3 is concerned. Other solvents tried were acetonitrile, water and tetrahydrofuran (THF). For a maximum product yield and an improved rate, the ratio (wt / wt) of *t*-butanol to reactant ratio was kept between 3 to 4. Table 4.4 represents the effect of solvent on the ammoximation reaction of methyl isobutyl ketone.

Table 4.4 : Influence of solvent on ammoximation of methyl isobutyl ketone

Solvent	Conversion (mole %)	Oxime selectivity (%)
t-Butanol	98.3	99.5
Tetrahydrofuran	78.4	96.4
Acetonitrile	72.3	96.2

4.3.2.2.5 Mechanistic Aspects :

There are mainly two types of mechanism for ammoximation of carbonyls reported[8,17,18], both involving titanium peroxo species in presence of H_2O_2 as shown in Scheme 4.2.

(A) Catalytic activation of ammonia through species III leads to hydroxyl amine, which in turn reacts with carbonyl group to form corresponding oxime in usual way.

(B) The reaction of ammonia occurs with carbonyls to form the corresponding

imine, which in turn undergoes catalytic oxidation through Ti-peroxo species into the respective oxime.

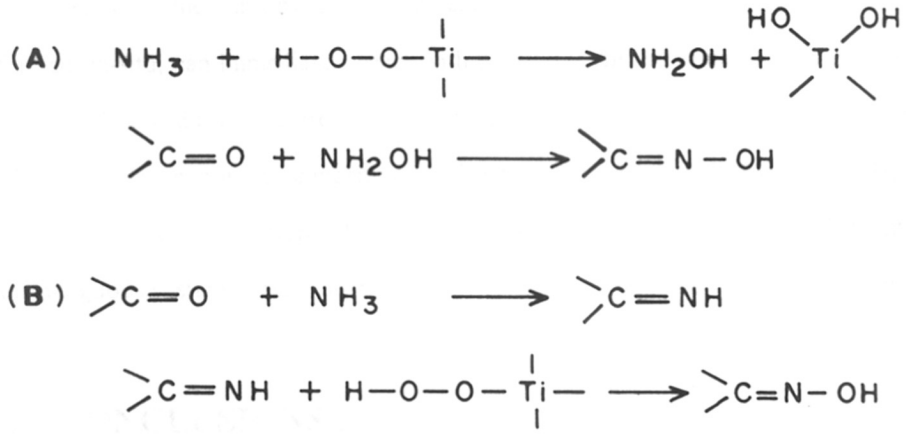

Scheme 4·2

If mechanism (A) is predominantly operative, the size of the carbonyls may not be very crucial and the reaction rate would be governed by the electronic nature of the substrates. However, the mechanism (B) involving imine formation, will be significantly influenced by diffusional limitation of the intermediate imine to reach the active sites in TS-1 / H_2O_2 pores. In fact, Reddy et al[19], have shown that during ammoximation of cyclohexanone, acetophenone and benzophenone by TS-2 / H_2O_2 / NH_3 system, the reactivity pattern was :

Cyclohexanone > Acetophenone >> Benzophenone

The size of the above ketones follows the reverse trend, suggesting that the diffusion of reactant carbonyl is crucial for catalytic ammoximation of carbonyls. This observation apparantly supports the mechanism (B).

However, the efficient utilization of relatively less stable NH_2OH may be expected when the carbonyl is also present around the active sites, so that NH_2OH formed, in-situ, can immediately react with substrates. In the case of bulky carbonyls, NH_2OH has to diffuse out from the zeolitic pores to react with carbonyl compounds. This may also cause decomposition, at least in part, during diffusion of NH_2OH, leading to less conversion of bulky substrates. Hence it is rather difficult to unambiguously state, based on the reactivity pattern, that the mechanism A is not operative.

4.4 CONCLUSIONS :

4.4.1 Chemoselective Epoxidation / Oxidation :

* Titanium silicate molecular sieve (TS-1) exhibit higher chemo-selectivity for epoxidation of allyl alcohol (rather than the oxidation of $-CH_2OH$ group to -CHO) compared to that obtained in the case of methallyl alcohol.
* The -CHO group, when present adjacent to the double bond (as in acrolein and methacrolein) suppresses both the total conversion (due to electron withdrawing effect) and chemoselective epoxidation of double bond (due to higher reactivity of -CHO group to $-CO_2H$ group).
* The influence of the $-CH_3$ group on epoxidation rates was more complex. The oxidation of methallyl alcohol was slower than that of allyl alcohol indicating steric inhibition by the $-CH_3$ group (reactant shape selectivity). Methacrolein, however, was converted at slightly higher rate over TS-1 than acrolein. The electron donating effect of methyl group may be predominating over steric inhibitory

effects in cases like this, wherein an electron withdrawing group (-CHO) is attached to the carbon - carbon double bond.

* The influence of the methyl group on chemoselective epoxidation also depends on the substrate nature. The chemoselectivity for epoxidation of the double bond (rather than $-CH_2OH$ group) was lower in the case of methallyl alcohol (vis-à-vis allyl alcohol) but higher in the case of methacrolein (vis-à-vis acroliein). The greater steric crowding at the reaction site (the C=C double bond) in methallyl alcohol, relative to allyl alcohol, is, perhaps, responsible for the lower reactivity of C=C double bond vis-à-vis the $-CH_2OH$ group. In fact, it is an interesting example of transition state shape selectivity leading to chemoselectivity in a molecule containing two oxidizable functional groups.
* Protic solvents like methanol, ethanol etc, suppress epoxide formation and facilitate the cleavage of carbon - carbon double bond.

4.4.2 Ammoximation :

* Titanium silicate molecular sieves are efficient catalyst for ammoximation of carbonyl compounds using dilute H_2O_2 as oxidizing agent in presence of solvent. Aldehydes gives their corresponding aldoximes at much faster rate than that of ketones of similar size.
* Both, the intrinsic activity as well as size of the carbonyl compound play significant role in determining product yield and selectivity.
* Two types of plausible mechanism are considered to be operating involving the formation of (i) hydroxyl amine from TS-1 - H_2O_2 - NH_3 and its further reaction with carbonyls to form the corresponding oxime, and (ii) imine of the carbonyls and its catalytic oxidation to the respective oxime.

4.5 REFERENCES :

1. Taramasso, M., Perego, G. & Notari, B., *US.Pat.*, 4410501 (1983).
2. Thangaraj, A., Kumar, R., Mirajkar, S.P. & Ratnasamy, P., *J.Catal.*, **130**, 1 (1991).
3. Reddy, J.S. & Kumar, R. & Sciscery, S.M., *J.Catal.*, **145**, 73 (1994).
4. Notari, B., *Stud.Surf.Sci.Catal.*, **37**, 413 (1987).
5. Ratnasamy, P. & Kumar, R., *Stud.Surf.Sci.Catal.*, **95**, 240 (1995).
6. Sheldon, A.A. & Kochi, J.K., "*Metal Catalyzed Oxidation of Organic Compounds*", Academic Press, New York (1981).
7. Petrini, G., Cesano, A., De Alberti, G., Genoni, F., Leofanti, G., Padovan, M., Paparatto, G. & Roffia, P., *Stud.Surf.Sci.Catal.*, **68**, 761 (1991).
8. Thangaraj, A., Sivasanker, S. & Ratnasamy, P., *J.Catal.*, **131**, 394 (1991).
9. Kumar,R., Bhaumik, A., Ahedi, R.K. & Ganapathy, S., *Nature*, **381**, 298 (1996).
10. Rossiter, B.E., Katsuki, T. & Sharpless, K.B., *J.Am.Chem.Soc.*, **103**, 464 (1981).
11. Mimoum, H., Saussine, L., Daire, E., Postel, M., Fishcher, R. & Weiss, R., *J.Am.Chem.Soc.*, **105**, 3101 (1983).
12. Kaneda, K., Jitsukawa, K., Itoh, T. & Teronishi, S., *J.Org.Chem.*, **45**, 3004 (1980).
13. Clerici, M.G. & Ingallina, P., *J.Catal.*, **140**, 71 (1993).
14. Bhaumik, A., Kumar,R. & Ratnasamy, P., *Stud.Surf.Sci.Catal.*, **84C**, 1883 (1994).
15. Tatsumi, T., Yoko, M., Nakamura, M., Yiuhara, Y. & Tominaga, H., *J.Mol.Catal.*, **78**, L41 (1993).
16. Bhaumik, A. & Kumar, R., "*Catalysis : Modern Trends*", (Eds. Gupta, N.M. & Chakrabarty, D.K.), Narosa Publishing House, 160 (1995).
17. Armor, J.N., *J.Catal.*, **70**, 72 (1981).
18. Uno, T., Gong, B. & Schultz, P.B., *J.Am.Chem.Soc.*, **116**, 1145 (1994).
19. Reddy, J.S., Sivasanker, S. & Ratnasamy, P., *J.Mol.Catal.*, 69, 383 (1991).

CHAPTER 5

TRIPHASE-CATALYSIS

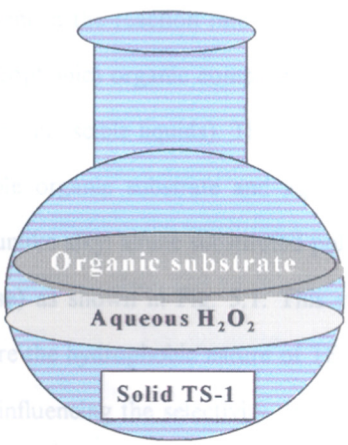

5.1 INTRODUCTION :

One of the major and frequently recurring problems encountered in liquid phase heterogeneous catalytic organic transformations is the reaction between mutually immiscible reagent(s) and substrate. If the chemical transformation takes place at the liquid-liquid phase boundary, rapid stirring may have an accelerating effect by increasing the interfacial contact[1]. Alternatively, the addition of cosolvent (viz., acetone, acetonitrile, methanol etc.) can bring about a homogeneous state and thereby completely eliminating the phase boundaries. Although, the use of cosolvents often finds its utility[2], product separation suffers from the drawback of complex work-up procedure. Phase-transfer catalysts[3-5] used to overcome this problem also suffer from the drawback that the catalyst used, promotes the formation of emulsions and thus giving severe problem in recycling and work-up. The use of solid catalyst, where the phase transfer catalysts were generally anchored / grafted in a polymer or inorganic supports[6-8] and the catalyst is sandwiched between organic and aqueous layers, is also reported.

Recently, using MFI type titanium silicate (TS-1) / H_2O_2 system[9-11], tremendous enhancement in the reaction rate was observed in the oxidation of some water immiscible (hydrophobic) organic compounds under triphase conditions[12] (solid catalyst along with two immiscible liquids). The three phase system consisting of solid TS-1, water immiscible organic substrate and aqueous H_2O_2 were physically non-interacting in nature (unlike alkyl amine substituted polystyrenes which form emulsions at the liquid interphase) as shown in Fig. 5.1. This system is an unique example of triphase catalysis where the hydrophobic nature of TS-1 plays a key role in enhancing the reaction rate and influencing the selectivity. In a broad sense, reactions occurring in the present three (tri, solvent-free) and two (bi, using cosolvent) phase system can be classified as :

(i) The reactions which occur in the biphase (using cosolvent) conditions but there is significant enhancement in the reaction rate and change in the product selectivity under triphase conditions.

(ii) In triphase conditions other routes are favoured compared to that exhibited in the presence of solvent, i.e., in biphase system.

(iii) Reactions that do not occur absolutely in the presence of solvent, can undergo in solvent-free conditions at least to some extent.

The present chapter deals with the oxidation of type (i) reactions involving some water immiscible organic substrates (benzene, toluene, anisole and *m*-cresol) over TS-1 / H_2O_2 system under triphase condition. The results are compared with those obtained under conventionally used biphase conditions employing a cosolvent. Apart from enhancement in activity and para-selectivity, present method offers distinct advantages of easier work-up, eco-safer and economic process.

5.2 EXPERIMENTAL :

The synthesis details of TS-1 catalysts are given in Chapter 2 and 3. It was ascertained through well known techniques such as XRD, FTIR, UV-VIS and adsorption measurements that the catalyst is free from amorphous and crystalline impurities. The reactions were conducted in a three neck glass batch reactor. In a typical reaction, 10 mmol of the substrate and catalyst (TS-1, 20 wt % with respect to the substrate) in presence of water (under triphase) or acetonitrile or acetone as cosolvent (in biphase)were taken in the batch reactor at an elevated temperature with rapid stirring. Then 10 mmol H_2O_2 (30 wt % aqueous) was added slowly into the mixture through feed pump. The substrate : water or substrate : cosolvent ratio is kept at 1 : 10 (m / m) so that the total volume of the reaction mixture remains same in both biphase and triphase. The products were collected at various intervals of reaction time and were analyzed through high resolution capillary gas chromatograph

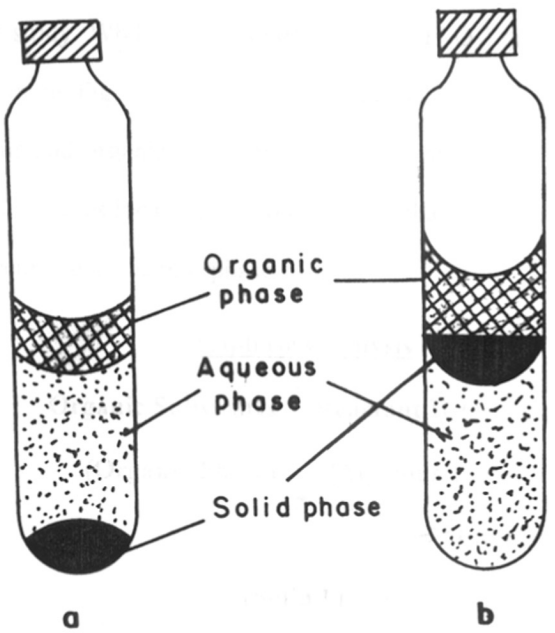

Fig. 5.1 : **Triphase system : (a) TS-1 / H_2O_2 / H_2O / organic substrate and (b) polymer supported alkyl amine / H_2O / organic substrate in solvent.**

(HP 5880, using Flame Ionization Detector). In all the cases two sets of experiments, one in biphase system using a cosolvent viz., acetonitrile, a commonly used solvent for TS-1 / H_2O_2 catalysis, and in triphase system, in the absence of any organic solvent, were carried out under similar conditions.

5.3 RESULTS AND DISCUSSION :

Fig. 5.1 illustrates the difference of triphase system used by Regan[8] and that used in the present study. While TS-1 (solid), 'water + H_2O_2' and substrate are non-interacting as shown in Fig. 5.1a, tetraalkyl amine substituted polystyrene resides between the aqueous and organic layers and forms an emulsion at the interface (Fig. 5.1b). Scheme 5.1 illustrates location of three distinct phases, under vigorous stirring, the reactions are occurring at the interphase.

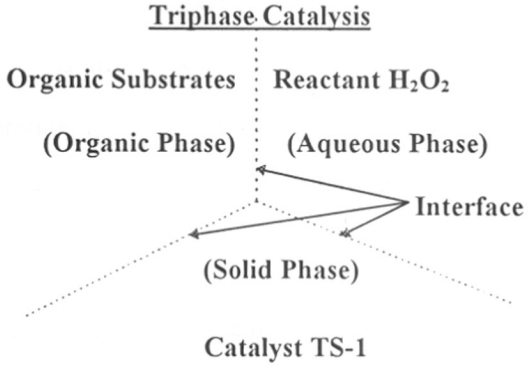

Scheme 5.1

The reactions studied in the present chapter are classified into two categories :

5.3.1 Hydroxylation of Aromatics (Benzene, Toluene, Anisole and m-Cresol) :

Benzene :

In Table 5.1, the results of the hydroxylation of benzene 1, over TS-1 / H_2O_2 system is reported. The conversion as well as the reaction rates (as indicated by Turn

Over Frequency per h, TOF h^{-1}) are considerably increased in triphase system over the biphase one. Whereas only 11.6 % conversion of benzene is obtained under biphase (using acetone as cosolvent) after 16 h, 78.5 % benzene was converted under triphase after only 2 h reaction time (entry 1 and 2, Table 5.1). However, the product distribution remains almost same in both the cases. Selectivity for phenol in triphase was 85.6 % and that for paranbenzoquinone was 9.3 %. Oxidation of phenol to parabenzoquinone is believed to be thermal reaction[13]. The H_2O_2 selectivity has shown a dramatic increase from mere 15.0 % (in biphase) to 89.8 % (in triphase). Table 5.1 also shows the effect of various substrate to H_2O_2 mole ratio on the conversion, H_2O_2 selectivity and product selectivities over TS-1 / H_2O_2 system under triphase.

Among the four benzene / H_2O_2 mole ratios used in the present study (i.e. 1, 1.5, 2 and 3), maximum H_2O_2 efficiency was observed in benzene / H_2O_2 mole ratio = 3, in line with earlier reports[13]. As the conversion level increases, H_2O_2 selectivity slowly decreases but its consumption (i.e. efficiency) is far better than that achieved in presence of organic cosolvent (biphase). Selectivity of phenol is also better at higher mole ratios.

In Fig. 5.2 the kinetics of benzene hydroxylation, i.e. plot of the conversion (in mole %) of benzene as a function of reaction time (in minute) under the triphase condition is shown. In the presence of cosolvent (acetone under biphase) reaction is very slow at the beginning and then gradually pick-up and then reaches a plateau after attaining the maximum conversion level of ca. 12 %. However, in present triphase condition the reaction is very fast from the very beginning and then gradually flattened at the maxima (curve a). From the nature of the curve it is clear that the activation energy barrier in triphase is relatively far low which facilitates the initial rapid hydroxylation. Whereas the selectivity for phenol gradually increases (curve b) and

Table 5.1 : Hydroxylation of benzene over TS-1[a] :

Entry	Benzene : H_2O_2	Phase	Conv. mole %	TOF h^{-1b}	H_2O_2 Sel (%)	Product Selectivities		
						Phenol	PBQ	Others[c]
1.	1.0	Triphase	78.5	61.2	89.8	85.6	9.3	5.1
2.		Biphase	11.6	2.3	13.7	82.0	18.0	-
3.	1.5	Triphase	56.7	45.7	94.0	89.5	7.5	3.0
4.		Biphase	9.8	1.7	16.6	86.9	13.1	-
5.	2.0	Triphase	43.2	36.8	95.6	90.4	6.1	3.5
6.		Biphase	8.7	1.5	19.2	90.1	9.9	-
7.	3.0	Triphase	31.2	19.5	97.5	95.9	4.1	-
8.		Biphase	6.4	1.1	20.6	92.8	7.2	-

a: Catalyst TS-1 (Si / Ti = 29) 15 wt % with respect to substrate, H_2O_2 was slowly feeded into the reaction mixture for a period of 0.5 h.

b: Turn Over Frequency = moles of benzene converted per mole of Ti, per hour.

c: Other product includes catechol and hydroquinone.

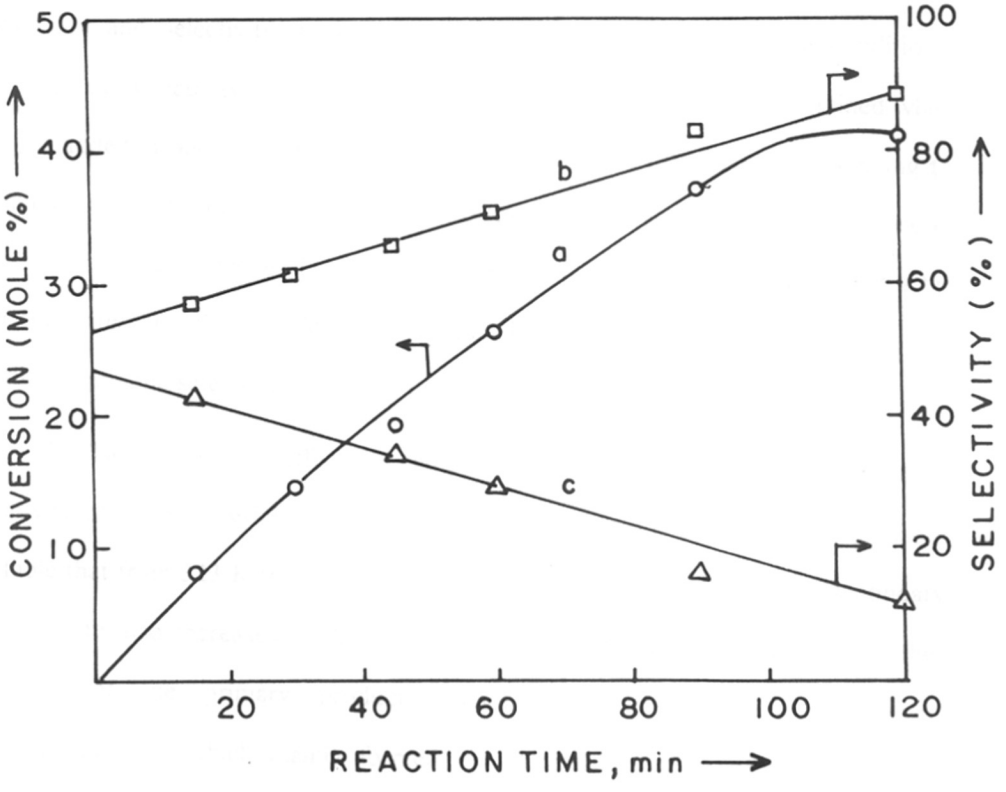

Fig. 5.2 : **Kinetics of benzene hydroxylation (a) and product selectivities for phenol (b) and parabenzoquinone (c) under triphase conditions.**

that for parabenzoqunione (PBQ, curve c) gradually decreases with time (Fig. 5.2). However, with time other secondary products e.g., catechol (CAT) and hydroquinone (HQ) also increase.

Table 5.2 illustrates the effect of continuous addition of H_2O_2 on the conversion and selectivity in the oxidation of benzene under triphase conditions. However, the selectivity of parabenzoquinone is slightly lower than that obtained when H_2O_2 is added in one lot. After exponential increase in the rate from the beginning to 75 minute reaction time, even the addition of extra H_2O_2 causes very little increase in the conversion of benzene. Table 5.2 also shows the amount of H_2O_2 added after different interval of times. With time phenol selectivity gradually increases and parabenzoquinone selectivity gradually drops down.

In Table 5.3, the effect of temperature on the conversion and product selectivity of the hydroxylation of benzene (under triphase) is shown. It is clear from the table that from 323 K to 353 K although the rate of reaction increases, secondary reaction rate also increases in the same way. Secondary reaction being the further oxidation of the primary product phenol to parabenzoquinone. However, parabenzoquinone, which mainly formed via thermal oxidation of phenol (in the presence of H_2O_2), finally gets converted into tars. Because of this tar formation not more than 12.5 wt % catalyst is recommended for this reaction.

Anisole :

In triphase conditions during the hydroxylation of the aromatic ring of anisole (2), high regioselectivity for the *para*-hydroxy products is observed. Unlike in benzene where only mono hydroxylation is possible, in other cases (viz. anisole, toluene and *m*-cresol) a significantly higher *para*-selectivity (i.e., low *ortho* / *para* mole ratio) for the products was observed under triphase conditions over conventional biphase

Table 5.2 :Effect of continuous addition of H_2O_2 on the conversion and selectivity in oxidation of benzene under triphase :

Reaction time (min)	15	30	45	60	90	120
H_2O_2 added (mmole)	3.0	6.0	9.0	12.0	18.0	24.0
Benzene conversion (%)	9.1	20.7	47.7	65.5	82.0	82.5
Product selectivity (%)						
Phenol	65.0	79.8	84.6	87.4	91.6	95.0
Parabenzoquinone	35.0	20.2	15.4	12.6	8.4	5.0

a: Reaction conditions : Temperature 333 K, Catalyst TS-1 (15 wt % with respect to benzene), 5 g water (as dispersion medium) for 2 g benzene, Benzene : H_2O_2 = 1 : 1 (mole / mole).

Table 5.3 : Effect of temperature on the activity and selectivity of oxidation of benzene over TS-1, under triphase :

Reaction temp.	Benzene conv.	H_2O_2 sel.	Reaction time	Product selectivity	
(K)	(mole %)	(%)	min[a]	Phenol	PBQ
323	67.8	70.5	180	96.0	4.0
333	82.5	89.1	150	92.0	8.0
343	78.6	89.2	120	86.5	13.5
353	72.3	87.9	60	78.4	21.6
373	40.6	56.8	30	59.9	40.1

a: Time at which maximum benzene conversion was achieved.

b: Benzene : H_2O_2 mole ratio = 1 : 1., other conditions are same as that given in Table 5.1, H_2O_2 was feeded for 0.5 h for reactions at 373 and 353 K, 1 h for 343 K and 2 h for reactions at 333 and 323 K, Catalyst 15 wt % with respect to the substrate.

one. In biphase system (using acetone or acetonitrile as cosolvent) high selectivity for the ortho-hydroxy products was obtained (Table 5.4). In the hydroxylation of anisole (2), 2-hydroxy anisole (2x guiacol) and 4-hydroxy anisole (2y) were formed at 26 :74 molar ratio (i.e. 0.35 : 1.0) under triphase conditions. Under biphase, the corresponding proportion was 68.5 : 31.5 mole percent (i.e. 2.22 : 1.0). This complete reversal of selectivity (i.e. *ortho / para* ratio) as well as, far better reactivity at much reduced reaction time are the outstanding outcome of triphase system over the conventional biphase one.

Fig 5.3 shows the kinetics of anisole hydroxylation under triphase condition together with product selectivity pattern during the course of reaction. The reaction rate is quite fast at the initial stages, but gradually decreases and reaches the plateau (curve a). However, with time the concentration of 4-hydroxy anisol slowly increases (curve b) and that of 2-hydroxy anisole (curve c) and the other heavy products decreases (curve d).

Toluene :

In the hydroxylation of toluene (3), both under bi- and triphase conditions, *o*-cresol (3x) and *p*-cresol (3y) are obtained. Once again, about five times increase was observed in TOF under triphase compared to that in biphase (Table 5.4). Among products, the *o*-cresol to *p*-cresol molar ratio was 2.45 : 1.0 under biphase, whereas the same in triphase condition was 0.75 : 1.0. The change in *para*-selectivity (i.e. change in *ortho / para* in biphase : triphase system) is more pronounced in the case of anisole, when compared to that in the case of toluene (Table 5.4). This may be attributed to greater +R effect along with relative bulkiness associated with $-OCH_3$ group of anisole compared to that of $-CH_3$ group of toluene. This is an interesting illustration of reversal of regioselectivity, amount of change being dependent on the substituent group present in the aromatic ring.

Table 5.4 : Hydroxylation of various substrates over TS-1[a] :

Substrates	Phase	Conv.	Reaction	TOF	Product selectivities			
		mole %	time, h	h^{-1}	x	y	z	Others
Anisole	Triphase	66.5	8.0	6.54	25.6	72.3	-	2.1
2	Biphase	42.2	16.0	2.07	66.6	30.3	-	3.1
Toluene	Triphase	14.8	6.0	2.28	41.4	55.9	-	2.7
3	Biphase	5.5	12.0	0.42	69.7	28.4	-	1.9
m-Cresol	Triphase	26.5	14.0	1.49	35.6	20.3	40.4	3.7
4	Biphase	10.7	14.0	0.60	38.2	39.4	18.5	3.9

a: Reaction temperature = 353 K, Substrate : H_2O_2 = 1 : 1, H_2O_2 was added for a period of 2 h, Catalyst (TS-1, Si / Ti = 29) 20 wt % with respect to the substrate.

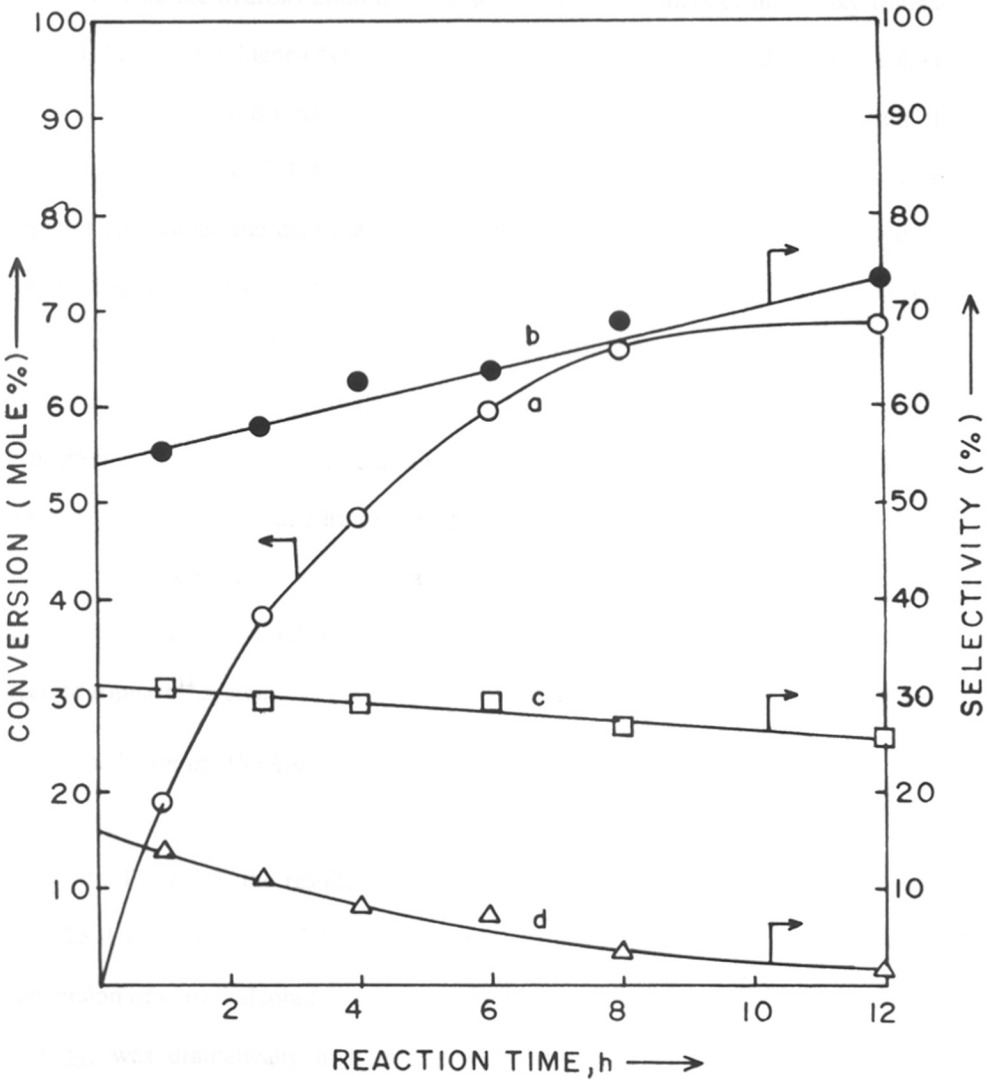

Fig. 5.3 : **Kinetics of anisole hydroxylation (a) and product selectivity for 4-hydroxy anisole (b), 2-hydroxy anilole (c) and others (d) under triphase.**

m-Cresol :

During the hydroxylation of *m*-cresol (4) all the isomers of dihydroxy toluene, viz. 3,4-dihydroxy toluene (4x), 2,3-dihydroxy toluene (4y) and 2,5-dihydroxy toluene (4z) (all being monohydroxylated products of *m*-cresol) were obtained. Although, the relative distribution of 3,4-dihydroxy toluene 4x was comparable in both, biphase and triphase conditions, the distribution of 2,3-dihydroxy toluene (4y) and 2,5-dihydroxy toluene (4z) isomers was found to be completely reversed. Both -OH as well as $-CH_3$ groups are *ortho-para* directing, +R being more pronounced in -OH group. Whereas the 2,3-dihydroxy isomer (incoming -OH group is *ortho* to both -OH and $-CH_3$ group) was predominant in the biphase system, the 2,5- dihydroxy toluene (incoming -OH group is *ortho* to $-CH_3$ but para to -OH group of *m*-cresol) was formed in large excess under triphase condition. Thus like anisole and toluene in the case of *m*-cresol also hydroxylation occurs preferentially *para* to the more stronger activating group in present triphase[12] system.

5.3.2 Oxidation of Alcohols (Benzyl alcohol and Cyclohexanol) :

Benzyl alcohol :

In Table 5.5, the results on the oxidation of benzyl alcohol and cyclohexanol over TS-1 under biphase and triphase conditions are shown. The enhancement in the conversion of benzyl alcohol 5 to benzaldehyde 5x and its further oxidation to benzoic acid 5y, was dramatically high in triphase system, exhibiting a nearly seven-fold increase in activity compared to that obtained in the biphase system (Table 5.5). In biphase, the reaction is very slow from the beginning but in triphase, reaction is very fast and within 4 h reaction time 60 % conversion level could be achieved. However, with time the reaction rate decreases very slowly and reaches the plateau. The selectivity for benzoic acid 5y, a further oxidation product of primary product 5x, was also quite high in triphase system, which may be a consequence of high conversion

Table 5.5 : Oxidation of alcohols over TS-1[a] :

Substrates	Phase	Conv.	Reaction	TOF	H_2O_2	Product sel. %		
		mole %	time, h	h^{-1}	sel %	x	y	Others
Benzyl-	Triphase	89.6	18.0	3.92	100.0	73.5	25.6	-
alcohol 5	Biphase	12.5	18.0	0.55	14.3	86.0	14.0	-
Cyclohexanol	Triphase	36.4	14.0	2.58	36.4	98.5	-	3.6
6	Biphase	12.8	14.0	0.60	12.8	96.2	-	4.2

a: Reaction conditions same as that given in Table 5.4

levels. Further, the oxidation of benzaldehyde to benzoic acid may result from thermal / aerial oxidation.

Cyclohexanol :

Similarly, in the oxidation of cyclohexanol 6 to cyclohexanone 6x, considerable increase in conversion was observed under triphase system, compared to that observed in biphase as depicted in the turn over frequency (TOF) shown in Table 5.5.

5.3.3 Explanation for High Activity and Para-Selectivity in Triphase Conditions :

MFI type structure is well known for its *para*-selective behavior. Bulkier *ortho* products may preferably be formed on external surface of the crystallites, while relatively less bulky *para* products are mainly formed inside the zeolite channels. Significantly higher *para*-selectivity obtained in the present triphase system indicates that the reaction takes place mainly inside the zeolite channels. However, in the biphase system, low conversion as well as very high *ortho*-selectivity probably indicate that the reaction takes place significantly on the external surface of the catalyst.

Since, high silica titanium silicate molecular sieves are highly hydrophobic in nature, it is expected that organic substrates will be competing more favorably with water vis-à-vis with organic solvent for diffusion and adsorption in triphase conditions which is free form organic solvents, resulting in higher conversions. When an organic solvent is present along with the reactant, the diffusion and adsorption of the reactant will be hindered by the solvent, thus lowering the conversion. To confirm this point some competitive adsorption experiments under bi- and triphase conditions (except the presence of H_2O_2) were carried out. The results of the thermogravimetric (TG) analysis of the solid catalyst obtained after saturating the catalyst with the substrate (anisole, taken as representative) in the presence of acetonitrile (biphase) and in the absence of acetonitrile (triphase, an equal amount of water is used instead of

acetonitrile) are recorded in Table 5.6. In fact, thermogravimetric analysis shows that the weight loss in TG occurred mostly due to acetonitrile and anisole in biphase and triphase system, respectively. Further, the desorption experiments (adsorbed catalyst was loaded in a tabular down flow reactor and was flushed with N_2 at an elevated temperature and the desorbed gas was collected and analyzed through capillary gas chromatograph using FID) over TS-1 / acetonitrile / anisole and TS-1 / water / anisole systems used for the adsorption experiments confirmed that acetonitrile was mostly (<90 %) desorbed from the former, while anisole was desorbed from the latter. Above results clearly suggest that the presence of organic solvent hinders the adsorption and diffusion of substrate inside TS-1 pores, while such diffusional hinderance was not experienced by hydrophobic organic substrates under triphase conditions.

The phenomenon of competitive diffusion as discussed above, is further supported chemically by the observation :

* When *tert*-butanol, which is too bulky to enter the TS-1 (MFI topology) pores, was used as solvent in place of acetonitrile (in biphase system), very high *para*-selectivity (*o*- / *p*- = 0.2) was observed in the hydroxylation of anisole, although the conversion was relatively low (28 %).

5.4 CONCLUSION :

In summary, it has been demonstrated that using triphase system (solid-liquid-liquid), in the absence of any cosolvent, considerable increase in conversion of water-immiscible organic compounds during their oxidation by TS-1 / H_2O_2 system can be achieved along with very high *para*-selectivity (vis-à-vis biphase system). Since titanium silicate molecular sieves are highly hydrophobic in nature, reactant will be competing more favorably with water for diffusion and adsorption under triphase

Table 5.6 : Thermogravimetric weight losses of various adsorbed components over TS-1[a] :

System	Temperature range (K)	Weight loss (%)	Total wt. loss (%)
TS-1 / CH_3CN	313-363 363-523	3.9 8.1	12.0
TS-1 / CH_3CN / $C_6H_5OCH_3$	313-363 363-523	3.7 7.8	11.5
TS-1 / $C_6H_5OCH_3$	363-573	11.7	11.7
TS-1 / H_2O / $C_6H_5OCH_3$	363-573	12.1	12.1
TS-1 / H_2O	313-423	2.0	2.0

a: 5 g of adsorbed TS-1 was loaded in a tabular downflow reactor and then flashed with dry helium by gradually increasing the temperature from 313 - 623 K (heating rate 10 degree min^{-1}). The desorbed material was cooled (at liquid nitrogen trap), collected and analyzed by GC.

conditions resulting in higher conversion and shape selectivity. Whereas in presence of cosolvent (conventionally used to homogenize the organic and aqueous layers) in biphase, cosolvent competes with the reactant for diffusion and adsorbtion at the active sites resulting in poor reactivity. Apart from enhancement in activity and *para*-selectivity, present triphase method offers distinct advantages in easier product separation and in the development of *eco-friendly* processes.

5.5 REFERENCES :

1. Menger, F.M., *J.Am.Chem.Soc.*, **92**, 5965 (1970).
2. Barton, A.F.M., *Chem.Reviews*, **75**, 731 (1975).
3. Starks, C.M., *J.Am.Chem.Soc.*, **97**, 195 (1971).
4. Dockx, J., *Synthesis,* 441 (1973).
5. Dehmlow, E.V., *Angew.Chem.Int.Ed.Engl.*, **13**, 170 (1974).
6. Regan, S.L., *J.Am.Chem.Soc.*, **97**, 5956 (1975).
7. Regan, S.L., *Angew.Chem.Int.Ed.Engl.*, **18**, 421 (1979).
8. Molinari, H., Monttanari, F., Quici, S. & Regan, S.L., *J.Am.Chem.Soc.*, **101**, 3920 (1979)
9. Notari, B., *Stud.Surf.Sci.Catal.*, **37**, 413 (1987).
10. Thangaraj, A., Kumar, R., Mirajkar, S.P. & Ratnasamy, P., *J.Catal.*, **130**, 1 (1991).
11. Notari, B., *Stud.Surf.Sci.Catal.*, **60**, 343 (1991).
12. Bhaumik, A. & Kumar, R., *J.Chem.Soc.Chem.Commun.*, 349 (1995).
13. Thangaraj, A., Kumar, R. & Ratnasamy, P., *Appl.Catal.*, **57**, L1 (1992).

CHAPTER 6

SOLVENT-FREE CATALYSIS

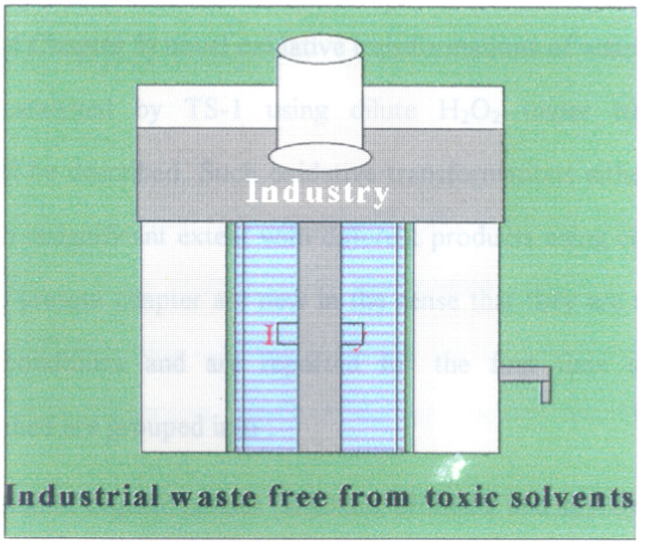

6.1 INTRODUCTION :

The researchers are becoming increasingly concerned about the need for developing new environmentally safer chemical transformations by reducing / removing the toxic waste and by-products obtained from the chemical processes making them ecologically more acceptable[1-4]. Now such concern is not merely a desirability but also becomes a necessity. One of the major problems encountered in various chemical processes is the use of organic solvents which are detrimental to nature. Hence, it is appropriate that the organic transformations under solvent-free conditions are attracting increasing attentions[3-5]. In the previous chapter, it is shown that titanium silicate molecular sieves (e.g., TS-1) can effectively catalyze the hydroxylation / oxidation of some hydrophobic organic compounds[6] (viz. benzene, toluene, anisole, *m*-cresol, benzyl alcohol etc.) under triphase conditions with significant enhancement in both activity and regio-selectivity compared to what obtained under conventional biphase conditions using solvents.

However, in the present chapter class (ii) and (iii) category of (as given in introduction of Chapter 5) novel oxidative transformations of water immiscible organic compounds catalyzed by TS-1 using dilute H_2O_2 under triphase, solvent-free conditions will be described. Such oxidative transformations either do not take place or occur to an insignificant extent with different products using cosolvents. Reactions studied in the present chapter are new in the sense that they are occuring only under solvent-free conditions and are reported for the first time over TS-1 catalyst. Reactions studied are grouped into :

(i) Oxidation of organic halides (aliphatic, aromatic and allylic).

(ii) Oxidation (mainly Baeyer-Villiger oxidation) of cyclic and aromatic ketones.

(iii) Oxidation of aromatic esters.

6.2 EXPERIMENTAL :

The liquid phase catalytic reactions were conducted in a three neck glass batch reactor (Fig. 4.1). 10 mmol of substrate and 10 mmol of H_2O_2 were reacted over the catalyst, TS-1 (20 wt % with respect to the substrate) in the presence of acetone or acetonitrile as solvent (in biphase at 333 K and 353 K respectively) or in absence of solvent (in solvent-free condition at 353 K, water was added for better dispersion of the catalyst in solid-liquid-liquid three phase system). Total volume of the reaction mixture is kept constant in both the cases. 1.0 mmol of concentrated sulphuric acid or hydrochloric acid was added in the case of acetophenone and cyclohexanone oxidation in both the cases to study the effect of added acid. Reactions were carried out at 333 K to 353 K temperature range and at various time intervals the products were collected and analyzed by high resolution gas chromatography (HP, 5880 and Shimadzu R-17A using FID), GC MS, GC IR, FTIR and ^{1}H NMR.

6.3 RESULTS AND DISCUSSION :

6.3.1 Oxidation of Organic Halides :

6.3.1.1 n-propyl halides :

In Table 6.1 oxidation of *n*-propyl chloride, *n*-propyl bromide and *n*-propyl iodide over TS-1 / H_2O_2 system under solvent-free conditons are given. Under conventional conditions using acetonitrile solvent *n*-propyl halides undergo hydrolysis with only about 5 % conversion, mainly producing propanol with very poor yield (< 4 %).

n-propyl chloride : In the case of *n*-propyl chloride the main reaction under solvent-free conditions was the oxyfunctionalization of β-C (ca. 90 %) resulting in alcohol

Table 6.1 : Oxidation of various alkyl halides over TS-1 / H_2O_2 system under solvent-free conditions:

	n-Propyl chloride **1**	*n*-Propyl bromide **2**	*n*-Propyl-iodide **3**
Conversion, mole%	37.9	65.8	76.5
H_2O_2 Efficiency, mole %	64.1	83.2	93.1
Products, mole %			
Propanal (**a**)	9.4	36.5	67.8
1-Halo-propan-2-ol (**b**)	37.2	15.0	19.8
1-Halo-propan-2-one (**c**)	53.4	31.5	6.2
1-Halo-propenes (**d**)	-	7.4	6.2
1-Halo-epoxy-propenes (**e**)	-	9.6	-
Sel. for α-C oxidation, %	9.4	36.5	67.8
Sel. for β-C oxidation, %	90.6	63.5	22.2

a : H_2O_2 selectivity = (moles of H_2O_2 consumed in the formation of oxy-products / moles of H_2O_2 taken initially) × 100.

b : Time required (in hours) for achieving maximum conversion = 6 h.

1b followed by its further oxidation to the corresponding ketone **1c**. The oxidation at α-C resulting in propanal **1a** was quite suppressed (ca. 10 %).

n-propyl bromide : On the other hand, in case of *n*-propyl bromide **2** the oxyfunctionalization of α-C (followed by HBr removal) and β-C (followed by further oxidation of primary formed 1-bromo-propan-2-ol, **2b**) occurs, simultaneously producing propanal **2a** and 1-bromo-propan-2-one (bromoacetone) **2c**, respectively (Table 6.1). The reaction path is shown in scheme 6.1. Small amount of bromopropenes **2d**, along with corresponding epoxides **2e**, were also obtained due to elimination of water from **2b**, followed by epoxidation.

Fig. 6.1 illustrates the conversion and product selectivities of *n*-propyl bromide oxidation (taken as representative) with reaction time. As the reaction progressed both the conversion of *n*-propyl bromide and H_2O_2 selectivity increased linearly before reaching a plateau. The selectivity for the oxidation of β-C (resulting in the formation of *sec.*alcohol and ketone) is comparable to the oxidation at α-C (resulting in the formation of propanal) in the beginning. As reaction time increases (with increasing conversion) relative yield of the product obtained via β-C oxidation vis-à-vis that obtained via α-C oxidation) increases and reaches a steady state. The small amount of propenes and corresponding epoxides were obtained during the course of the reaction.

n-propyl iodide : In the case of *n*-propyl iodide **3**, although, the reaction is relatively fast, major product being propanal **3a**. β-C oxidation occurs to very minor extent giving **3b** and **3c**. I^- being good leaving group, α-C oxidation is favoured here.

Here it is pertinent to mention that all earlier methods reported in the literature, for preparing **2a** and **2c** are based on the oxidation of 1-propanol[7] and bromination of acetone[8] respectively. This is probably the first report of the formation of **2a** and **2c** by direct oxidation of **2** in one-pot reaction. In the case of *n*-propyl chloride path 2 of

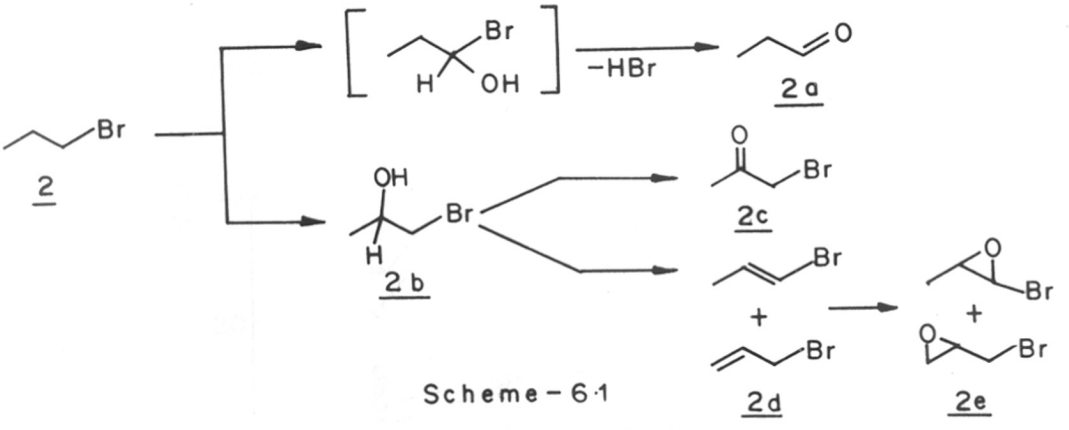

Scheme - 6·1

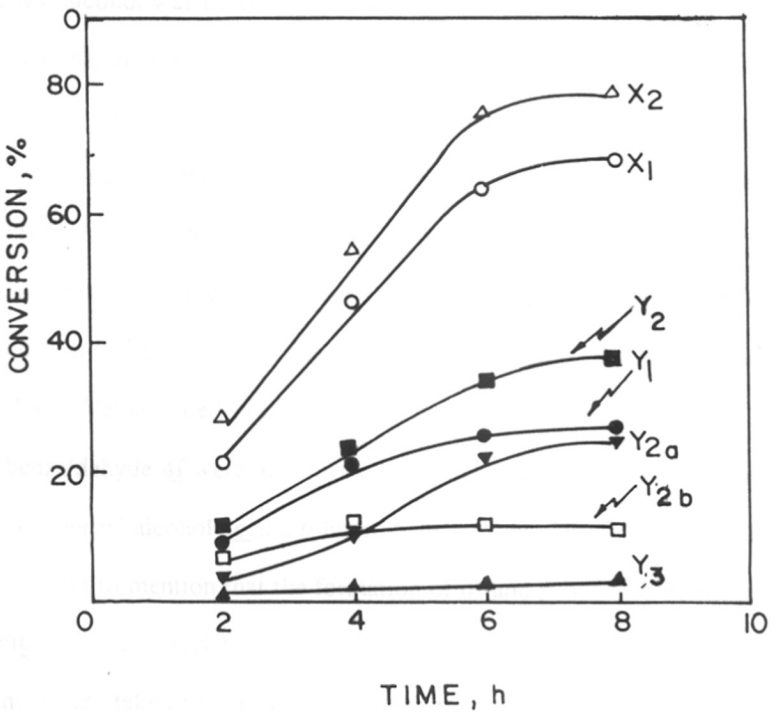

Fig. 6.1 : Reaction kinetics of *n*-propyl bromide oxidation under solvent-free condition : X_1 = conversion, X_2 = H_2O_2 selectivity, Y_1 = yield of propanal, Y_{2a} = bromoacetone, Y_{2b} = 1-bromo-propan-2-ol, Y_2 = yield of β-oxidation products (Y_{2a}+Y_{2b}) and Y_3 = mainly propenes and epoxides.

Scheme 6.1, i.e., β-C oxidation predominates over α-C (path 1 of Scheme 6.1). Other solvents like acetone, methanol also behave in a similar way as acetonitrile does.

6.3.1.2 Benzyl chloride :

In the case of benzyl chloride (aromatic halide) not only side chain oxyfunctionalization, followed by HCl removal, directly producing benzaldehyde **4a** (as no benzyl alcohol was detected in solvent-free conditions even in the initial stages of the reaction), ring hydroxylation also occurs to a considerable extent (75 % selectivity vis-à-vis 25 % selectivity for side chain oxidation) producing valuable *o*- and *p*-hydroxy benzyl chloride **4c** and **4d** respectively (Table 6.2, Scheme 6.2). Remarkably high *para*-selectivity, obtained in this case (*para* / *ortho* = 85 : 15, Table 6.2), is consistent of with the earlier results on the oxidation of activated molecules like anisole and toluene[6] presented in Chapter 5, and may be attributed to confined void space of TS-1. Value added products like *ortho*-hydroxy benzaldehyde **4e** and *para*-hydroxy benzaldehyde **4f** were also formed in small quantities by side chain oxidation of *o*-hydroxy benzyl alcohol **4c** and *p*-hydroxy benzyl chloride **4d**, respectively. Here it may be pertinent to mention that the formation of *o*- and *p*-hydroxy benzaldehyde was not through the hydroxylation of benzaldehyde. In a control experiment when benzaldehyde was taken as substrate, only benzoic acid was formed. In the presence of cosolvent (acetonitrile) only 3 % conversion was obtained solely due to the hydrolysis of C-Cl bond, forming mainly benzyl alcohol (80 %), followed by its further oxidation to benzaldehyde (15 %) and benzoic acid (5 %).

Table 6.3 depicts the effect of benzyl chloride to H_2O_2 mole ratios on conversion and product selectivities. As expected, at high ratios (Table 6.3), the H_2O_2 efficiency was increased. Among products the selectivity for ring hydroxylation was also higher compared to side chain oxidation (Table 6.3).

Table 6.2 : Oxidation of benzyl chloride over TS-1 under solvent-free conditions :

Conv. (mole %)	H_2O_2 sel. %	Time, h	Products	Selectivity (mole %)
40.2	45.4	8.0	Benzaldehyde **4a**	21.5
			Benzoic acid **4b**	3.6
			o-Hydroxy benzyl chloride **4c**	6.5
			p-Hydroxy benzyl chloride **4d**	59.0
			o-Hydroxy benzaldehyde **4e**	2.1
			p- Hydroxy benzaldehyde **4f**	7.3
			$\sum$Side chain oxidation **4a** + **4b**	25.1
			$\sum$Ring hydroxylation **4c** + **4d** + **4e** + **4f**	74.9

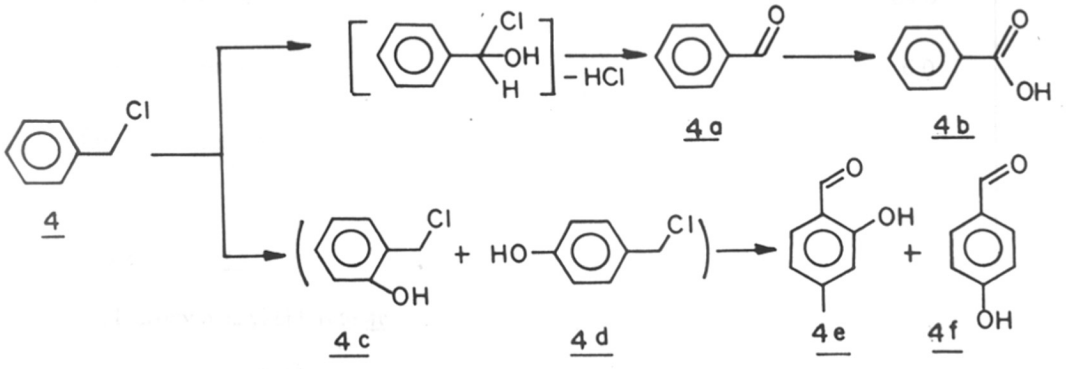

Scheme-6·2

Table 6.3 : Effect of H_2O_2 concentration in oxidation of benzyl chloride :

	Substrate / H_2O_2 mole ratio[a]		
	1	2	3
Conversion, mole % Theoratical Max.	37.8	52.8	54.0
H_2O_2 Efficiency, %	43.1	57.5	64.0
Reaction time, h	8.0	6.0	6.0
Products, mole %			
Benzaldehyde **4a**	31.6	20.0	17.5
Benzoic acid **4b**	7.4	1.5	1.4
o-Hydroxy benzyl chloride **4c**	6.2	7.5	9.1
p-Hydroxy benzyl chloride **4d**	49.2	63.1	64.7
o-Hydroxy benzaldehyde **4e**	2.2	2.4	3.0
p- Hydroxy benzaldehyde **4f**	3.4	5.5	4.3
$\sum$Side chain oxidation **4a** + **4b**	39.0	21.5	18.9
$\sum$Ring hydroxylation **4c** + **4d** + **4e** + **4f**	61.0	78.5	81.1

a : H_2O_2 was added in a lot in all the cases.

6.3.1.3 Dihydroxylation of Allylic Halides (Allyl and Methallyl chlorides):

Epoxidation of olefin over titanium silicate molecular sieves is well documented[9,10]. In the case of allylic chlorides also in presence of a cosolvent (acetone or acetonitrile) it is the sole reaction product[11,12] (Chapter 4, section 4.3.2). However, present solvent-free triphase condition leads to direct dihydroxylation of allylic halide over TS-1 / H_2O_2 system. Asymmetric dihydroxylation is of great interest in synthetic organic chemistry[13,14]. Dihydroxylation of the present type proceeds through ring opening of epoxides. Unsymmetrical epoxides viz. epoxide of allylic halides are ambident substrates where incoming nucleophile can take up two different positions, depending on the nature of substituents (which may exhibit different steric or stabilizing effect) and restricted geometry of the zeolite channels[15].

Allyl chloride : In Table 6.4, results of dihydroxylation of allyl chloride **5** and methallyl chloride **6** over TS-1 / H_2O_2 system are given. In the presence of cosolvent (biphase) epoxide is the sole product (entry 2 and 4, Table 6.4). However, the rate of reaction (as reflected in TOF for the respective entries), as well as product distribution pattern completely changes when the reaction is switched over to the present triphase solvent-free conditon. In the case of allyl chloride after 4 h reaction time 90 % conversion occurs (at 333 K) together with 92 % selectivity for 2,3-dihydroxy propyl chloride (Fig. 6.2; Scheme 6.3; Table 6.4, entry 1,). Fig. 6.2 shows the reaction kinetics of allyl chloride dihydroxylation under solvent-free conditions. With time epoxide selectivity drops down (curve b) and diol concentration increases (curve c). However, conversion level (curve a) reaches maxima at 90 - 95 % within 1 h reaction time.

Methallyl chloride : In the case of methallyl chloride under identical conditions after 6 h 96 % conversion and 85 % selectivity for diol 2,3-dihydroxy-2-methyl propyl chloride (Scheme 6.3; Table 6.4, entry 3) mixtures were obtained. In the presence of

Table 6.4 : Dihydroxylation of allylic halides over TS-1 :

Substrate	Condition	Conversion	Reaction	Product sel. %		
		mole %	time, h	diol	epoxide	others
Allyl chloride **5**	Triphase	98.5	4.0	92.3	5.2	2.5
Allyl chloride **5**	Biphase	90.0	8.0	-	95.0	5.0
Methallyl chloride **6**	Triphase	96.6	6.0	90.0	6.0	4.0
Methallyl chloride **6**	Biphase	63.0	8.0	-	92.0	8.0

a: Reaction condition same as given in Table 6.1.

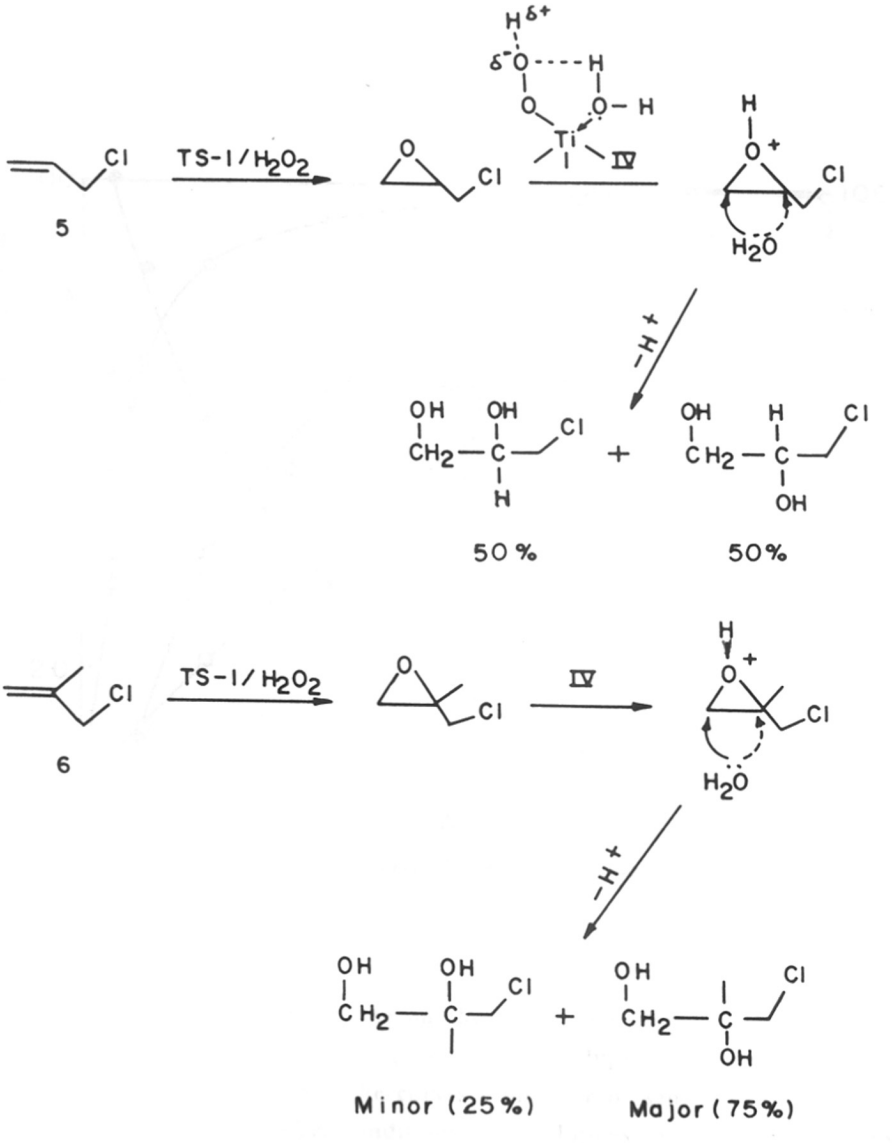

Scheme 6·3

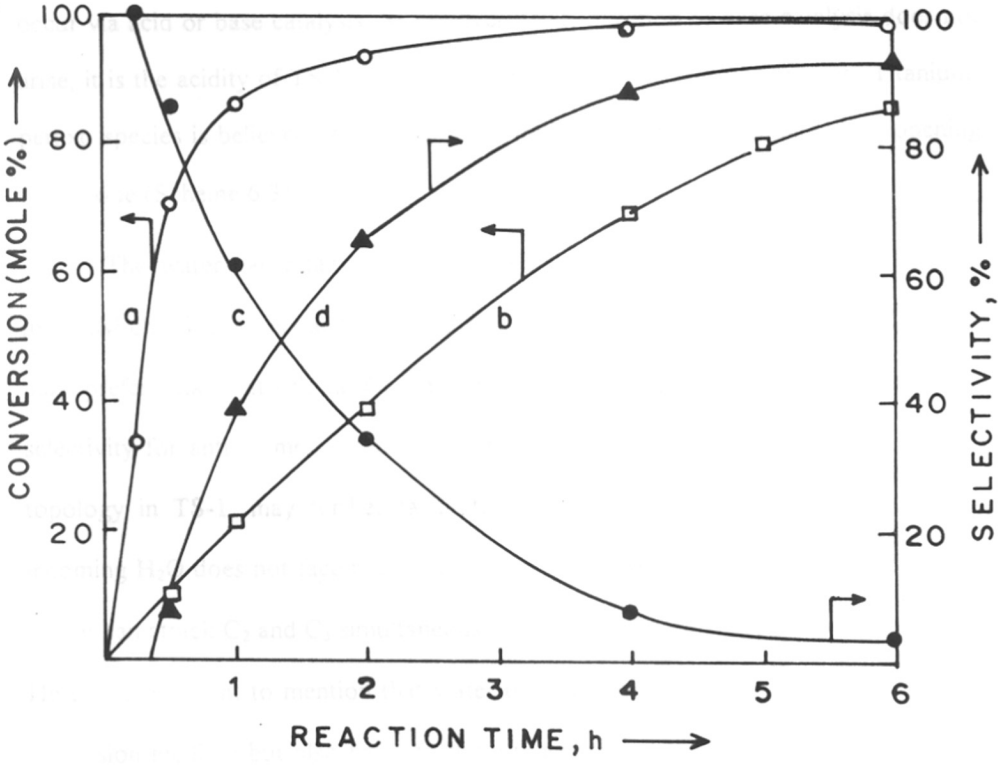

Fig. 6.2 : **Effect of reaction time on the conversion of allyl chloride under solvent-free, triphase (curve a) and biphase using acetonitrile solvent (curve b). The curves c and d represent epoxide and diol under solvent-free conditions. Under biphase epoxide was the only product and hence not shown in Fig.**

acetone solvent, only 63 % of methallyl chloride was converted into the corresponding epoxide (with 90 % selectivity) after 8 h reaction time. In the initial stages of dihydroxylation reaction considerable amount of epoxide is formed which is subsequently converted into diols as the reaction proceeds for longer time. This indicates that diol formation proceeds via ring opening of epoxide which can occur via acid or base catalysis. Since, over TS-1, question of base catalysis does not arise, it is the acidity of TS-1 which is responsible for the said observation. Titanium-peroxo species is believed to generate Brönsted acidity which facilitates ring opening of epoxide (Scheme 6.3).

The water can attack the epoxide either at C_2 or C_3. Since, in the case of methallyl chloride, C_2 is much crowded than C_3 (because of methyl group at C_2) water may preferentially attack at C_3 and thereby probably leading to higher sterio selectivity for anti isomer. Restricted pore openning and channel dimention of MFI topology in TS-1, may further facilitate this attack. In the case of allyl chloride, incoming H_2O does not face much hinderance due to smallar size of allyl chloride and thus it can attack C_2 and C_3 simultaneously, giving rise to corresponding diol mixtures. Here it is pertinent to mention that water used in solvent-free system not only act as dispersion medium but also helps to drive (clean) away the products from the active reaction sites of the zeolite channels, since the product diol is more hydrophilic in nature than the substrate.

6.3.2 Oxidation of Cyclic and Aromatic Ketones :

Baeyer-Villiger (B.V.) rearrangement, induced by peroxy acid[16] or H_2O_2 / Lewis acid[17] systems, organometallics[18] and metalloenzymes[19,20] is an important class of chemical transformation for synthesizing esters and lactones from acyclic and cyclic ketones, respectively. B.V. oxidation falls in the (ii) category of reactions given above.

6.3.2.1 Cyclohexanone :

Table 6.5 represents the results obtained in the B. V. oxidaiton of cyclohexanone **7**. The conversion is significantly higher along with higher selectivity for ε-caprolactone in the triphase solvent-free condition (compared to that obtained in biphase with cosolvent) system (entry 1 vs 2, Table 6.5). Further in the presence of a small amount of added acid (commonly used in B.V. oxidation) the conversion as well as selectivity to ε-caprolactone increases considerably (entry 1 vs 3). In the presence of cosolvent and in the absence of any added acid very little reaction (ca. 5 % conversion) with no ε-caprolactone was observed. Apart from ε-caprolactone, a Baeyer-Villiger oxidative rearrangement product, other products, hydroxy ketones and diketones (1,2-; 1,3- and 1,4- all three, i.e., α-C, β-C and γ-C oxidation products, respectively, occur simultaneously. 1-Hydroxy cyclohexene and its corresponding epoxide are also formed to some extent (Scheme 6.4).

6.3.2.2 Acetophenone :

In Table 6.6, the results of B.V oxidation of acetophenone **8** are recorded. Like the oxidation of cyclohexanone discussed above, in this case also under solvent-free condition some conversion of acetophenone and high selectivity for phenyl acetate, which is a B.V. oxidation product (entry 1 and 3, Table 6.6, Scheme 6.4), were observed. Further, the presence of catalytic amount of aadded acid, considerably enhances both the conversion and ester selectivity (entry 1 vs. 2). Under biphase conditions no conversion was observed at all. When few drops of acid were added in biphase reaction mixture, about 5 % conversion was obtained.

The ester so formed undergoes acid hydrolysis to produce phenol (PH) [followed by its further oxidation products catechol (CA) and hydroquinone (HQ)] and acetic acid (AA). The other major reaction observed under solvent-free conditions with added acid, is the direct hydroxylation of acetophenone to give quite important

Table 6.5 : Oxidation of cyclohexanone over TS-1[a]

Entry	System	Phase[b]	Conv[c]	Product selectivities (mole %)			
			mole %	ε-capro lactone	hydroxy ketone	diketone	cyclohexene + epoxide
1.	TS-1/H_2O_2	Tri	31.0	19.6	31.3	33.6	15.5
2.	TS-1/H_2O_2/H^+	Tri	64.0	45.2	17.0	14.0	23.8
3.	TS-1/H_2O_2	Bi	5.0	-	64.0	36.0	-
4.	TS-1/H_2O_2/H^+	Bi	30.2	28.4	25.5	31.0	15.1
5.	H_2O_2/H^+	Bi	11.2	94.5	-	-	5.5
6.	H_2O_2/H^+	Mono[d]	-	-	-	-	-

a: a: Reaction conditions : Substrate : H_2O_2 = 1:1, catalyst TS-1 (Si / Ti = 29) 20 wt % with respect to substrate, Temp. 353 K.

b: Tri = solid caatalyst + two immiscible liquid phases (organic substrate + H_2O_2 in water); Bi: solid catasyst + one homogeneous liquid phase (organic substrate + aq H_2O_2 + CH_3CN as cosolvent).

c: Maximum conversion achieved during the reaction after 6 h reaction time.

d: One homogenize liquid phase, no catalyst.

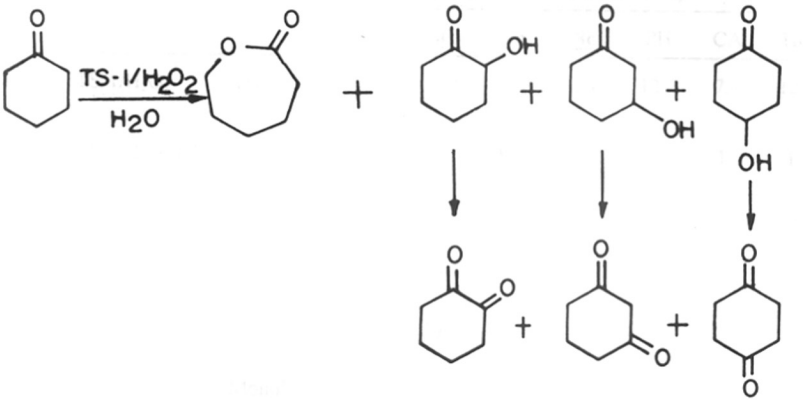

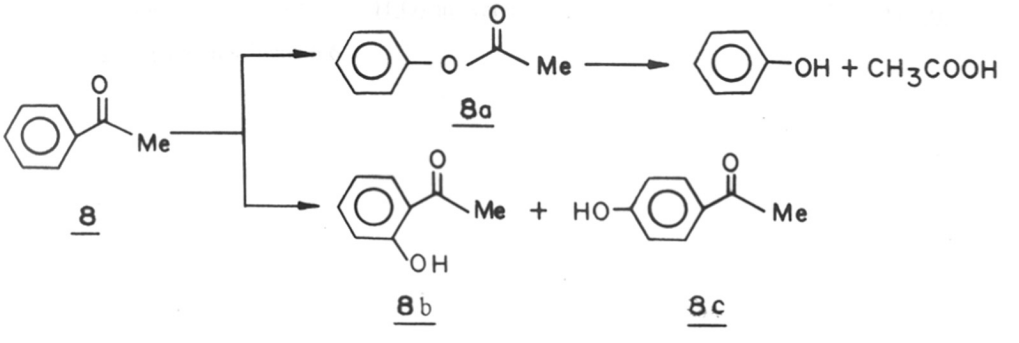

Scheme-6·4

Table 6.6 : Baeyer-Villiger rearrangement and hydroxylation of acetophenone over TS-1 / H_2O_2 system[a]:

Entry	System	Phase[b]	Conv[c]	Product selectivities (mole %)						
			(%)	**8a**	**8b**	**8c**	PH	CA	HQ	AA
1.	TS-1/H_2O_2	Tri	7.0	27.0	2.8	5.6	12.6	7.4	12.3	32.3
2.	TS-1/H_2O_2/H^+	Tri	31.0	49.7	16.6	16.0	7.0	1.0	1.1	8.6
3.	TS-1/H_2O_2	Bi	-	-	-	-	-	-	-	-
4.	TS-1/H_2O_2/H^+	Bi	6.1	61.0	-	-	4.6	10.8	4.4	19.0
5.	Blank/H_2O_2/H^+	Bi[d]	5.5	31.8	6.9	-	24.9	2.8	3.5	30.1
6.	Blank/H_2O_2/H^+	Mono[e]	-	-	-	-	-	-	-	-

a, b and c: same as given in Table 6.1 except that the reaction time was 12 h.

d: two liquid phases (substrate + H_2O_2 in water).

e: one liquid phase (substrate + H_2O_2 in water + CH_3CN as cosolvent). Products **8a**, **8b** and **8c** as given in scheme 6.6.

products namely, *o*- and *p*-hydroxy acetophenone (32 %), which are the raw materials for the production of *o*- and *p*-acetamol (very important bulk chemical for pharmaceutical industry), respectively. The formation of hydroxy acetophenones (particularly *ortho* isomer) can also be possible due to the acid catalyzed Fries rearrangement of the initially formed B.V. product phenyl acetate. To check this point, phenyl acetate was taken as substrate and the reaction was carried out under identical conditions. Interestingly, around 70 % of the substrate was converted into corresponding hydrolyzed products, phenol and acetic acid. No *o*- and *p*-hydroxy acetophenone were detected, indicating that the formation of hydroxy acetophenone, particularly *p*-isomer occurs via direct hydroxylation of acetophenone. This is further supported by the fact that, when the blank reaction was carried out in absence of any catalyst and cosolvent (i.e., acetophenone + H_2O_2 + H_3O^+) nearly 5 % conversion was achieved (with the formation of *o*-hydroxy acetophenone and no *p*- hydroxy acetophenone), whereas no reaction was observed in the presence of cosolvent and in absence of catalyst (entry 6, Table 6.6). Under TS-1 / H_2O_2 triphase conditions higher selectivity for *p*-hydroxy acetophenone (vis-à-vis *o*-isomer, *p*-/*o*- = 2:1), characteristic of TS-1, was observed. However, in the presence of added H_2SO_4 almost 1:1 *p*-/*o*- ratio was obtained, mainly due to the contribution of *o*-isomer via acid catalyzed Fries rearrangement of ester mainly to *o*-hydroxy acetophenone.

6.3.3 Oxidation of Methyl Benzoate, an Aromatic Ester :

In the oxidation of methyl benzoate **9** (Scheme 6.4) under solvent-free reaction conditions, the formation of perester **9a** and hydroxylated products *ortho* hydroxy methyl benzoate **9d** and *para*-hydroxy methyl benzoate **9e** was observed (Table 6.7). Hydrolysis of methyl benzoate to perbenzoic acid **9b** and methanol **9c** also occurs to

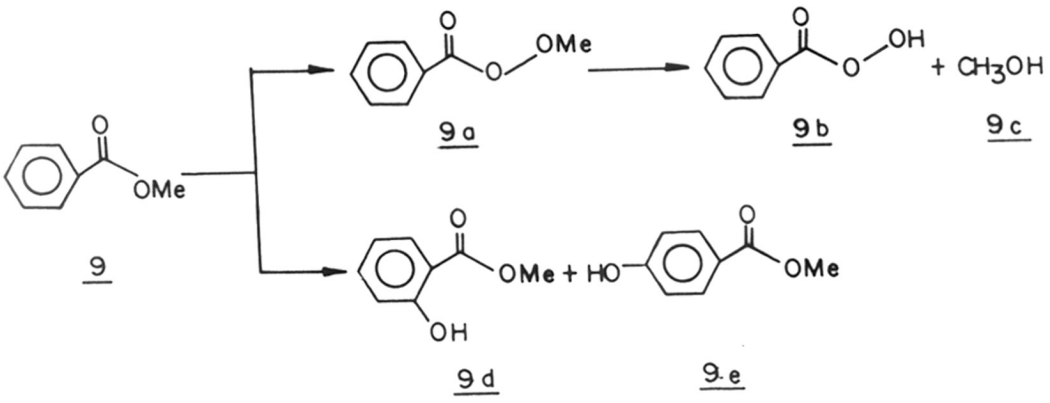

Scheme-6.5

Table 6.7 : Oxidation of methyl benzoate over TS-1 under solvent free conditions :

Conv. (mole %)	H_2O_2 sel. %	Time, h	Products	Selectivity (mole %)
21.2	24.8	12.0	Methyl perbenzoate 9a	21.8
			Per benzoic acid 9b	12.1
			Methanol 9c	7.0
			o-Hydroxy methyl benzoate 9d	12.2
			p-Hydroxy methayl benzoate 9e	6.8
			o- Hydroxy benzoic acid 9f	20.2
			p-Hydroxy benzoic acid 9g	14.7
			Others[a]	5.2
			$\sum$Side chain oxidation 9a + 9b + 9c	40.9
			$\sum$Ring hydroxylation 9d + 9e + 9f + 9g	53.9

a : Oxidation products of methanol, i.e. HCHO and HCO_2H.

some extent. Hydrolysis of *o*- and *p*-hydroxy methyl benzoate resulted in the formation of *o*-hydroxy benzoic acid and *p*-hydroxy benzoic acid (which are important bulk chemical for pharmaceutical industry), respectively. However, under biphase reaction conditions using solvent no reaction was observed.

6.3.4 Mechanistic Aspects **:**

An interesting observation in the formation of *o*- and *p*-hydroxy acetophenone, particularly the *para* isomer which is not formed in blank or in the presence of cosolvents. It seems that under solvent-free conditions, TS-1 / H_2O_2 system can favor hydroxylation of deactivated aromatic ring. Bellussi and Fattore[21] have reported that TS-1 exhibits Brönsted acidity in the presence of H_2O_2, due to the formation of titanium peroxo species (Scheme 6.6, species **II**) stabilized by protic solvent like water (Scheme 6.5, species **III**) and alcohols[21,22]. However, this acidity is solvent dependent[21]. Under solvent-free conditions, TS-1 seems to act both as oxidation and Brönsted acid catalyst. That is why, even in the absence of any added acid, TS-1 under solvent-free conditions (entry 1, Table 6.6) exhibits the formation of ester and aids its hydrolysis. The "≡Ti-O-O...H" moiety stabilized in the presence of water is proposed to attack, through nucleophilic oxygen, the *o*- and *p*- positions (which is partially deactivated in the presence of electron withdrowing CH_3CO- group) forming *o*- and *p*-hydroxy acetophenones.

A plausible reaction path in the oxidation of acetophenone taken as representative, is depicted in Scheme 6.7. The species **II** may act as nucleophile, particularly in presence of water (species **III**, Scheme 6.6) under solvent-free conditions, to attack the electron defficient carbonium ion produced after initial protonation step, thus forming species **8a** (Scheme 6.7) via a plausible intermediate **2** through the migration of phenyl gorup[23]. Similarly, the species **III** can also attack the partially electron defficient *o*- and *p*- positions of the deactivated aromatic ring of

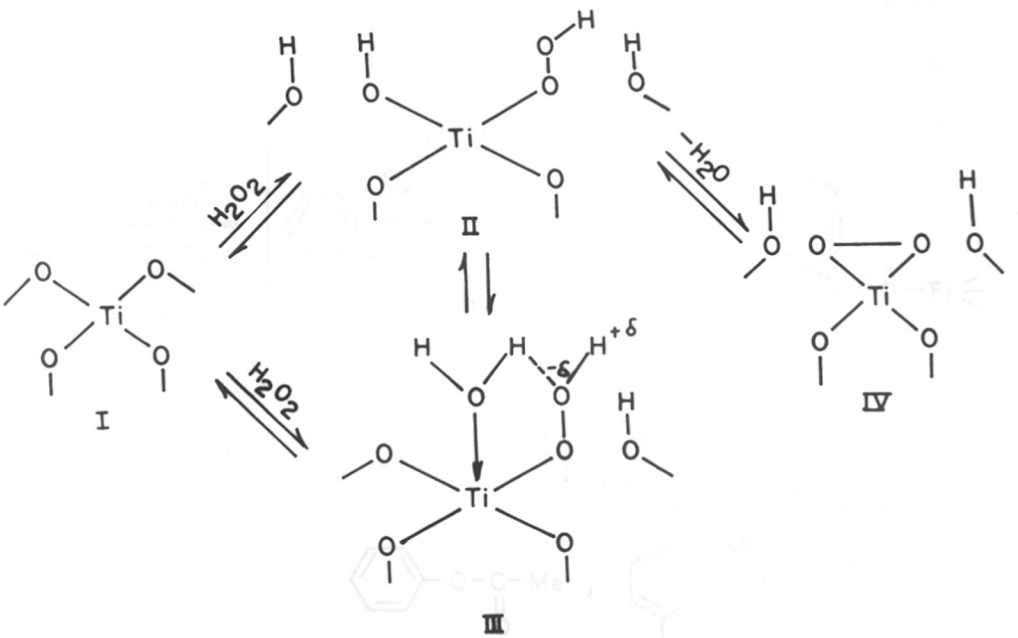

Scheme-6·6

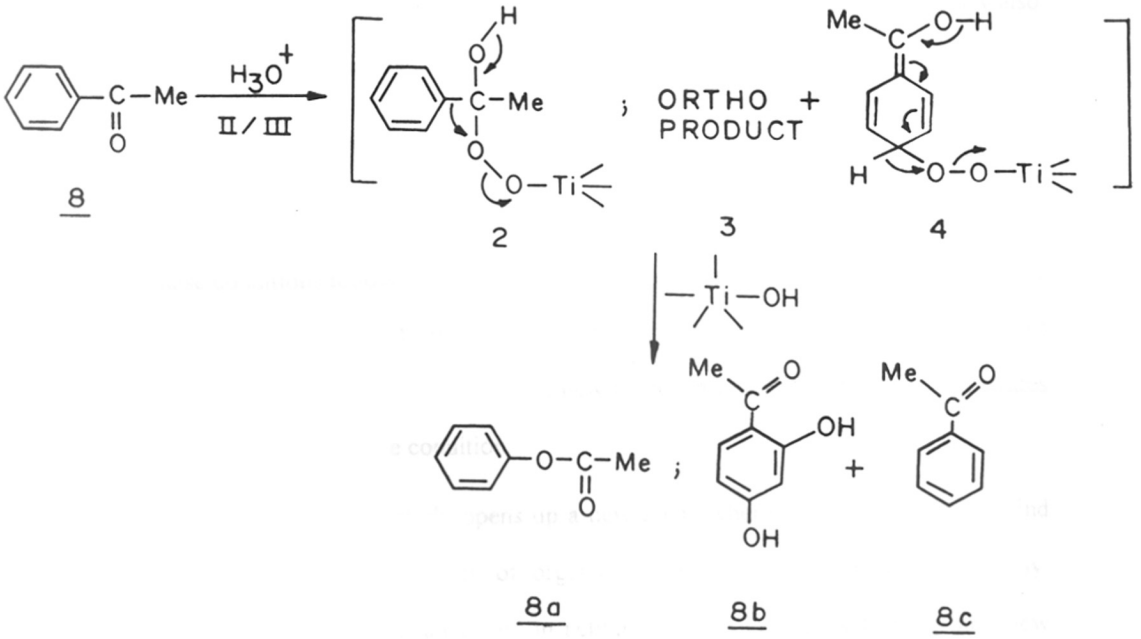

Scheme–6·7

acetophenone, thus producing *o*- and *p*-hydroxy acetophenones (species **8b** and **8c** via species **3** and **4**, respectively). Significantly higher activity of TS-1 under solvent-free condition compared to that in presence of solvent can be attributed to the higher hydrophobic nature of TS-1[6], where an organic solvent, when present (as in biphase), will favorably compete with the substrate for the diffusion and absorption at the active sites. Whereas, in present triphase solvent-free condition organic substrate will not face such diffusional competition with water in TS-1. Further, the higher Brönsted acidity of TS-1 / H_2O_2 system in the presence of water[21] (vis-à-vis cosolvent) may also be responsible for higher yields of Baeyer-Villiger rearrangement products.

6.4 CONCLUSION :

From the above results it can be concluded that under present solvent-free / triphase conditions following can be achieved : (i) enhancement of activity of the water immiscible (hydrophobic) substrates, (ii) drastic change (in some cases reversal) in regio-selectivity of the products, (iii) new routes in oxidation of various substrates over conventional biphase condition.

Thus the present study opens up a new arena where titanium silicate can find tremendeous utility in a variety of organic transformations, in an eco-safer way. Factors responsible for enhancement in activity, change in regio-selectivity and new routes are summarized as :

(i) Competitive diffusion of substrate with solvents.

(ii) More hydrophobic nature of the products than the substrates.

(iii) Relative hydrophobic nature of titanium silicates.

(iv) Restricted pore openings and void volume in zeolite channels.

(v) Brönsted acidity of titanium silicates in the presence H_2O_2 and water.

6.5 REFERENCES :

1. Ameto, J., *Science*, **259**, 1538 (1993).
2. Kaupp, G., *Angew.Chem.Int.Ed.Engl.*, **33**, 1452 (1994).
3. Tanko, J.M. & Blackert, J.F., *Science*, **263**, 203 (1994).
4. Metzer, J.O. & Mahler, R., *Angew.Chem.Int.Ed.Engl.*, **34**, 902 (1995).
5. *Ullman's Encyclopidia of Industrial Chemistry*, Vol. A22, 5th Ed., VCH, Weinheim, pp411 (1993).
6. Bhaumik, A. & Kumar, R., *J.Chem.Soc.Chem.Commun.*, 349 (1995).
7. Perego, G., Bellussi, G., Corno, C., Taramasso, M., Buonomo, F. & Esposito, A., *Stud.Surf.Sci.Catal.*, **28**, 129 (1986).
8. Ronny, N. & Igal, A., *J.Chem.Soc.Chem.Commun.*, 1285 (1988).
9. Tatsumi, T., Yoko, M., Nakamura, M., Yinhara, Y. & Tominaga, H., *J.Mol.Catal.*, **78**, L41 (1993).
10. Sato, T., Dakka, J. & Sheldon, R.A., *J.Chem.Soc.Chem.Commun.*, 1887 (1994).
11. Bhaumik, A., Kumar, R. & Ratnasamy, P., *Stud.Surf.Sci.Catal.*, **84C**, 1883 (1994).
12. Clerici, M.G. & Ingallina, P., *J.Catal.*, **140**, 71 (1993).
13. Van Nieuwenhze, M.S. & Sharpless, K.B., *J.Am.Chem.Soc.*, **115**, 7864 (1993).
14. Corey, E.J., Noe, M.C. & Guzman-Perez, A., *J.Am.Chem.Soc.*, **117**, 10817 (1995).
15. Onaka, M., Kawai, M. & Izumi, Y., *Chem.Lett.*, 779 (1985).
16. Emmons, W.D. & Lucas, G.D., *J.Am.Chem.Soc.*, 77, 2287 (1955).
17. McClure, J.D. & Williams, P.H., *J.Org.Chem.*, **27**, 24 (1962).
18. Balur, C., Schingfoff, G. & Weickhardt, K., *Angew.Chem.Int.Ed.Engl.*, **33**, 1848 (1994).
19. Gognon, R., Gronan, G., Roberts, S.M., Villa, R. & Willetts, A.J., *J.Chem.Soc. Perkin. Trans.1*, 1505 (1995).
20. Lemoult, S.C., Richardson, P.F. & Roberts, S.M., *J.Chem.Soc.Perkin.Trans.1*, 89 (1995).
21. Bellussi, G. & Fattore, V., *Stud.Surf.Sci.Catal.*, 69, 79 (1991).
22. Bellussi, G. & Fattore, V., *Stud.Surf.Sci.Catal.*, 85, 177 (1994).
23. Palmar, B.W. & Fry, A., *J.Am.Chem.Soc.*, 92, 2580 (1970).

CHAPTER 7

SUMMARY AND CONCLUSIONS

Chapter 2 reports about the synthesis and use of a *new organic template, 1,6-hexamethylene bis (benzyl dimethyl ammonium* bromide / hydroxide). This new template is *quite suitable to produce large pore ZSM-12, medium pore ZSM-48 and small pore ZSM-39* zeolites by varying its concentration (along with Si / Na and Si / Al mole ratios) in the hydrogel. Using this organic additive MTW type alumino-silicate, pure-silica polymorph as well as *titanium-silicate (Ti-MTW) and vanadium-silicate (V-MTW)* analogs are synthesized. Framework IR and UV-VIS spectroscopy as well as catalytic activity indicate the incorporation of Ti in silicate lattice. ESR spectra of V-MTW samples indicate that isolated V^{4+}/V^{5+} ions are firmly anchored in the silicate network. V-MTW samples have been found to be quite active in the oxidation of a variety of organic substrates including bulkier ethylbenzene.

In Chapter 2, *first report of arseno-silicate (As in both III and V oxidation state) analogs of various zeolite structures (MFI, MEL, MTW and ZSM-48) are made*. These materials particularly As(V)-silicates have been synthesized *at much lower temperature and at much reduced crystallization time* compared to their silicalite and alumino-silicate analogs. Further, with increase in As(V) content of the gel, the crystallization becomes faster, contrary to the observations made in the case of all other high silica zeolites and metallo-silicates.

Chapter 3 describes an important invention of *a novel and generalized concept of using 'promoters' in enhancing zeolite crystallization*. Use of a small amount of one of the promoter oxyanions / oxyacids (perchlorate, nitrate, phosphate, carbonate, arsenate etc.) can enhance the crystallization of a variety of zeolite structures, independent of its Si/Al ratio (FAU to MFI), pore size (large pore Beta to small pore NU-1) or hetero-element content (silicalite or Ti-silicates) in the hydrogel. In some cases it reduces the crystallization temperature also. Liquid-state ^{29}Si and ^{31}P NMR experiments indicate the interaction of these promoter oxyanions with the soluble

silicate species in facilitating the condensation process. Further, the use of these promoters not only the *saves time and energy*, but also produces zeolite crystals having better crystallinity and more uniform and smaller particles which are quite important from catalytic point of view.

Chemoselective oxidation of various organic compounds containing more than one functional groups over TS-1 is reported in Chapter 4. A generalized study on the use of TS-1 in ammoximation of various carbonyls (ketones and aldehydes) is reported in this chapter.

Application of triphase catalysis over high silica zeolite TS-1 is reported for the first time (Chapter 5), in the oxidation of various hydrophobic organic compounds. Not only the *enhancement in activity* and drastic change in *para*-selectivity (in some cases *complete reversal of ortho-para selectivity*), present method offers distinct advantages in *easier work-up* of products. Using relatively hydrophobic titanium-silicates catalysts, in the presence of H_2O_2, under triphase (absence of cosolvents) organic substrates selectively diffuse through the zeolite pores vis-à-vis that in the presence of cosolvents (commonly used to homogenize the immiscible liquid layers), where cosolvent competes with the substrates for diffusion and adsorption at the active sites located inside the zeolite channels and thereby adversely affecting the conversion.

Solvent-less chemistry, one of the most desirable and challenging objective of present days chemical research, is focused over silica based molecular sieves (TS-1) for the first time. Present methodology of *solvent-free* conditions (given in Chapter 6) gives rise to new routes in TS-1 / H_2O_2 catalyzed organic transformation (viz., direct oxidation of organic halides, Baeyer-Villiger oxidation of ketones etc.) in an *eco-friendly* way.

List of Publications:

Papers:

1. Promoter-induced enhancement of the crystallization rate of zeolites and related molecular sieves, Rajiv Kumar, **Asim Bhaumik**, Ranjeet Kaur Ahedi and S.Ganapathy, *Nature, 381, 298-300* (1996).

2. Titanium silicate molecular sieve (TS-1) / H_2O_2 induced triphase catalysis in the oxidation of hydrophobic organic compounds with significant enhancement of activity and para-selectivity, **Asim Bhaumik** and Rajiv Kumar, *J.Chem.Soc.Chem.Commun.*, 349-350 (1995).

3. A new MFI type As(III)-silicate molecular sieve, **Asim Bhaumik** and Rajiv Kumar, *J.Chem.Soc.Chem.Commun.*, 349-350 (1995).

4. Chemoselective oxidation of organic compounds having two or more functional groups. **Asim Bhaumik**, Rajiv Kumar and Paul Ratnasamy, *Stud. Surf. Sci. & Catal.*, 84 C 1883-1888 (1994).

5. Low temperature, efficient synthesis of new As(V)-silicate molecular sieves with MFI topology and their catalytic properties in oxidation reactions, **Asim Bhaumik,** S.G.Hegde and Rajiv Kumar, *Catal.Lett.*, 35, 327-334 (1995).

6. Synthesis of MTW type microporous materials and its vanadium silicate analogue using a new diquaternary ammonium cation as a template, **Asim Bhaumik,** M.K.Dongere and Rajiv Kumar, *Microporous Materials*, 5, 173-178 (1995).

7. Sn-ZSM-12, a new large pore MTW type molecular sieve: synthesis, characterization and catalytic properties in oxidation reactions, N.K.Mal, **A.Bhaumik,** R.Kumar and A.V.Ramaswamy, *Catal.Lett.*, 33, 387-394 (1995)

8. Ammoximation of different carbonyl compounds over titanium silicate molecular sieve, TS-1, using dilute H_2O_2 and ammonia, **Asim Bhaumik** and Rajiv Kumar, *Catalysis Modern Trends*, (Eds., N.M.Gupta and D.K.Chakrabarty), Narosha Publishing House, New Delhi, 160-165 (1995).

9. Synthesis of Al-free Sn-containing molecular sieves of MFI, MEL and MTW types and their catalytic activity in oxidation reactions, N.K.Mal, **A.Bhaumik**, V.Ramaswamy, A.A.Belhekar and A.V.Ramaswamy, *Stud. Surf. Sci. & Catal.*, 91, 387-396 (1995).

10. Baeyer-Villiger rearrangement catalyzed by titanium silicate molecular sieve (TS-1) / H_2O_2 system, **Asim Bhaumik**, Prashant Kumar and Rajiv Kumar, *Catal.Lett.*, (in press).

11. New method of enhancement of the crystallization rate of zeolites in presence of Gr. VA and VIIA oxyacids / oxysalts as promoter, **Asim Bhaumik**, A.A.Belhekar and Rajiv Kumar, *11th Int.Zeol.Conf., Seoul, South Korea*, (1996) (Accepted).

12. New oxidative transformations over TS-1 / H_2O_2 system under solvent-free conditions, **Asim Bhaumik** and Rajiv Kumar, *J. Org. Chem.*, (Communicated).

13. Triphase Catalysis over Titanium - Silicate Molecular Sieves under Solvent - Free Coditions: I, Hydroxylation of Benzene and Substituted Benzens, **Asim Bhaumik** and Rajiv Kumar, *J.Catal.*, (communicated)

14. Zeolite crystallization - an in-situ liquid state NMR study, **Asim Bhaumik** Rajiv Kumar and S.Ganapathy, *J.Phys.Chem.*, (To be communicated).

15. Role of liquid crystalline quatarnery ammonium salts in zeolite crystallization, **Asim Bhaumik** and Rajiv Kumar, *J.Chem.Soc.Chem.Commun.* (To be communicated)

Patents

1. An improved process for oxidation of olefinic compounds, R.Kumar, G.C.G.Pieas, **A.Bhaumik**, P.Kumar and B.Pandey, Filed, Indian: NF-201/93.

2. A process for the preparation of arsenic modified porous crystalline silicas, **A.Bhaumik** and R.Kumar, Filed, India: 290/DEL/95.

3. An improved process for the production of zeolites, **A.Bhaumik** and R.Kumar, Applied India and U.S., Indian Appl. No.NF-138/95.

4. A new process for the preparation of MTW type molecular sieves, **A.Bhaumik** and R.Kumar, Filed, India: 289/DEL/95.

5. A single-step process for production of phenol, **A.Bhaumik** and R.Kumar, Applied (India and U.S.).